To the Graduate Council:

I am submitting herewith a dissertation written by Hanchang Henry Chen entitled "Transient Simulation and Sensitivity Analysis for Transport of Radionuclides in a Saturated-Unsaturated Groundwater Flow System." I recommend that it be accepted in partial fulfillment of the requirements for the degree of Doctor of Philosophy, with a major in Nuclear Engineering.

James C. Robinson, Major Professor

We have read this dissertation
and recommend its acceptance:

Accepted for the Council:

Vice Chancellor
Graduate Studies and Research

TRANSIENT SIMULATION AND SENSITIVITY ANALYSIS FOR TRANSPORT OF RADIONUCLIDES IN A SATURATED-UNSATURATED GROUNDWATER FLOW SYSTEM

A Dissertation

Presented for the

Doctor of Philosophy

Degree

The University of Tennessee, Knoxville

Hanchang Henry Chen

December 1980

ACKNOWLEDGEMENTS

The author wishes to express his gratitude to the Technology for Energy Corporation which has funded this work to its completion.

The author wishes to express his sincere appreciation to Dr. J. C. Robinson, who served as his major professor, for his support and encouragement. The author is also very grateful to Dr. A. H. Eraslan for his enthusiasm in assisting the development of the numerical method employed in this work. Appreciation is given to Dr. H. L. Dodds of the University of Tennessee for his encouragement and suggestions. Appreciation is also extended to Joyce Wallace and Frank Fox of Technology for Energy Corporation, who assisted in the preparation of this manuscript.

Special appreciation is given to my wife, Margaret, who has been exercising her patience and encouragement throughout the course of this study. Finally, this dissertation is dedicated with gratitude to my Lord Jesus Christ, who has been faithfully guiding my life.

ABSTRACT

Radionuclide transport by groundwater flow is an important pathway in the assessment of the environmental impact of radioactive waste disposal to the biosphere. A numerical model was developed to simulate radionuclide transport by groundwater flow and predict the radionuclide discharge rate to the biosphere. A sensitivity analysis methodology was developed to address the sensitivity of the input parameters of the radionuclide transport equation to the specified response of interest (space-average radionuclide concentration and radionuclide discharge rate at a final time).

A transient, two-dimensional radionuclide transport code RADMIG, based upon the Fluid in Discrete Element (FLIDE) numerical formulation, was developed to simulate the radionuclide transport in a given groundwater flow system. The radionuclide transport code was employed to simulate tritium transport in a hypothetical saturated-unsaturated groundwater flow system.

The sensitivity analysis methodology for the radionuclide transport problem was developed based on generalized perturbation theory. The adjoint transport equation was first derived using variational principle formulation. Sensitivity coefficients were formulated for four input parameters: longitudinal and transverse dispersivities; retardation factor; and radioactive decay constant.

Sensitivity coefficients were computed by combining the solved time-dependent concentration and adjoint fields together. The computational

procedure for performing the radionuclide transport sensitivity analysis is presented. Relative sensitivity coefficient fields of two responses to four input parameters are presented and discussed.

The radionuclide transport sensitivity theory was validated by comparing the relative sensitivity coefficients obtained from both the perturbation predictions and direct calculations. The agreement between the sensitivity results from both approaches is good. Linearity ranges of the parameters for two responses were estimated.

It is concluded that the generalized perturbation theory provides a feasible, economic means to perform sensitivity analysis on radionuclide transport problems.

TABLE OF CONTENTS

LIST OF TABLES

LIST OF FIGURES

FIGURE PAGE

CHAPTER I

INTRODUCTION AND BACKGROUND

The management of low-level radioactive wastes generated by nuclear power plants, hospitals and research laboratories has long been a major problem confronting the nuclear industry and its regulators. These radioactive wastes should be properly treated and disposed of in order to prevent them from imposing any unacceptable environmental impact on the present and future generations. Reposition of the radioactive wastes by shallow land burial is one of the methods that has been used, and it necessitates the evaluation of the potential for transport of radionuclides from the burial site to the biosphere by groundwater flow. One of several pathways by which buried wastes can enter the biosphere is by leaching and seepage of the wastes into the groundwater system. The earth science community generally perceives that transport by groundwater is the most important natural mechanism for bringing buried wastes to the biosphere.[1] Therefore, a methodology is required (a) to describe the radionuclides transport by groundwater flow in the hydrogeologic system of a given site from the bottom of the burial trench to the discharge surface where the radionuclides become accessible to the biosphere, (b) to predict the movement of the radionuclides, and (c) to estimate the radiological doses to human beings. A radionuclides transport model based on the physical conservation principles can be employed to simulate the transport of

radionuclides in a groundwater flow system and estimate the radiation doses accessible to the biosphere.

For any computer simulation of the radionuclides transport by groundwater flow, the following sensitivity questions arise (a) what is the uncertainty in the calculated result due to uncertainties in the input parameters (hydrogeologic characteristics), (b) how sensitive (important) is the calculated result to each one of the input parameters, and (c) where are the most sensitive regions in the groundwater flow system in which the input parameters must be specified (or measured) more accurately in order to obtain a more accurate simulation. The first question can be answered by performing a sensitivity analysis on the radionuclides transport by groundwater flow in conjunction with an uncertainty analysis. The latter two questions can be addressed by calculating the spatial (space-dependent) distributions of the relative sensitivity coefficients of the calculated result to the input parameters.

A. Radionuclide Transport Models

Radionuclides must be dissolved in the water of the burial trench before they can begin to infiltrate the bottom of the burial trench and be transported by the groundwater through the porous media. Transport of radionuclides by groundwater may be modeled by considering (1) groundwater flow transport, and (2) mass transport.

The groundwater flow transport is described by the equation of motion for the groundwater flow and the appropriate initial and boundary conditions. The groundwater flow transport problem has been solved in a

number of real hydrological field-specific problems by numerical methods.[2-8] Finite element methods have widely been employed to simulate the groundwater flow transport in either saturated flow systems (e.g., aquifer) or saturated-unsaturated flow systems. Reeves and Duguid[9] have developed a computer model for groundwater movement through saturated-unsaturated porous media by finite element method. This model has been utilized to simulate the transient, two-dimensional (vertical cross-section) groundwater flow transport in a saturated-unsaturated region and compute the Darcian velocity field and water content field. Since the development of a groundwater flow transport model is not our purpose in this study, we shall use Reeves and Duguids' model to obtain the groundwater flow information which will then be read as input data into a radionuclide transport model.

The mass transport of contaminants dissolved in the groundwater through the porous media has been simulated by both analytical and numerical methods.[10-18,21] The mathematical model for mass transport of dissolved material in groundwater flow is basically convective transport, hydrodynamic dispersion, chemical interaction with soil and radioactive decay processes. The governing equation is a diffusive-convective time-space-dependent linear differential equation which is formulated by applying the principle of conservation of mass to a differential control volume. This equation together with the specified initial and boundary conditions may be solved for the time-dependent spatial distribution of contaminant concentration in a given hydrogeological region. This dispersion-convection equation has been solved analytically.[11,18]

Numerical methods have long been employed to simulate the transport of the contaminants dissolved in groundwater in a number of different hydrologic systems.[12,17] The most commonly used numerical methods for solving the dispersion convection mass transport equation are the method of characteristics, finite-difference, and finite-element methods.

The method of characteristics[17] was developed to solve hyperbolic differential equations. This method involves a particle tracking scheme to solve the transport equation. Depending on the velocity field, the particles are advected through the finite-difference grid. Next, a dispersion equation is solved and the concentration in a cell is modified according to the solution. If solute transport is dominated by convective transport, as is common in many field problems (e.g., in aquifer), then the mass transport equation may closely approximate a hyperbolic partial differential equation and be highly compatible with the method of characteristics. However, the groundwater velocities in the unsaturated region in our case are generally small, that is, the radionuclide transport is "not" dominated by convective transport. Therefore, the method of characteristics is not appropriate as the numerical method to solve the radionuclide transport equation in the saturated-unsaturated porous media.

Several investigators have employed finite-difference methods for the solution of the mass transport equation.[12,19,20] The direct application of finite-difference methods to field problems has experienced numerical dispersion effects which cause oscillations in the concentrations in the region of the front.[22] As pointed out by

Bredehoeft,[20] the numerical dispersion produced by these methods was of the same order as the physical dispersion. As a result, higher order techniques which minimize numerical dispersion have appeared.

To reduce the effect of numerical dispersion, Rubin and James,[14] and Pinder[13] have used Galerkin finite-element methods. These methods appear to be better suited for the solution of the dispersion-convection transport equation because numerical dispersion is small and because multidimensional irregular regions can be treated. In Galerkin finite-element methods, the region of interest in two-dimensional space is discretized into either triangular or quadrilateral finite elements. The governing differential equation is then integrated over the finite elements by using Galerkin's formulation. The resulting nodal system of equations is then solved implicitly. The time derivative is approximated by a fully implicit backward difference scheme to gain stability. Galerkin finite-element models have been developed to simulate the transport of dissolved contaminants in various site-specific problems in two and three-dimensional geometries.[15,16,23] Specifically, Duguid and Reeves[15] have developed a transient, two-dimensional computer model to simulate the transport of dissolved contaminant through porous media utilizing the Galerkin finite-element method. This computer code was intended to be employed in conjunction with a formerly developed groundwater flow transport model[9] (also using Galerkin finite-element method) to simulate the contaminant transport by groundwater flow.

Eraslan has developed a unified transport mathematical model utilizing the FLIDE (Fluid-In-Discrete-Element) method (also called

discrete-element method) for numerical simulations of fast-transient, one- and two-dimensional transport of thermal, radiological, chemical, and biological properties in rivers, estuaries, lakes, and coastal regions for assessing the impact of power-plant operations.[24-29] For example, a fast-transient, two-dimensional discrete-element thermal transport model was formulated and developed to simulate the transient temperature distribution under specified flow conditions in lakes, estuaries, and coastal regions for predicting the thermal impact of power plant operations.[24] Another fast-transient, two-dimensional, dissolved radionuclide transport model was also developed by converting temperature formulations into radionuclide concentrations. The discrete-element method employs the integral forms of the conservation principles for mass and thermal energy in variable-sized discrete elements that span the specified flow region. In the case of dissolved radionuclide transport, the rate of change in the radionuclide concentration in the control volume (discrete element) is equal to the net transportive mass flow rate in the control volume due to the mechanisms of convection, hydrodynamic dispersion and radioative decay. The convective transport term is formulated by using "upwind differencing" scheme to attain the simulation stability. The resulting system of time-dependent differential equations is numerically integrated, from arbitrarily specified initial conditions, by the multi-time step numerical integration technique (e.g., the Runge-Kutta-Gill method) with a time-step size based on a stability criterion for explicit methods. The discrete-element transport model has demonstrated its numerical stability in transient simulations in various site-specific

problems.[24,26,28,29] Like finite-difference methods, the mathematical formulation of the discrete-element transport model is physics-oriented and the representation of spatial derivatives is straight-forward. The discrete-element method has the flexibility of placing the higher density of discrete elements in the subregions where the concentrations are considered more important. In contrast to the finite-element method where large systems of equations must be solved simultaneously and, thus, a large amount of computer core memory is required to store system matrices and variables, the discrete element method explicitly solves the system of discrete-element equations, and the calculational procedure is more direct, efficient, and meaningful.

B. Sensitivity Analysis Methodologies

Sensitivity analysis of radionuclide transport by groundwater is very important and has become one of the major items in national radioactive wastes management programs.[31,32] Sensitivity analysis can be used to determine the uncertainty in the simulation results (e.g., radionuclide discharge rate) due to the uncertainties in the hydrogeological parameter data and to identify the most sensitive (important) parameters and their regions where the parameters need to be measured more accurately. Therefore, it is beneficial to perform sensitivity analysis for radionuclide transport problems.

If the radionuclide transport equation is solved by analytical methods and the results of interest can be expressed in a closed form in terms of input parameters, the parametric analysis can be done by calculating the result with each parameter varying over its potential range

of values while holding the other parameters fixed at their reference values. The sensitivity analysis can be performed by taking partial derivative of the result of interest with respect to each parameter and then calculating the relative sensitivity coefficients using the reference values of the input parameters.

For the case of numerical simulations, the parametric and sensitivity analyses are usually based upon the response-surface method. In this method, a set of reference parameter values needed as input data for the computer simulation is first chosen for study. To perform a parametric analysis, a specified input parameter value is varied over a certain value range while holding the other parameters at their reference values, and the computer code is run to compute the changes made in the calculated results using the altered data sets. To perform a sensitivity analysis, the relative sensitivity coefficient of the result of interest to the specified parameter is obtained from the ratio of percent change in the calculated result to percent change in the specified parameter about its reference value. It is assumed that the result is linear with respect to the input parameter near the reference point. In general, a response surface (i.e., the behavior of the result as a function of input parameters) can be constructed by assembling the calculated results from repetitive runs of the computer code with varied input parameters. Sensitivities of the result to input parameters can then be derived from the response surface. For example, Dickens and Lennox[16] performed a sensitivity analysis on the problem of transient, two-dimensional transport of contaminants in a steady saturated groundwater flow system, which was simulated by the Galerkin finite-element

method. The simulation was repeated by varying the input value of the dispersivity while holding other parameters fixed at their reference values.

This conventional sensitivity analysis method has two disadvantages: (1) the calculated sensitivity of the result to a parameter depends on the variation range of the parameter value in the vicinity of the reference data point and (2) this method requires a large number of time-consuming calculations and hence is very expensive for a large computer simulation code such as the radionuclide transport code. To remedy the situation just outlined, a more advanced sensitivity analysis methodology is desirable to address the sensitivity problems for the radionuclide transport by groundwater flow.

A general sensitivity analysis methodology has been widely and successfully applied to some reactor engineering design work over the past several years.[33-40] Oblow[34] has developed the general sensitivity theory based on the differential formulation to address the sensitivity analysis for the radiation transport problems and reactor thermal-hydraulic problem. Williams,[41] in his dissertation, has developed a perturbation and sensitivity theory for the nonlinear reactor fuel burnup equation describing the time-dependent behavior of the neutron and nuclide fields in a reactor core. The adjoint equations were derived using a variational principle technique described by Pomraning[39] and Stacy.[40] The sensitivity theory to be developed for the numerical simulation of the radionuclide transport by groundwater flow has some analogy with that for reactor burnup analysis. The radionuclide concentration field in the radionuclide transport equation

is analogous to the nuclide field in the burnup equations for the case of uncoupled approximation. And responses of interest (the calculated results) for both cases are final-time functionals of the radionuclide fields.

C. Objectives

The objectives of this dissertation are stated as follows:

1. To develop a transient, two-dimensional radionuclide transport computer code by employing the discrete-element numerical method to simulate the transport of radionuclides in a saturated-unsaturated groundwater flow system.
2. To derive the adjoint equation for the radionuclide transport equation based on generalized perturbation theory.
3. To formulate and compute the relative sensitivity coefficients of responses to the input parameters.
4. To validate the sensitivity theory by comparing the sensitivity results obtained from both the perturbation prediction and direct calculation.

D. Scope of Text

Chapter II is devoted to the description of the Galerkin finite-element model to be used for the simulation of groundwater flow transport, and the development and implementation of a transient, two-dimensional discrete-element numerical model for the transport of radionuclides by groundwater flow. Chapter III contains the description of the transient, two-dimensional computer simulations of the

radionuclide transport by groundwater flow for a hypothetical sample problem by using the computer code developed in Chapter II. The results of the simulations will be presented as contour plots. In Chapter IV, the general sensitivity theory will be developed for the radionuclide transport equation, based on the perturbation theory of the variational principle approach. The adjoint transport equation will be derived and sensitivity coefficients, uncertainty equations formulated. Chapter V contains the solutions of the adjoint transport equation, presentation and interpretation of the solutions. The implementation of the relative sensitivity coefficients calculations will be presented in Chapter VI. Comparisons of the sensitivities results obtained from the direct calculations and the general sensitivity method will be given in Chapter VII, along with some discussions of the results. Finally, Chapter VIII contains the conclusion and recommendations for future work.

CHAPTER II

GROUNDWATER TRANSPORT MODELS

A. Introduction

In this chapter, we shall examine the mathematical models which will be used to simulate the groundwater transport in the porous media. Two mathematical models have been formulated and their numerical models employed for simulations of radionuclide transport as well as sensitivity calculations. They are (1) groundwater flow transport model and (2) radionuclide transport model. The groundwater flow transport model will provide the necessary groundwater flow information for a given hydrological condition. Then the computed groundwater flow data can be utilized by the radionuclide transport model to compute the time-dependent radionuclide concentration distribution in the associated groundwater flow system. The development of the radionuclide transport model by discrete-element numerical formulation will be presented in detail in this chapter.

First consider a typical physical model for a radioactive wastes burial trench. There are three basic conditions which must all occur before the radionuclide source can be produced in the waste burial trench. These conditions are (1) water must enter the waste burial trench, (2) the water must come in contact with the radioactive waste, and (3) the radionuclides must leach out of the waste material. It is assumed that these three conditions occur. As a result, the radioactive

contaminants dissolved in the water inside the trench will begin to seep through the bottom of the burial trench and will be transported within the saturated-unsaturated porous media toward the discharge locations such as a nearby river or a well. The radionuclides will then become accessible to the biosphere after they have passed through the discharge surfaces. The purposes of an environmental impact statement of the radioactive wastes disposal problem are composed of (1) the prediction of time-dependent radionuclide concentration distributions in the groundwater flow system, and (2) the estimation of radiological doses to man calculated from the discharge rate (μCi/day) passing through the discharge (outflow) boundary. We will first address the groundwater flow transport model which will be utilized to obtain the groundwater flow field.

B. Groundwater Flow Transport

Although there are a number of numerical models for groundwater flow transport,[2-8] a transient, two-dimensional model for groundwater flow transport through saturated-unsaturated porous media developed by Reeves and Duguid at the Oak Ridge National Laboratory was used. One governing equation for groundwater flow transport through saturated-unsaturated porous media was formulated by combining equations of (1) continuity of the fluid, (2) continuity of the solid, (3) motion of the fluid, (4) consolidation for the medium, and (5) state for the compressibility of water. The air phase has been assumed to be

continuous and is at atmospheric pressure. After some derivations the governing equation is finally reduced to:

$$F \frac{\partial H}{\partial t} = \nabla \cdot \overline{\overline{K}} \nabla H \qquad (2.1)$$

where F represents a generalized storage constant and is defined as

$$F = \frac{\theta}{n}\alpha' + \theta\beta' + \frac{d\theta}{dh}, \qquad (2.2)$$

and $H = h + z$,

H = hydraulic head,

h = pressure head,

z = elevation relative to an arbitrary datum,

θ = volumetric water content,

n = porosity,

α' = modified coefficient of compressibility of the medium,

β' = modified coefficient of compressibility of water,

$\overline{\overline{K}}$ = hydraulic conductivity tensor.

The water content, porosity and the hydraulic conductivity are all functions of space and pressure head. Equation 2.1 is therefore in general nonlinear because the soil properties F and $\overline{\overline{K}}$ depend on pressure head h. Note that Equation 2.1 is valid for both saturated and unsaturated flow.

The transient, two-dimensional groundwater flow transport model developed by Reeves and Duguid was used to solve Equation 2.1. This model was formulated and implemented using quadrilateral finite elements for geometrical configuration, bilinear Galerkin interpolation for

spatial integration and Gaussian elimination for the solution of the resulting matrix equations. Since Equation 2.1 is highly nonlinear in the soil property F and $\overline{\overline{K}}$, a soil-properties iteration loop is necessary to attain a converged solution. The computer code is capable of having different kinds of boundary conditions including the constant-flux, constant-head, and pressure-dependent boundary conditions. The computer code was first employed to solve Equation 2.1 for the pressure head field in the groundwater flow system region. Then the Darcian velocity field and the water content field were computed from the solution (pressure head field) and the hydraulic conductivity of the porous medium. From Darcy's law, the Darcian velocity field was calculated by using the following equation.

$$\overline{v} = - \overline{\overline{K}} \cdot \nabla H \tag{2.3}$$

where $\overline{\overline{K}}$ is the hydraulic conductivity tensor evaluated by interpolating the specific curve of hydraulic conductivity vs pressure at the calculated pressure head. The water content was calculated by interpolating the water content vs pressure at the calculated pressure head.

In general, the groundwater flow transport is a transient hydrodynamic problem because the boundary conditions are time-dependent. For example, the water flux seeping through the bottom of the trench can be a function of time or the water depth in the burial trench may vary with time. In addition, the precipitation rate is also a function of time. As a result, time-dependent groundwater flow fields are computed, which in turn will be used as the input data in the radionuclide transport simulation. Nevertheless, a steady-state groundwater flow transport

calculation, a less complicated case was performed in this study to provide the groundwater flow data needed in the radionuclide transport model. As suggested by Pinder,[13] inasmuch as there has been no net water table elevations (for example, no sudden heavy rainfall) in the region of interest, a steady-state groundwater flow pattern can be considered adequate for the radionuclide transport simulation.

For a steady-state groundwater flow, Equation 2.1 is reduced to

$$\nabla \cdot \bar{\bar{K}} \nabla H = 0 \ . \tag{2.4}$$

From Equation 2.3, Equation 2.4 becomes

$$\nabla \cdot \bar{v} = 0 \tag{2.5}$$

which is the continuity equation for steady-state groundwater flow motion. The calculation of a steady-state groundwater flow field will be performed (Chapter III) for a sample problem by using the Galerkin finite-element numerical model.

C. Radionuclide Transport Model

The mathematical model for the transport of radionuclides by groundwater flow through porous media is considered in this section. The transport of dissolved radionuclides by groundwater flow is governed by such mechanisms as convective transport, hydrodynamic dispersion, chemical interaction between radionuclides and porous media, and radioactive decay. The governing equation of the contaminant transport model has been formulated and solved numerically by many investigators.[12-17] For example, Bredehoeft and Pinder[12] presented the

formulation and numerical solution of mass transport equation for a specific saturated isothermal groundwater flow system. The radionuclide transport equation used in our study is based on the one formulated by Duguid and Reeves.[15] This model encompasses the convective transport, hydrodynamic dispersion of a dissolved radionuclide carried by the fluid phase, chemical adsorption, and radioactive decay. The adsorption of radionuclide by the solid is assumed to occur at a rapid rate (i.e., a fast exchange reaction) such that the dissolved material in the carrier is in equilibrium with the material adsorbed by the solid. The concentration of the dissolved radionuclide is assumed to be sufficiently small that changes in concentration do not affect transport of the fluid. We further assume that transport of different radionuclides in the porous medium are completely independent so that the transport simulation of different radionuclides can be performed one at a time.

Consider an arbitrary material volume element of saturated-unsaturated porous medium. The volume element is composed of fluid and solid. After excercising the physical principle of mass conservation to the radionuclide transport in the volume element and making some approximations, the governing transient radionuclide transport equation is derived to be

$$\theta R_d \frac{\partial C}{\partial t} = \nabla \cdot \bar{\bar{D}} \nabla C - \nabla \cdot \bar{v} C - \left(R_d \frac{\partial \theta}{\partial t} + \alpha' \theta R_d \frac{\partial h}{\partial t} + \lambda \theta R_d\right) C \qquad (2.6)$$

where

C = space-time-dependent radionuclide concentration in $\mu Ci/cm^3$,

R_d = $1 + \rho k_d/n$ = retardation factor, dimensionless,

ρ = bulk density of the solid,

k_d = distribution coefficient of the medium for the radionuclide being carried by the fluid, defined as the ratio of quantity of adsorbed material per mass of solid to quantity of dissolved material per volume of fluid, cm^3/g,

λ = radioactive decay constant, and

$\overline{\overline{D}}$ = hydrodynamic dispersion coefficient tensor.

Note that those parameters that are pertaining to groundwater flow transport equation have previously been defined.

In a homogeneous medium which is assumed to be isotropic with respect to dispersivity, the element of D can be written as

$$D_{ij} = a_T v \delta_{ij} + (a_L - a_T)\, v_i v_j / v + a_m \tau \delta_{ij} \qquad (2.7)$$

where i,j are indices of components in the rectangular coordinate system, δ_{ij} is the Kronecker delta, a_L is the longitudinal dispersivity, a_T is the transverse dispersivity, a_m is the molecular diffusion coefficient, τ is the tortuosity, v_i, v_j are components of hydraulic velocity, and v is the magnitude of the velocity.

For a steady-state groundwater flow, θ, h are independent of time. Equation 2.6 is then reduced to

$$R_d \theta \frac{\partial C}{\partial t} = \nabla \cdot \overline{\overline{D}} \nabla C - \nabla \cdot \overline{v} C - R_d \theta \lambda C \,. \qquad (2.8)$$

The steady-state Darcian velocity field $\overline{v}$ and water content field θ were computed from the solution of the steady-state groundwater flow

transport equation. Equation 2.8 is the governing equation for the radionuclide transport simulation considered in the next chapter.

Before Equation 2.8 can be solved for a specific radionuclide transport problem, the appropriate initial and boundary conditions must be specified and the input parameter data must be given for the problem. The initial conditions can be either that no radionuclide concentrations are in the system region or that a known concentration field exists prior to the start of the simulation. The former case will be assumed, that is, no radioactive waste is present in the system region at the initial time when the radioactive waste was first deposited in the burial trench. The boundary conditions for the radionuclide transport are determined by the flow conditions on the boundaries from the groundwater flow transport simulation. For example, the boundary surface where water is flowing into the system from outside (e.g., water seeping through the bottom of the trench into porous medium) is characterized as inflow boundary. The boundary surface where water is flowing out of the system is called outflow boundary.

As was mentioned in Chapter I, the discrete-element numerical simulation model will be developed in this dissertation to simulate the transport of radionuclides by groundwater flow. In the formulation of this simulation model, the numerical method, FLIDE (FLuid-In-Discrete-Element) was evolved from the methods of PIC[30] (Particle-In-Cell) by Evans and Harlow, MAC[30] (Marker And Cell) by Harlow and Welch, and FLIC[30] (FLuid-In-Cell) by Gentry, Martin and Daly. The formulation of the radionuclide transport model by the FLIDE method is based on the control volume approach, which results in the necessary computational

system of difference equations by applying the macroscopic conservation forms of mass, momentum and energy principles for a cell of rectangular enclosure surfaces. The region of interest (also called system region hereafter) is divided into a sufficient number of cells which span the entire system region, and then the conservation principles are carried out for each cell at each time step.

Five phases of the computational procedure in the formulation of the FLIDE numerical model are presented as follows:

(a) Computational element discretization in the system region:

First of all, the system region of saturated-unsaturated porous media with groundwater flowing through it is partitioned into an appropriate number of rectangular discrete elements of arbitrary size. The system region is usually confined by the boundary surface (or the boundary line in two-dimensional case) which may consist of the ground surface, the bottom of the burial trench, impermeable bottom boundary such as the interface of the porous medium with bedrock, slope surface, and stream interface boundary. The domain of the system region depends upon the flow information. Usually the region for the radionuclide transport simulation is the same as that for the groundwater flow transport. Once a flow region is specified in the groundwater flow model and the flow information is obtained on the boundary by solving the flow transport equation, the same region will be used in the radionuclide transport model. The size of each discrete element is determined by the concentration importance in different areas of the system region. For instance, finer elements are appropriate near the

outflow boundary across which radionuclides become accessible to the biosphere. After the discrete-element grid system has been constructed by drawing lines parallel to x- and z-axes throughout the system region, element type (interior, boundary, external) is assigned to each element and the region values of element x-, z-enclosure dimensions, element area for each element are calculated.

(b) Input data preparation:

There are three kinds of input data that need to be prepared for the radionuclide transport simulation by FLIDE method. They are (1) geometric region data, (2) groundwater flow data, and (3) input parameter data.

The geometric region data consist of the associated data for interior, boundary and external discrete elements. External discrete elements are not used in calculation. Two typical 2-D interior and boundary elements are shown schematically in Figure 2.1. The interior element has two enclosure lengths in x and z directions. The boundary element contains four enclosures. Each of the enclosures is assigned an enclosure-type identification number depending on the type of the discrete element with which the enclosure interfaces. The enclosure type consists of interior enclosure, close enclosure (impermeable boundary), and open enclosure (either inflow or outflow boundary). Each enclosure has its length as shown in Figure 2.1.

The groundwater flow data consist of the volumetric groundwater flow rates $G_{x_{i,k}}$, $G_{z_{i,k}}$ at the interfacing enclosures between any two adjacent discrete elements. For example, $G_{x_{i,k}}$ is the water flow rate

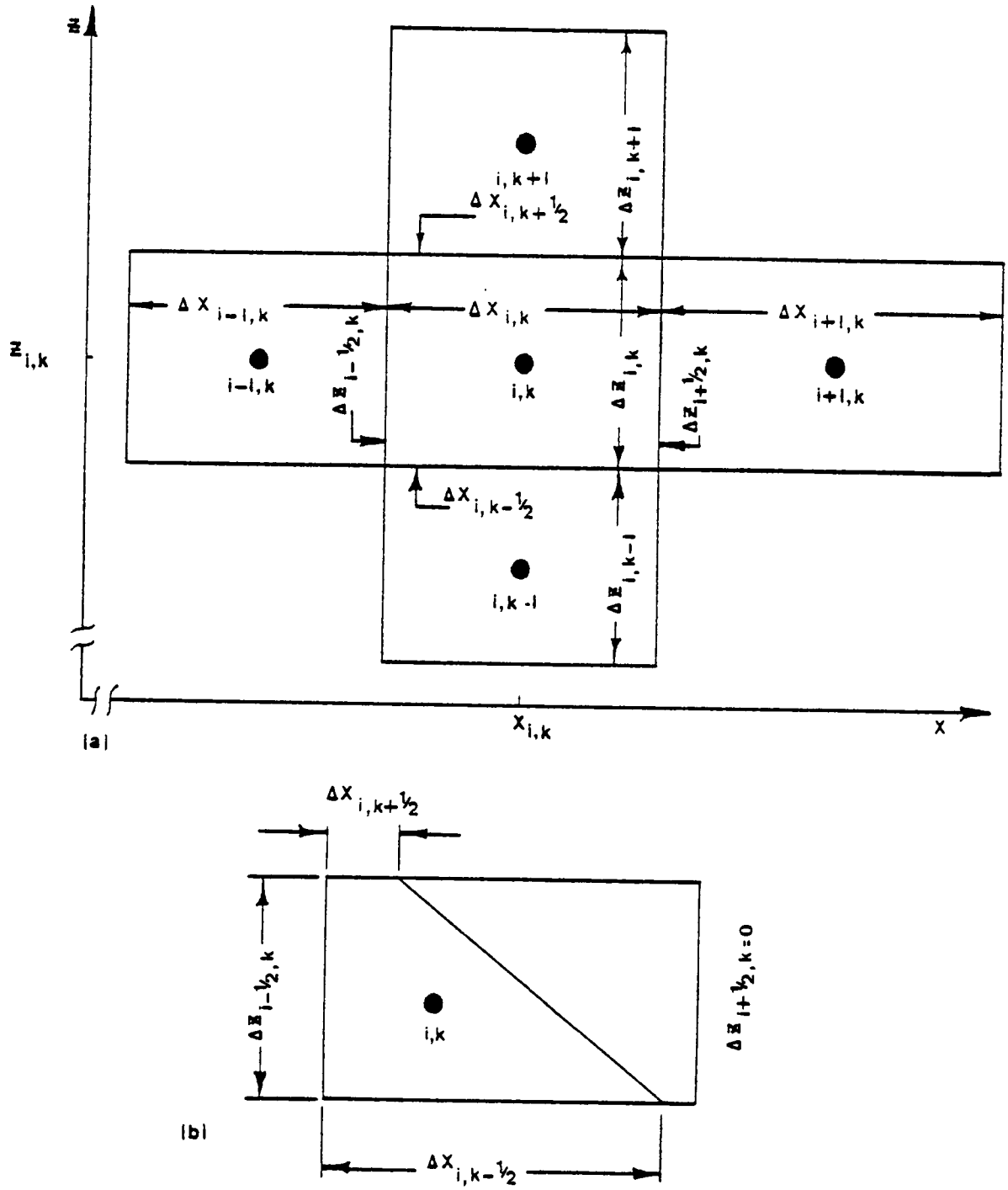

Figure 2.1. Geometrical Configuration of Discrete Elements for the FLIDE Method, (a) Interior Element and Its Adjacent Elements, (b) Boundary Element.

evaluated at the interfacing enclosure $(i+1/2,k)$ between the discrete elements (i,k) and $(i+1,k)$; and $G_{z_{i,k}}$ is the flow rate evaluated at the interfacing enclosure $(i,k+1/2)$ between the discrete elements (i,k) and $(i,k+1)$. Boundary elements have boundary water flow rates on the boundary lines. For example, $G_{xb_{i,k}}$ represents the boundary flow rate evaluated on the boundary enclosure $(i+1/2,k)$. If it is an outflow boundary line, a positive outgoing water flow rate $G_{xb_{i,k}}$ is specified. If it is an inflow boundary line, a negative $G_{xb_{i,k}}$ is specified. The water flow rate on a close boundary is zero. Having the water flow rate data described above, we can calculate the element-center velocities by the following equations:

$$v_{x_{i,k}} = \frac{1}{2}\left(\frac{G_{x_{i-1,k}}}{\Delta z_{i-1/2,k}} + \frac{G_{x_{i,k}}}{\Delta z_{i+1/2,k}}\right), \tag{2.9}$$

$$v_{z_{i,k}} = \frac{1}{2}\left(\frac{G_{z_{i,k-1}}}{\Delta x_{i,k-1/2}} + \frac{G_{z_{i,k}}}{\Delta x_{i,k+1/2}}\right). \tag{2.10}$$

Finally, input parameter data consist of values for longitudinal, transverse dispersivities, retardation factor determined by Equation 2.6, and radioactive decay constant for the specified radionuclide.

(c) Formulation of FLIDE computational equations:

We now begin to formulate the computational equations for the radionuclide transport equation based on the FLIDE numerical method. Refer to the schematic representation of the flow and radionuclide transport in a discrete element shown in Figure 2.2 In the formulation of the two-dimensional FLIDE method, the control volume is a rectangular

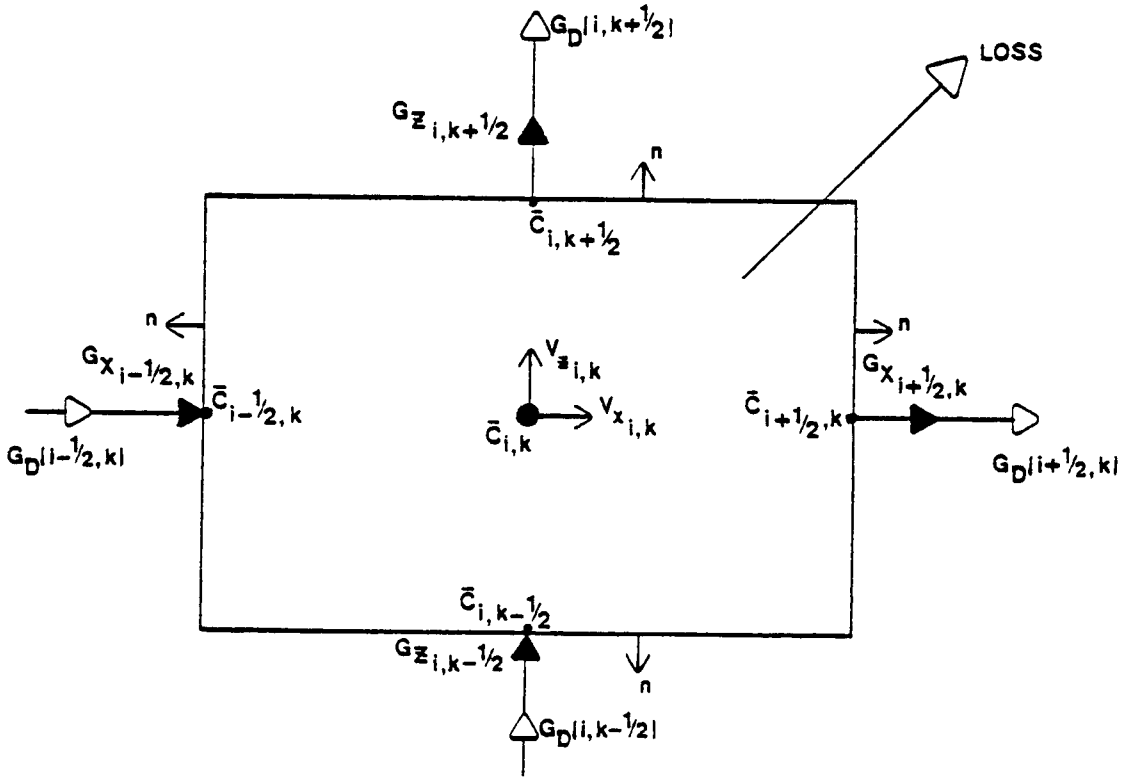

Figure 2.2. Schematic Representation of the Flow and Radionuclide Transport in a Discrete Element.

discrete element on x-z plane with unit width in y direction. Taking a volume integral on Equation 2.8 over a control volume V gives:

$$\int_V R_d\theta(\bar{r})\frac{\partial C(\bar{r},t)}{\partial t}\,d\bar{r} = \int_V \nabla\cdot\bar{\bar{D}}(\bar{r})\nabla C(\bar{r},t)d\bar{r} - \int_V \nabla\cdot\bar{v}(\bar{r})C(\bar{r},t)d\bar{r}$$

$$-\int_V R_d\theta(\bar{r})\lambda C(\bar{r},t)d\bar{r}\ . \qquad (2.11)$$

Consider each volume integral in Equation 2.11 for the control volume of a two-dimensional discrete element (i,k) as shown in Figure 2.2. The left-hand side of Equation 2.11 becomes

$$\int_V R_d\theta(\bar{r})\frac{\partial C(\bar{r},t)}{\partial t}\,d\bar{r} = R_d\bar{\theta}_{i,k}\frac{\partial \bar{C}_{i,k}(t)}{\partial t}\Delta A_{i,k} \qquad (2.12)$$

where $\bar{\theta}_{i,k}$ and $\bar{C}_{i,k}(t)$ represent the volume-average water content and time-dependent radionuclide concentration evaluated at the center of the discrete element, and $\Delta A_{i,k}$ is the area of the element.

The first term on the right-hand side of Equation 2.11 is the radionuclide transport rate in the control volume due to the hydrodynamic dispersion. This term will be represented by DISPERSION hereafter. Using the divergence theorem, the dispersion transport term can be changed from volume integral to surface integral as follows:

$$\text{DISPERSION} = \int_V \nabla\cdot\bar{\bar{D}}(\bar{r})\nabla C(\bar{r},t)d\bar{r} = \int_A \hat{n}\cdot\bar{\bar{D}}(\bar{r})\nabla C(\bar{r},t)d\bar{r}$$

$$= -\int_A \hat{n}\cdot\bar{q}_D(\bar{r},t)d\bar{r} \qquad (2.13)$$

where

$$\bar{q}_D(\bar{r},t) = -\bar{\bar{D}}(\bar{r})\nabla C(\bar{r},t), \qquad (2.14)$$

is the dispersive transport flux at space $\bar{r}$ and time t, and $\hat{n}$ is the outwardly directed normal unit vector on the surface A.

There are four enclosure surfaces with unit width in y-direction for a 2-D rectangular discrete element. They are designated as enclosure $(i-\frac{1}{2},k)$, $(i+\frac{1}{2},k)$, $(i,k-\frac{1}{2})$, and $(i,k+\frac{1}{2})$. The dispersive transport term is equal to the sum of the four dispersive transport rates on the four enclosures. As can be seen from Equation 2.14, the dispersive transport flux is due to the concentration gradient. On the enclosures perpendicular to x-axis, $(i-\frac{1}{2},k)$ and $(i+\frac{1}{2},k)$, we assume that we only have concentration gradient $\partial C/\partial x$ in x-direction. And we only have concentration gradient $\partial C/\partial z$ in z-direction on the enclosures $(i,k-\frac{1}{2})$ and $(i,k+\frac{1}{2})$. Since we only have dispersive transport flux on each enclosure due to the concentration gradient in the direction perpendicular to that enclosure in the FLIDE formulation, Equation 2.13 can be expressed as

$$\text{DISPERSION} = (q_{D_x}(t)\,\Delta z \Big|^{*}_{(i-\frac{1}{2},k)} - (q_{D_x}(t)\,\Delta z \Big|_{(i+\frac{1}{2},k)} + (q_{D_z}(t)\,\Delta x \Big|_{(i,k-\frac{1}{2})} - (q_{D_z}(t)\,\Delta x \Big|_{(i,k+\frac{1}{2})} \qquad (2.15)$$

---

*($\Big|_{(i-\frac{1}{2},k)}$ represents the quantity between the left parenthsis and the vertical bar is to be evaluated on the enclosure $(i-\frac{1}{2},k)$.

where the dispersive transport fluxes in x and z directions are

$$q_{D_x}(t) = -D_{xx} \frac{\partial C(\bar{r},t)}{\partial x} , \tag{2.16}$$

and

$$q_{D_z}(t) = -D_{zz} \frac{\partial C(\bar{r},t)}{\partial z} . \tag{2.17}$$

D_{xx} and D_{zz} are the principal elements in the hydrodynamic dispersion coefficient tensor $\bar{\bar{D}}(\bar{r})$ and can be evaluated by Equation 2.7.

Equation 2.15 can be regarded as the net dispersive transport mass flow rate passing through the four enclosures, i.e.,

$$\text{DISPERSION} = G_D(i-1/2,k) - G_D(i+1/2,k) + G_D(i,k-1/2) - G_D(i,k+1/2) . \tag{2.18}$$

Assuming first order approximation at the half-points (i.e., on the enclosures), we have the following dispersive transport flow rates:

$$G_D(i-1/2,k) = -D_{xx}(i-1/2,k) \frac{\bar{C}_{i,k} - \bar{C}_{i-1,k}}{\Delta x_{i-1/2,k}} \Delta z_{i-1/2,k} , \tag{2.19}$$

$$G_D(i+1/2,k) = -D_{xx}(i+1/2,k) \frac{\bar{C}_{i+1,k} - \bar{C}_{i,k}}{\Delta x_{i+1/2,k}} \Delta z_{i+1/2,k} , \tag{2.20}$$

$$G_D(i,k-1/2) = -D_{zz}(i,k-1/2) \frac{\bar{C}_{i,k} - \bar{C}_{i,k-1}}{\Delta z_{i,k-1/2}} \Delta x_{i,k-1/2} , \tag{2.21}$$

$$G_D(i,k+1/2) = -D_{zz}(i,k+1/2) \frac{\bar{C}_{i,k+1} - \bar{C}_{i,k}}{\Delta z_{i,k+1/2}} \Delta x_{i,k+1/2} . \tag{2.22}$$

The time variable was suppressed for notation simplicity. The dispersion coefficients at the half-points are:

$$D_{xx}(i\pm 1/2,k) = [(a_L v_x^2 + a_T v_z^2)/v + a_m \tau]_{(i\pm 1/2,k)}, \tag{2.23}$$

$$D_{zz}(i,k\pm 1/2) = [(a_T v_x^2 + a_L v_z^2)/v + a_m \tau]_{(i,k\pm 1/2)}. \tag{2.24}$$

The x, z components and the magnitude of the Darcian velocity are evaluated at the center of each associated enclosure, and are calculated by the linear interpolation between the velocity values at two adjacent element centers. The dispersive transport term can thus be determined from Equations 2.18 through 2.24.

Now let us examine the second integral term on the right-hand side of Equation 2.11. This term gives the net convective transport flow rate in the control volume and will be represented by CONVECTION because it accounts for the convection of the radionuclide concentration in the control volume. The divergence theorem is employed again to change the convective term to surface integral:

$$\text{CONVECTION} = -\int_V \bar{v}(\bar{r})C(\bar{r},t)d\bar{r}$$

$$= \int_A \hat{n} \cdot [-\bar{v}(\bar{r})C(\bar{r},t)]d\bar{r} \ . \tag{2.25}$$

For a control volume of a 2-D discrete element having four enclosures, the convection term becomes:

$$\text{CONVECTION} = G_{x_{i-1/2,k}}\bar{C}_{i-1/2,k} - G_{x_{i+1/2,k}}\bar{C}_{i+1/2,k} +$$

$$G_{z_{i,k-1/2}}\bar{C}_{i,k-1/2} - G_{z_{i,k+1/2}}\bar{C}_{i,k+1/2} \tag{2.26}$$

where $G_{x_{i-1/2,k}}$, $G_{x_{i+1/2,k}}$, $G_{z_{i,k-1/2}}$, and $G_{z_{i,k+1/2}}$ represent the volumetric water flow rates passing through the corresponding enclosures. Water flow rates passing through the enclosures of all the discrete elements were computed from the steady-state groundwater flow transport model and are the input data to the present model.

Before the formulation for the convective transport term can be completed, the half-point values of concentration, i.e., $\overline{C}_{i-1/2,k}$, $\overline{C}_{i+1/2,k}$, $\overline{C}_{i,k-1/2}$, and $\overline{C}_{i,k+1/2}$ must be evaluated in terms of the mean concentrations at the centers of the discrete elements, which are the solutions of the radionuclide transport equation. One must note how to evaluate the half-point concentration values because the stability of the numerical methods, particularly the explicit ones, critically depends upon the forms of the convective term.[24] Roache[30] pointed out that the mass conservation property and the flow transportive property must be satisfied in order to obtain an accurate simulation for a computational fluid dynamic problem. The most successful form, from the computational point of view, for eliminating the half-point values in terms of the solution values (mean values in the discrete elements), is the "second upwind differencing" method. This particular form, which is based more on physical reasoning about fluid flow conditions than on rigorous mathematical derivations, possesses both the conservative and transportive properties for the explicit finite difference formulations of conservation equations. This method has proven to be very dependable from numerical stability considerations.

The second upwind differencing forms for the half-point concentration values are expressed as follows:

$$\bar{C}_{i-1/2,k} = \begin{cases} \bar{C}_{i,k} & \text{for } G_{x_{i-1/2,k}} < 0 \\ \bar{C}_{i-1,k} & \text{for } G_{x_{i-1/2,k}} > 0 \end{cases}, \tag{2.27}$$

$$\bar{C}_{i+1/2,k} = \begin{cases} \bar{C}_{i+1,k} & \text{for } G_{x_{i+1/2,k}} < 0 \\ \bar{C}_{i,k} & \text{for } G_{x_{i+1/2,k}} > 0 \end{cases}, \tag{2.28}$$

$$\bar{C}_{i,k-1/2} = \begin{cases} \bar{C}_{i,k} & \text{for } G_{z_{i,k-1/2}} < 0 \\ \bar{C}_{i,k-1} & \text{for } G_{z_{i,k-1/2}} > 0 \end{cases}, \tag{2.29}$$

$$\bar{C}_{i,k+1/2} = \begin{cases} \bar{C}_{i,k+1} & \text{for } G_{z_{i,k+1/2}} < 0 \\ \bar{C}_{i,k} & \text{for } G_{z_{i,k+1/2}} > 0 \end{cases}. \tag{2.30}$$

The final form of the convective transport term is obtained by substituting Equations 2.27 through 2.30 into 2.26.

The last term in Equation 2.11 is the radionuclide loss in the discrete element due to the radioactive decay. The radioactive decay loss is proportional to the concentration in the discrete element, which can be represented by the mean concentration at the element center $\bar{C}_{i,k}$. Therefore the formulation of the loss term due to radioactive decay by the FLIDE method is

$$\begin{aligned} \text{LOSS} &= -\int_V R_d \lambda \theta(\bar{r}) C(\bar{r},t) d\bar{r} \\ &= -R_d \lambda \bar{\theta}_{i,k} \bar{C}_{i,k} \Delta A_{i,k} \, . \end{aligned} \tag{2.31}$$

Assembling the FLIDE forms for the terms in Equation 2.11, we can write a difference equation for the rate of change of the mean concentration $\bar{C}_{i,k}$ in the discrete element (i,k) in terms of the mean concentrations, input flow rate data and system parameters. Substituting Equations 2.12, 2.18, 2.26, and 2.31 into Equation 2.11 and dividing both sides by $R_d\bar{\theta}_{i,k}\Delta A_{i,k}$, the final simulation form of radionuclide transport equation for an arbitrary discrete element (i,k) by the FLIDE method becomes

$$\frac{\partial \bar{C}_{i,k}}{\partial t} = \left[\frac{1}{R_d\bar{\theta}_{i,k}\Delta A_{i,k}} \left(G_D(i-1/2,k) - G_D(i+1/2,k) + G_D(i,k-1/2) - G_D(i,k+1/2)\right)\right]$$

$$+ \left[\frac{1}{R_d\bar{\theta}_{i,k}\Delta A_{i,k}} \left(G_{x_{i-1/2,k}}\bar{C}_{i-1/2,k} - G_{x_{i+1/2,k}}\bar{C}_{i+1/2,k}\right.\right.$$

$$\left.\left. + G_{z_{i,k-1/2}}\bar{C}_{i,k-1/2} - G_{z_{i,k+1/2}}\bar{C}_{i,k+1/2}\right)\right] - \left[\lambda\bar{C}_{i,k}\right] \qquad (2.32)$$

for all interior and boundary discrete element (i,k), where $G_D(i-1/2,k)$, etc., $\bar{C}_{i-1/2,k}$, etc. are taken from Equations 2.19-2.24 and 2.27-2.30, respectively. Equation 2.32 is the system equation for solving the radionuclide transport equation by the FLIDE method. The time rate of change of the mean radionuclide concentration in the discrete element is equal to the sum of the dispersive transport rate, convective transport rate and the radioactive decay loss rate. Before we can solve the system of differential equations as formulated by Equation 2.32, the initial and boundary conditions need to be addressed.

(d) Initial and boundary conditions

The solution of a partial differential equation in space and time requires the specifications of the initial and boundary conditions. For the system of coupled, ordinary, first-order differential equations in time, represented by Equation 2.32, the initial conditions were specified at any arbitrarily assigned time t_0 for all the discrete elements in the system region, that is,

$$\bar{C}_{i,k}(t_0) = \bar{C}_{0_{i,k}}, \text{ for all } i,k \ . \tag{2.33}$$

Either zero initial conditions, assuming that the system region contains no radionuclides, or a known radionuclide concentration distribution at the initial time t_0 can be used. In this study, zero initial conditions were used.

In the formulation of the FLIDE method, the discrete element on the boundary may take any geometrical configuration with a straight boundary line across any two enclosures in order to closely approximate the real boundary configuration of the system region. Note that the boundary conditions are normally specified at the discrete-element enclosures of the physical and imaginary boundaries in the system region. The physical boundaries are such as the ground surface geometry, burial trench configuration, and the river-pore interface geometry. The physical boundary is also based on the geological consideration such as the impermeable boundary which interfaces the porous medium with a impervious medium such as bedrock. In order to deal with a finite region, some imaginary boundaries in the underground region must be specified

from a practical computational consideration. Usually, the geometry of the system region for the radionuclide transport problem is in conformity with the groundwater flow transport problem. That is, both transport problems share the same boundary. And the boundary characteristics are determined by the flow condition on the boundary obtained from the simulation of the groundwater flow transport model. The relevant boundary conditions specified on the half-point enclosures of boundary elements are categorized into the following three types:

(1) Close boundary: This is also known as impermeable boundary. In a realistic situation, there might be a region full of impervious material such as clay or bedrock that no groundwater can flow through it. The interface between the porous medium and the impervious medium is then specified as the close boundary. Therefore, there is no radionuclide transfer across the enclosure of the boundary element which corresponds to the section of the close boundary. For example, the boundary conditions for the groundwater flow rate and the concentration at the close boundary enclosure $(i,k-1/2)$ of discrete element (i,k) are

$$G_{z_{i,k-1/2}} = 0, \ \bar{C}_{i,k-1/2} = \bar{C}_{i,k} \ . \tag{2.34}$$

(2) Inflow boundary: The inflow boundary is characterized by the flow condition on the physical or imaginary boundary where water is flowing from the outside region into the system region. Examples of the inflow boundary are such as (1) source seepage surface, (2) ground surface, and (3) imaginary boundary that separates the system region from the outside region where water inflow rate is known. The source

seepage surface is the bottom surface of the burial trench through which the radionuclides dissolved in the water infiltrate. The ground surface may become the inflow boundary as well because precipitation may fall on the ground surface and percolate into the groundwater flow system. For the case of a steady-state groundwater flow system, the inflow boundary remains inflow boundary because the water flow direction does not change with time. The water flow rate on the inflow boundary was determined from the simulation of the steady-state groundwater flow transport. We only need to specify the half-point values for the radionuclide concentration on the inflow boundary.

In the formulation of the FLIDE method, the second upwind differencing technique requires that the "upstream" values of the system variable (i.e., concentration in this case) be used as the enclosure values in the boundary elements to evaluate the convective term. Therefore, it is essential to know the mean concentration values as a function of time in the additional imaginary discrete elements just outside the inflow boundary elements. Usually it is assumed that the homogeneous concentration of the radionuclide dissolved in the water of the burial trench is known. However, the evaluation of the radionuclide concentration as a function of time inside the burial trench is quite a complex process[11] and is beyond the scope of this dissertation. We simply assume that the radionuclide concentration in the burial trench can be represented by a box-car function of time with known source concentration and source duration. For example, if discrete element (i,k) is an inflow boundary element located beneath the source seepage surface

with the enclosure $(i,k+1/2)$ being part of the bottom of the burial trench, then the concentration in the additional imaginary element $(i,k+1)$ is

$$C_{i,k+1} = \begin{cases} C_S, & \text{for } t \leq T_D \\ 0, & \text{for } t > T_D \end{cases} \tag{2.35}$$

where C_S is the source concentration, and T_D is the source depletion time. Both are input data.

With regard to the boundary condition in concentration on the inflow boundary other than the source seepage boundary, such as an imaginary inflow boundary crossing an aquifer, zero concentration outside that boundary is assumed because we assume that the source seepage boundary is the only boundary through which the radionuclide can enter into the system region.

(3) Outflow boundary: The outflow boundary is determined by the flow condition on the boundary where the groundwater is flowing out of the system region. From the steady-state flow rates obtained from the groundwater flow transport calculation, the portion of the system boundary where the flow rate is directed outward is specified as the outflow boundary. The outflow boundary may include a slope portion of the ground surface through which the groundwater may seep out of the system, or a river interface surface through which the groundwater may also discharge into the river.

It is very difficult to specify the boundary condition in concentration on the outflow boundary, for the numerical experiences have shown that catastrophic instabilities may propagate upstream from the

outflow boundary and destroy the solution.[30] The computational outflow boundary condition should be specified in such a way to best simulate the real condition near and on the outflow boundary that interfaces two different media.

The second upwind differencing formulation for the convective term does not require the specification of the concentrations in the discrete elements outside the outflow boundary. However, the concentrations external to the outflow boundary elements are required to evaluate the concentration gradients for the dispersion term. There is no way to guess what these "artificial" concentrations may be. We cannot specify zero concentrations as the ambient conditions because this will cause very high concentration gradient near the outflow boundary. As a result, it would produce unrealistic results and the solutions would become extremely sensitive to the dimensions of the outflow boundary elements.

Since the main contribution to the radionuclide flux passing through the outflow boundary comes from the convective term, it is assumed that the dispersive term or the concentration gradient components in x and z directions vanish, that is,

$$\hat{n} \cdot \overline{\overline{D}} \nabla C(\bar{r},t) = 0, \ \bar{r} \text{ on the outflow boundary,} \tag{2.36}$$

or

$$\frac{\partial C(x,z,t)}{\partial x} = 0, \ \frac{\partial C(x,z,t)}{\partial z} = 0 \text{ on the outflow boundary.} \tag{2.37}$$

For example, in the discrete element formulation, we have outflow boundary element (i,k) with (i+1,k) and (i,k+1) the external elements

adjacent to the boundary element, the boundary conditions specified by Equation 2.37 are equivalent to:

$$\overline{C}_{i+1,k}(t) = \overline{C}_{i,k}(t), \tag{2.38}$$

and

$$\overline{C}_{i,k+1}(t) = \overline{C}_{i,k}(t). \tag{2.39}$$

(e) Solution of the initial-value problem by numerical time integration:

So far we have formulated the system of simultaneous oridnary differential equations in time (Equation 2.32 for all the discrete elements) for the radionuclide transport equation by the FLIDE method. Initial and boundary conditions were also specified. We will now attempt to solve this set of system equations. This system of simultaneous ordinary differential equations and the associated initial and boundary conditions constitute an initial-value problem. Unique and continuous solutions for radionuclide concentration $\overline{C}_{i,k}(t)$ can be obtained in time for the initial-value problem by numerical time integration methods. Since each differential equation for $\overline{C}_{i,k}(t)$ depends only upon five discrete-element concentrations $\overline{C}_{i,k}(t)$, $\overline{C}_{i-1,k}(t)$, $\overline{C}_{i+1,k}(t)$, $\overline{C}_{i,k-1}(t)$, and $\overline{C}_{i,k+1}(t)$, the simultaneous system of ordinary, first-order differential equations is suitable for numerical integration. The time-dependent concentrations are solved by numerically integrating the system equations from the known initial conditions using some well-established computational marching schemes. For example, the explicit methods which basically approximate the time

derivatives by the forward time difference may consist of from the simplest form of one time step to multistep and multilevel time formulation (e.g., midpoint leap-frog[42,43] and Du Fort-Frankel[44] methods). In the solution of the present FLIDE mathematical model for transient radionuclide concentration distributions, the explicit method was considered.

The initial-value problem, Equations 2.32 and 2.33, will be directly integrated by the standard fourth-order Runge-Kutta method with Gill coefficients which were successfully employed in numerious studies for the numerical solution of the semidiscretized finite-difference equations associated with external flow problems. Since the Runge-Kutta method employs four time levels for one time step integration, and is a higher-order-accuracy, modified form of the basic Euler-Cauchy method with more stable properties for approximate integration, it should give more stable and accurate solutions to the mathematical model. For an explicit formulation like the Runge-Kutta method, it is essential to establish the necessary stability criteria for the application of the method to the solution of the mathematical system.

In regard to the stability criterion for the numerical simulation of the present initial-value problem, the time marching step size Δt was deduced from the stability analysis for the one-dimensional case[30] to be

$$\Delta t \leq \Delta t_{max} = \frac{\text{Min}(\Delta x_{i,k}, \Delta z_{i,k})}{\text{Max}(\omega_{x_{i,k}}, \omega_{z_{i,k}})} \text{ , for all } i,k \qquad (2.40)$$

where $\Delta x_{i,k}$, $\Delta z_{i,k}$ are the sizes of the discrete element (i,k) in x and z directions, $\omega_{x_{i,k}}$ and $\omega_{z_{i,k}}$ are the x and z components of the

effective radionuclide moving velocity at the discrete element (i,k) and is defined as $\bar{\omega} = \bar{v}/(R_d\theta)$, where $\bar{v}$, R_d, θ represent the Darcian velocity, the retardation factor, and the water content, respectively. A maximum time step size Δt_{max} was first computed using Equations 2.40 and the input data, and then an appropriate smaller time step size Δt was chosen to be used in the transient radionuclide transport simulation.

(f) Computer Simulation Procedure:

In this section, the computation procedure for the radionuclide transport simulation will be outlined and each one of the computer program modules will be briefly described. The flow diagram for the radionuclide transport simulation computer code RADMIG (RADionuclide MIGration) is shown in Figure 2.3. RADMIG was programmed in a modular form. Each program module is dedicated to undertaking a specific task.

The computer simulation of RADMIG begins with the initialization mode by setting the control key word KRUN=0. The module SMLPRP is intended to read in the required simulation input data. The input data includes the dispersivities, retardation factor, radionuclide half-life, initial time, final time, time-step size Δt, and the regional specification of the final-time response of interest. Then the module REGION IS used to input the two-dimensional discrete-element grid system data for the groundwater flow region in x-z plane. The geometric data was prepared separately, as previously described. Module FLOWER is intended to input the steady-state Darcian velocities, water contents at the element centers, and groundwater flow rates on the enclosures of the elements. Module BOUNDS is used to input the flow and boundary conditions on the boundary elements. All flow and boundary data were

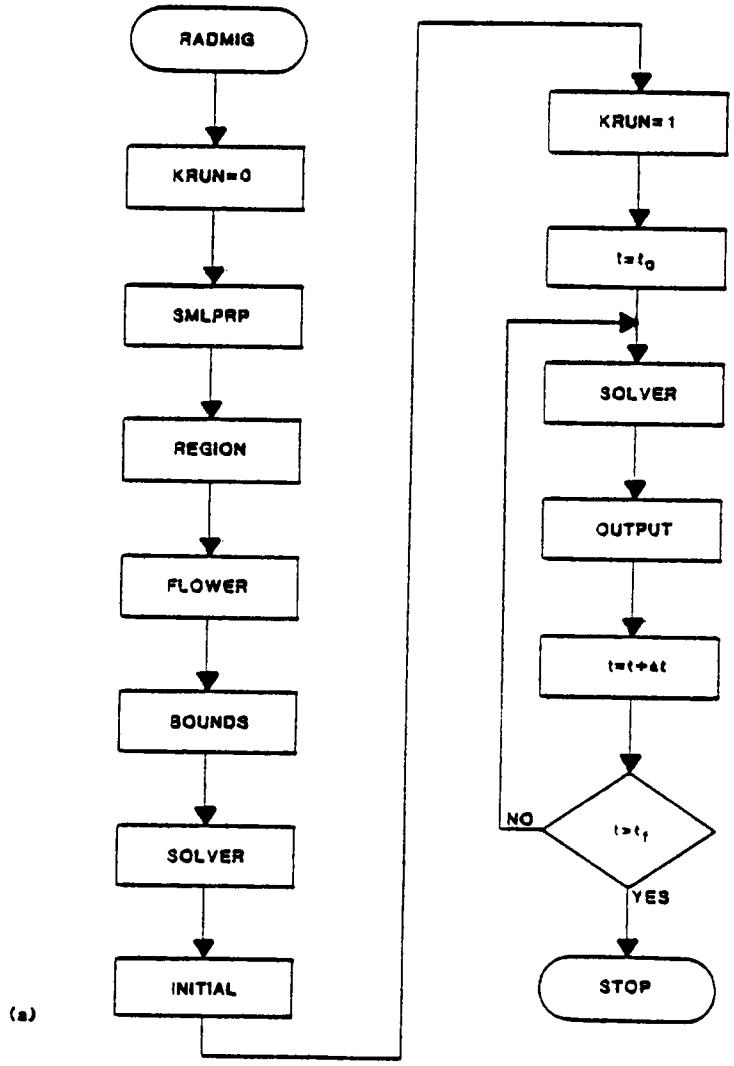

Figure 2.3. Flow Diagram of the Radionuclide Transport Simulation Computer Code RADMIG.

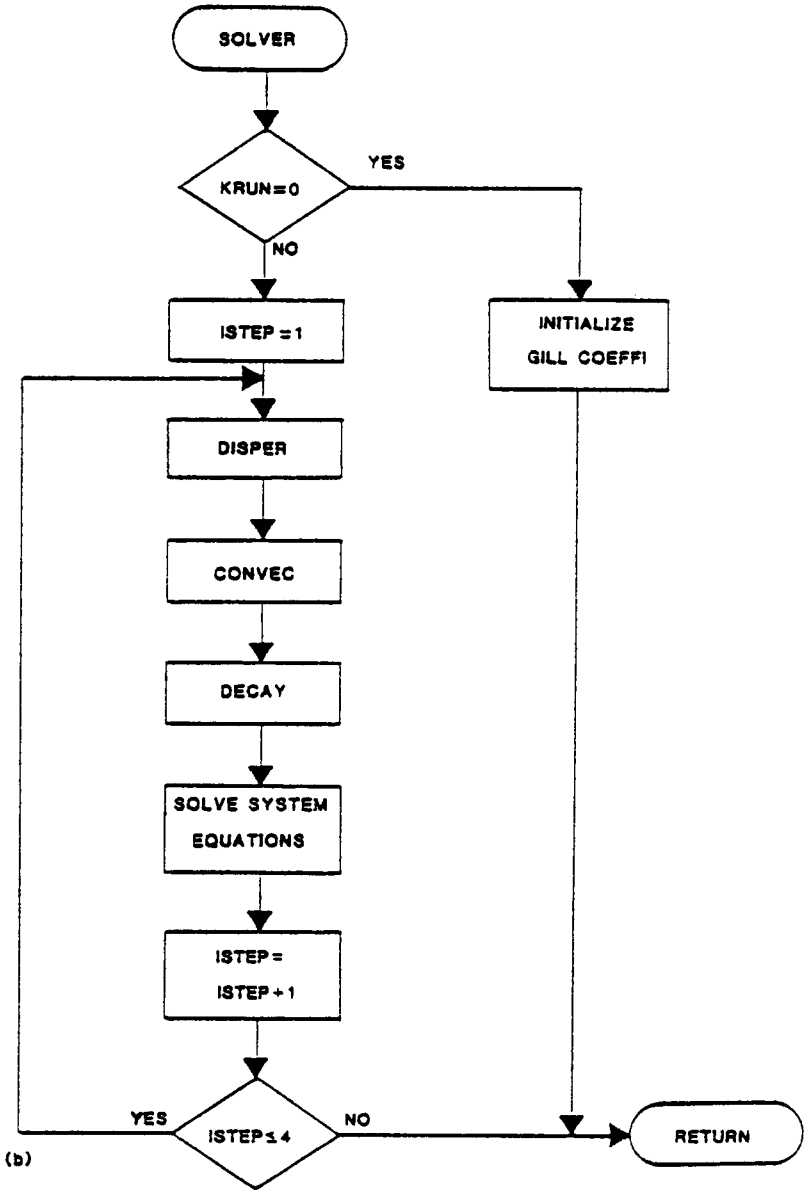

Figure 2.3. (Continued)

prepared off-line. Since these data do not vary with time, they are read in along with the region data only once for each simulation. The Gill coefficients for the fourth-order Runge-Kutta numerical integration method are set in the module SOLVER. Before the transient simulation begins, the module INITIAL must be called to set the initial condition (i.e., initial concentration values).

The transient simulation of the radionuclide transport by groundwater flow begins when KRUN is set to one. The simulation time period from initial time t_0 to final time t_f was divided into a number of the time-step size. For each time step integration, there are four time levels. Within each time level, the module DISPER, CONVEC are called to compute the dispersive, convective radionuclide flow rates in the discrete elements, respectively, based on the current concentration values. Then DECAY is called to account for the radioactive decay loss and construct a system of time derivatives of concentration in the discrete elements. This system of first-order time differential equations is then solved in the module SOLVER. The solved concentrations at each discrete time are written onto a magnetic disk for the future utilization. The output data (concentration values) are also printed on a line printer in a form that conforms to the geometric configuration of the system region for the purpose of easy view. Such a procedure as outlined above is iterated for each time step until the end of the simulation time period. Finally, the response of interest is computed from the final-time concentrations and printed out.

CHAPTER III

RADIONUCLIDE TRANSPORT SIMULATION FOR A SAMPLE PROBLEM

A computer simulation model of the radionuclide transport by groundwater flow for a hypothetical sample problem is presented in this chapter. This model will be employed for the numerical demonstration of the general sensitivity theory for the radionuclide transport model. The sample problem used was taken from Duguid[19] which represents a typical radionuclide transport by groundwater for the low-level radioactive wastes disposal using the shallow-land burial technique. The steady-state, two-dimensional groundwater flow transport model will be solved by the Reeve and Duguids' mositure transport computer code.[9] The transient, two-dimensional radionuclide transport model will be simulated by the computer code, RADMIG, developed in Chapter II by using the mathematical formulation of the Fluid-In-Discrete-Element (FLIDE) method. The computational process and the results of the simulation will be presented in this chapter.

A. Groundwater Flow Transport Calculation

A hypothetical shallow-land burial trench for low-level radioactive wastes disposal is situated above a saturated-unsaturated porous medium near a stream as shown in Figure 3.1(a). The hydrogeological system is composed of a highly permeable sand with soil properties of hydraulic conductivity and moisture content versus pressure head as shown in

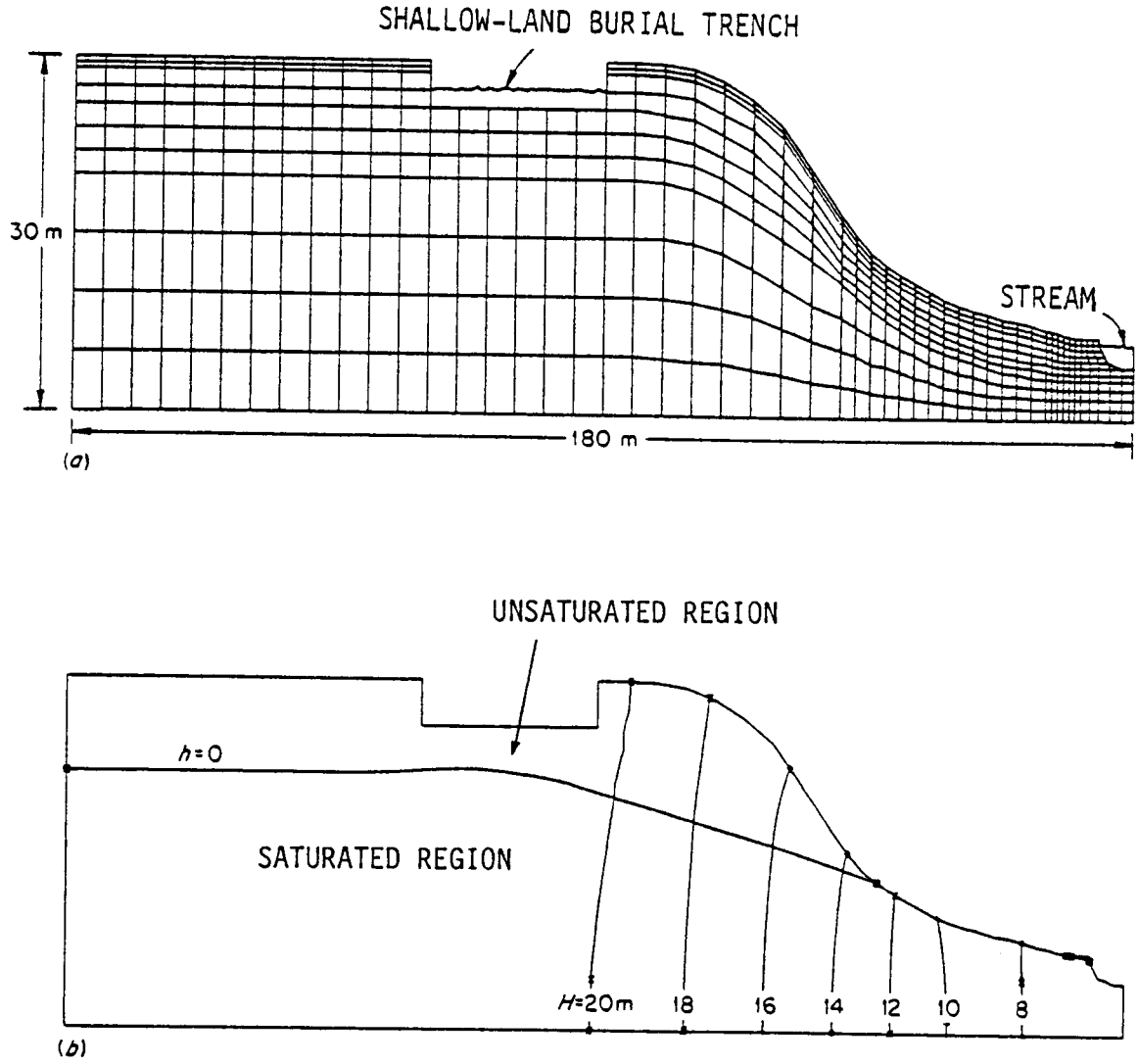

Figure 3.1. (a) Spatial Discretization, (b) Water Table (h=0) and Total Head (H) Configurations for Moisture Transport from a Shallow-Land Burial Trench to a Stream.

Figure 3.2. A water flux of 4.0×10^{-4} $cm^3/cm^2/sec$ with radionuclide dissolved in it, directed vertically downward from the bottom of the trench, provides the only driving force for moving the radionuclide toward the nearby stream because the precipitation is taken to be negligible.

The steady-state groundwater flow transport calculation was performed by employing the moisture-transport computer code developed by Reeves and Duguid[9] to obtain the steady-state Darcian velocity field and water content (moisture content) field. These two hydraulic data will be needed as input data to the radionuclide transport model. The computational steps for performing the steady-state groundwater flow transport calculation are as follows:

(1) Discretize the system region into 528 quadrilateral finite elements with four corner nodes in each element. There are totally 595 finite-element nodes (nodal points). The finite-element geometrical system is shown in Figure 3.1(a). The nodal point data of the x and z coordinates and the global nodal point numbers for all elements are prepared as the input data to the moisture-transport code where all the necessary geometry information will be generated automatically.

(2) Prepare a table of the hydraulic conductivity values and moisture content values versus corresponding pressure head values by linear interpolation from the soil properties depicted in Figure 3.2. This table of hydraulic property values, along with other miscellaneous input data such as acceleration of gravity, viscosity of water, and the steady-state convergence tolerance were prepared as input data to the moisture-transport code.

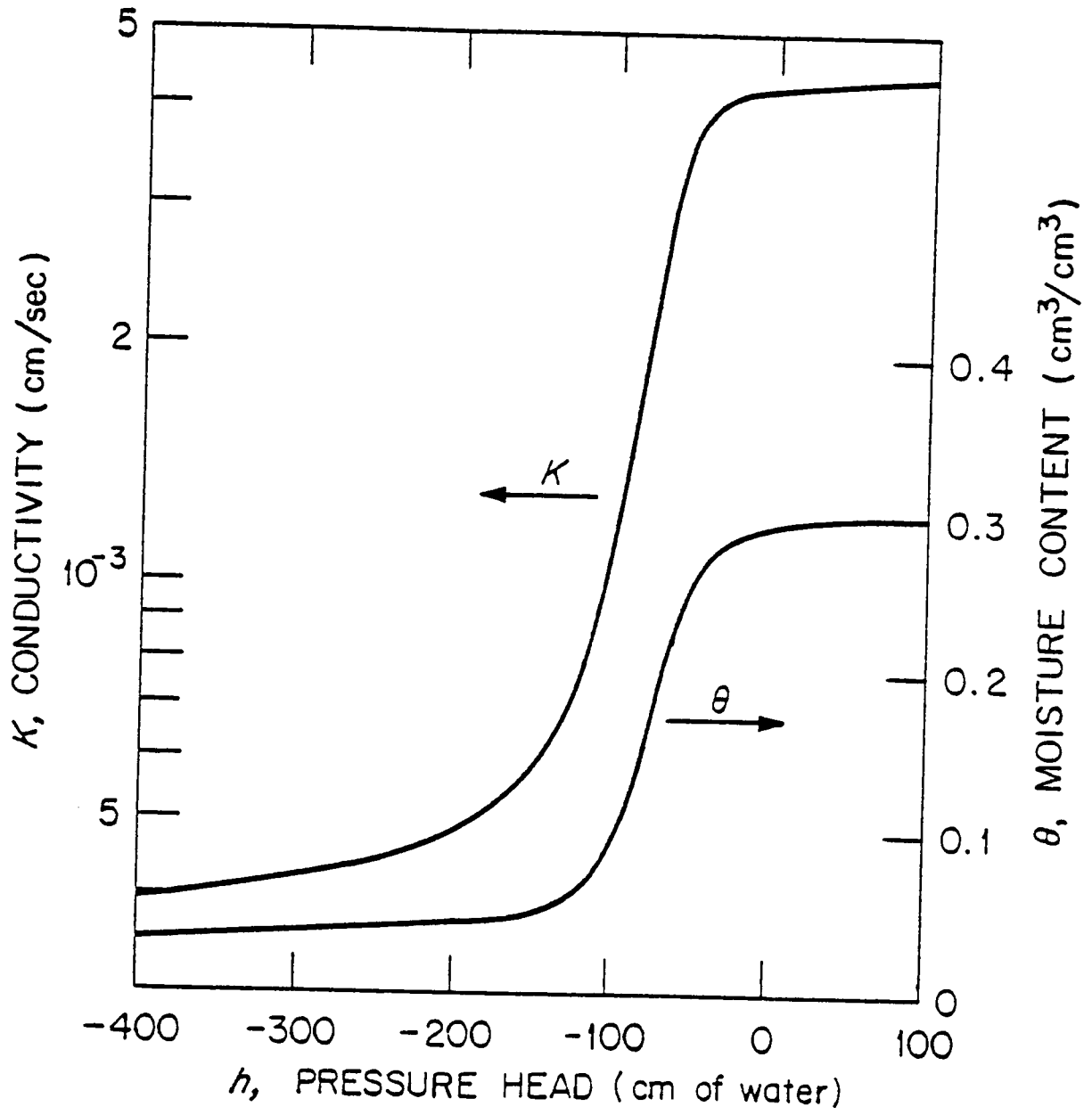

Figure 3.2. Hydraulic Conductivity and Soil-Moisture Characteristics of a Hypothetical Sandy Soil.

(3) Specify steady-state boundary conditions. Neumann boundary conditions were specified on the bottom surface of the burial trench as the source seepage boundary condition with water flux of 4.0×10^{-4} $cm^3/cm^2/sec$ at each nodal points of the boundary elements. Dirichlet boundary conditions were specified at the nodal points of the interfacing elements between the porous medium and the stream. The pressure head values at these nodal points are fixed values equal to the water depths in the stream. The slope and porous medium-stream interface portions of the system were specified as the outflow boundary. The rest of the boundary in the system region, including the bottom line were treated as Neumann condition with zero flux crossing the boundary (close boundary).

(4) Run the moisture-transport code with the input data prepared in steps (1)-(3) to obtain the pressure head at all nodal points. The unsaturated and saturated regions are separated by the water table shown in Figure 3.1(b). The water content field was calculated by interpolating the pressure head vs water content table using the calculated pressure head at each nodal point. The x and z components of Darcian velocities were computed at four corner nodes of each finite element.

B. Radionuclide Transport Simulations

We now present the computer simulation of the radionuclide transport in the porous medium by employing the discrete-element transport model developed in Chapter II.

First the system region was partitioned into a rectangular discrete-element grid system as described in Chapter II. The entire

burial site region situated in an x-z rectangular coordinate system frame was partitioned into 21 by 9 rectangular discrete elements of which 82 elements are interior elements, 55 elements are boundary elements. The remaining are external elements which are not used in the model calculation. The discrete-element grid system is shown in Figure 3.3. The grid system may be composed of discrete elements of various sizes. Finer meshes were placed near the outflow boundary where the radionuclide concentrations are of most concern. The coordinates of the region boundary and the discretization control parameters such as the data associated with x and z grid lines were input to the program module REGION to generate the necessary geometrical data to be used in the main body of the simulation code. Three types of boundary conditions were specified in this sample problem. They are close (i.e., impermeable) boundary, inflow boundary, and outflow boundary conditions. Inflow boundary condition was specified for the elements at the bottom of the burial trench, outflow boundary condition for the elements on the slope and stream interface. The remaining boundary elements were specified to have close boundary condition.

Secondly, the steady-state Darcian velocity and water content fields were prepared in the discrete-element grid system as the input data to the radionuclide transport discrete-element model. Since no groundwater flow transport model by the discrete-element method was available, the flow-field data (Darcian velocities and water contents) were transformed from finite-element form to discrete-element form. The four sets of Darcian velocities, each set consisting of 528 nodal point values of the finite elements, were transformed to the Darcian velocities at the

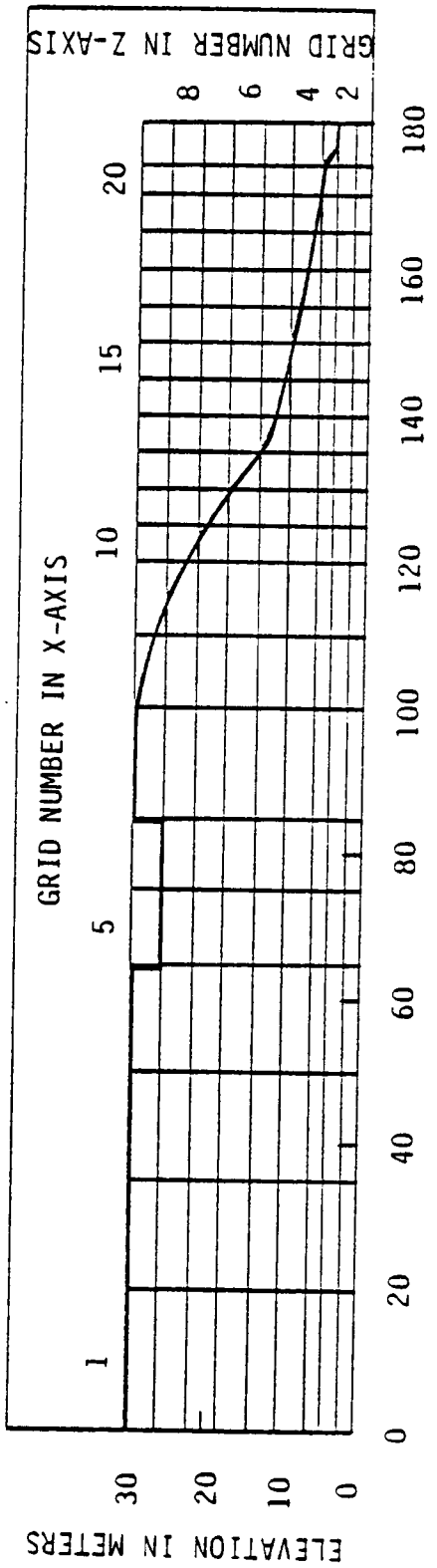

Figure 3.3. Discrete-Element Grid System for the Geometry of the Hypothetical Sample Problem.

centers of 137 discrete elements as well as the Darcian flow rates passing through the enclosures of these 137 discrete elements. Bilinear interpolation was employed to transform the flow field data from 528 quadrilateral finite elements to 137 rectangular discrete elements. The water content field at 595 finite-element nodal points were also transformed to that at the centers of 137 discrete elements. Before bilinear interpolation was applied, the four sets of Darcian velocities x and z components at the four corner nodes of 528 finite elements had been combined into one Darcian velocity field at the 595 nodal points of the finite-element grid system. This was done by averaging the velocity components values at each nodal point shared by its adjacent finite elements. Then these averaged nodal Darcian velocities and water contents were bilinearly interpolated into the Darcian velocity and water content fields, respectively, at 137 discrete elements by using the following equation:

$$\bar{F}_i = \frac{\sum_{n=1}^{N} \frac{F_n}{|\bar{r}_n - \bar{r}_i|^m} \delta_{ni}}{\sum_{n=1}^{N} \frac{1}{|\bar{r}_n - \bar{r}_i|^m} \delta_{ni}}, \text{ for } i = 1 \ldots I \qquad (3.1)$$

where

F_n = nodal variable value at nodal point n,

$\bar{F}_i$ = interpolated variable value at discrete-element point i,

$\bar{r}_n$, $\bar{r}_i$ = two-dimensional coordinates at nodal point n, discrete-element point i, respectively,

N = total number of finite-element nodal points,

I = total number of interplation points in discrete-element grid system,

m = bilinear interplation power and,

$$\delta_{ni} = \begin{cases} 1, \text{ if } |\bar{r}_n - \bar{r}_i| < R \\ 0, \text{ otherwise} \end{cases}$$

where R = radius of convergence.

Equation 3.1, along with m = 2 and R = 10 meters was used to interpolate the Darcian velocity and water content fields. The Darcian flow rates of the elements were calculated by multiplying the bilinearly interpolated Darcian velocity components at the enclosure centers by the associated enclosure lengths. The hydraulic velocity field in the discrete-element grid system was computed by dividing the Darcian velocity by the water content at the center of each element, as shown in Figure 3.4.

The use of bilinear interpolation to obtain the flow-field data in the discrete-element grid system can only be regarded as an "art" rather than a science because no strict mathematical equations have been derived to give unique bilinearly interpolated variable values.[47] The interpolated results depend upon the chosen bilinear interpolation power and the radius of convergence. For example, m = 2 would give more "centralized influence" on the interpolated value than m =1 would. And R = 10 m in the interpolation calculation involves only those variable values whose locations are within the range of 10 m radius from the interpolated location. Though the flow field so obtained is not unique, a good estimation of the bilinearly interpolated flow field can be

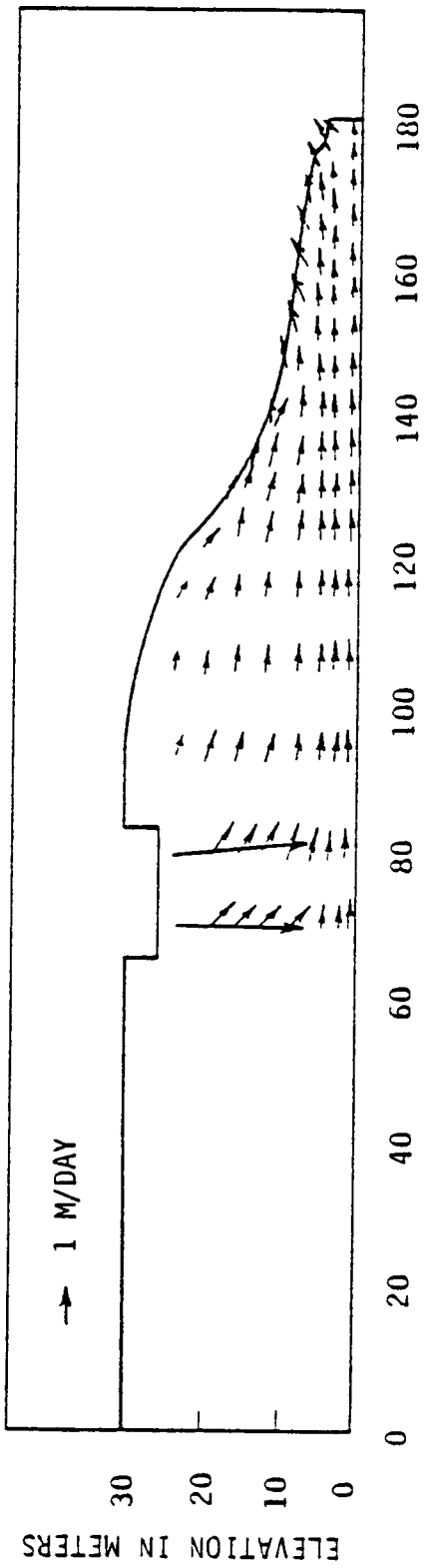

Figure 3.4. Steady-State Hydraulic Velocity Field of the Sample Problem in the Discrete-Element Grid System.

obtained as long as reasonable values of m and R are chosen. Since it was not the purpose of this dissertation to develop and solve the groundwater flow transport model by the discrete-element method, bilinear interpolation served as a means to provide the necessary Darcian velocity and water flow fields in the discrete-element grid system.

In addition to the needed geometrical data and flow-field data (Darcian velocities and water contents) for the sample problem, some other input parameters are also required for the simulation of the radionuclide transport. They are longitudinal dispersivity a_L, transverse dispersivity a_T, retardation factor R_d, and decay constant λ for the addressed radionuclide with half life $t_{1/2}$.

The initial conditions for the time-dependent radionuclide transport problem (i.e., initial-value problem) were assumed to be zero for our simulation, i.e., $\bar{C}_{i,k}(t = 0) = 0$ for all (i,k) in the discrete-element grid system. Three simulation examples have been accomplished and time-dependent radionuclide concentration fields as a result of simulations will be presented and discussed in the following sections. In these three examples, the radionuclide dissolved in groundwater was assumed to be tritium with $R_d = 1$ and $t_{1/2} = 12.7$ years. The time-step size Δt for the transient simulation of H-3 transport was calculated from Equation 2.43 to be 0.1 day. The input parameter data for the three examples are summarized in Table 3.1.

Simulation Example 1

In this example, longitudinal and transverse dispersivities a_L, a_T were assumed to have hypothetical values of 10 m and 5 m, respectively. Tritium concentration in the water of the burial trench

Table 3.1. Input Parameter Data for Radionuclide Transport Simulation Examples

Parameter	Example 1	Example 2	Example 3
Radionuclide	H-3	H-3	H-3
a_L (m)	10	10	10
a_T (m)	5	5	1
R_d	1	1	1
$t_{1/2}$ (years)	12.7	12.7	12.7
Δt (days)	0.1	0.1	0.1
t_f[a] (days)	10	10	10
T[b] (days)	>10	1	>10

[a] t_f = final simulation time.

[b] T = source depletion time.

(i.e., at the source boundary) was assumed to remain a fixed value (e.g., 1 Ci/m^3) during the entire simulation period. That is to say, the source depletion time (source duration time) mentioned in Chapter II was set to be greater than the final simulation time. The radionuclide transport period of time (total simulation time) for the computer simulations was 10 days, i.e., the number of time steps used was 100. The computer code was run on the DEC-10 system at the University of Tennessee Computing Center. A computer run for 10 time steps took less than 4 seconds CPU time.

The results of the simulations are tritium concentrations at 137 discrete-elements at every simulation time (multiple of time step size).

The time-dependent tritium concentration fields are presented in concentration-contour plots (isoconcentration lines drawn in 2-D plots) as shown in Figure 3.5.

As can be seen from these plots, H-3 concentrations are moving away from the source (the bottom of the burial trench) toward the outflow boundary as the simulation time increases. The concentrations in the system are fractions of the source concentration at the bottom of the burial trench. The concentrations to the left of the trench drop rapidly because the groundwater velocities there are very small. From the steady-state hydraulic velocity plot (Figure 3.4, page 52), we see that groundwater is flowing at very small velocity from the lower-left corner of the trench to the left. The behavior of the concentrations plumes near the lower-left corner of the trench can be accounted for by groundwater flowing in the lower-left direction as well as the large transverse dispersion effect resulting from the large seepage velocities near the bottom of the trench. The concentrations below the trench bottom are moving downward and toward the right-hand side of the trench. In general, the concentrations move faster to the right than to the left because groundwater is flowing faster in the right-hand side region. The concentration field is closely associated with the groundwater flow field because radionuclides are convected in the groundwater flow directions.

Simulation Example 2

The input parameter data in this example were the same as those in the first example except the source depletion time was 1 day. It means that the source concentration was kept to a constant value

Normalized Isoconcentration Contours 1-8 at Values of 0.01, 0.025, 0.05, 0.075, 0.1, 0.25, 0.5, and 0.75

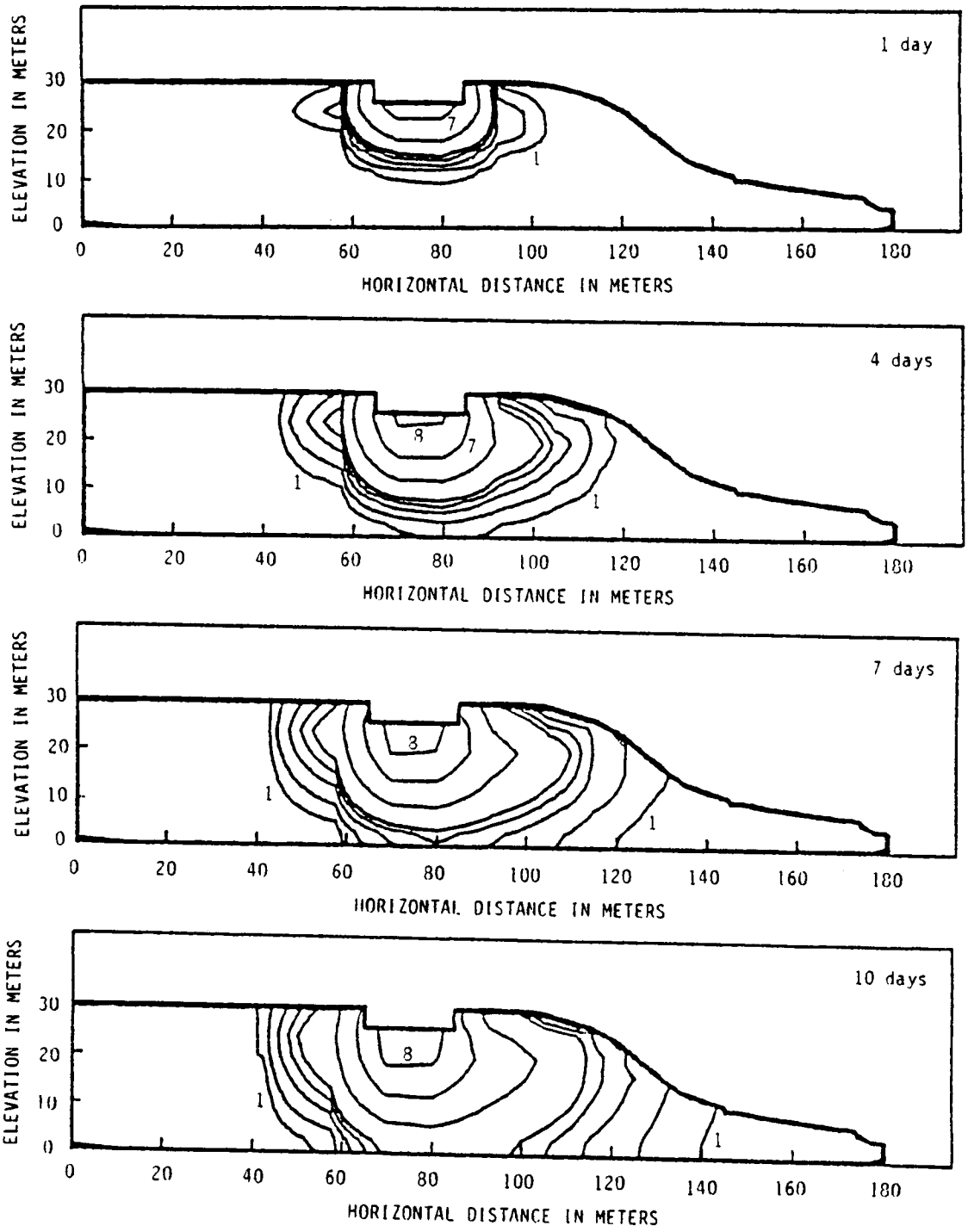

Figure 3.5. Time-Dependent Tritium Concentration Distributions for Simulation Example 1.

(e.g., 1 Ci/m^3) for the first day and was zero thereafter. This "band-release" of source concentration can be thought of as having the infiltration of radionuclide-dissolved water for one day, and then replacing the radioactive liquid with uncontaminated water to flush the porous medium. The band release of radionuclides can be assumed to model a realistic condition of the radioactive wastes disposal in which the radionuclide leach rate is assumed constant for a certain period of time and then becomes zero thereafter.

The simulation history of the concentration field for this example is displayed in Figure 3.6 from the first through the tenth day. It can be seen from these figures that the concentration near the bottom of the trench are gradually decreasing with time after the source has been cut off after the first day. Closed isoconcentration contours begin to form beneath the trench bottom. The concentrations are spreading out with time from the central region (where the concentrations are the highest). This spreading mechanism is primarily due to the hydrodynamic dispersion. As we examine these plots one by one, it can be seen that the concentration "peak" is broadening and flatening. The concentrations in the inner regions decrease with time (note the inner contours move inwardly and some disappear at later times). The outer contours can be seen moving faster to the right-hand side of the trench (outflow boundary) than to the left.

Simulation Example 3

The input parameter data in this example were the same as in the first example except the transverse dispersivity a_T was reduced from

Normalized Isoconcentration Contours 1-7 at Values of 0.01, 0.025, 0.05, 0.075, 0.1, 0.25, and 0.5

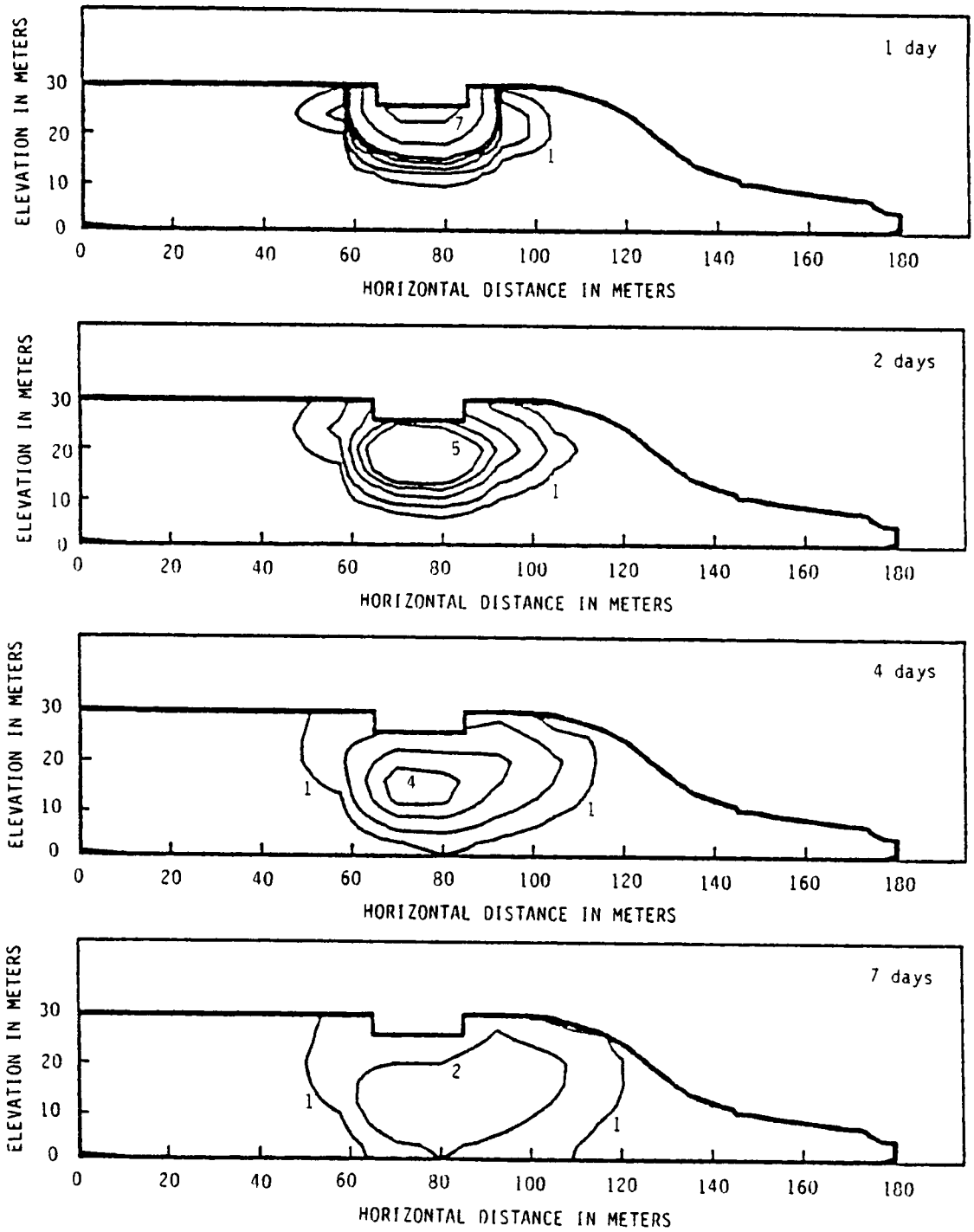

Figure 3.6. Time-Dependent Tritium Concentration Distributions for Simulation Example 2.

10 m to 1 m. The transient concentration fields are presented in Figure 3.7. As was expected, the transversal dispersion effect decreases because the value of transverse dispersivity a_T used was five times smaller than that used in the first example. Since the groundwater flow near the bottom of the system region is essentially horizontal, increasing the value of transverse dispersivity causes the radionuclides to move further toward the bottom of the flow system. In the present case the outer concentration contours are observed to move down toward the bottom of the flow system slower than those do in the first example. From Figures 3.5 and 3.7 we note the radionuclide plume extends slightly farther longitudinally (to the right) for small value of a_T. The reduction of the transversal dispersion effect is obvious near the lower-left corner of the trench, where the concentration contours hardly move (note that there are large seepage velocities pointing downward beneath the bottom of the trench).

We have demonstrated the performance of the transient, two-dimensional radionuclide transport discrete-element model by using this model to simulate the above three cases of the radionuclide transport problem. We will use this model as a computational method in addressing the sensitivity analysis for the radionuclide transport problem.

Normalized Isoconcentration Contours 1-8 at Values of 0.01, 0.025, 0.05, 0.075, 0.1, 0.25, 0.5, and 0.75

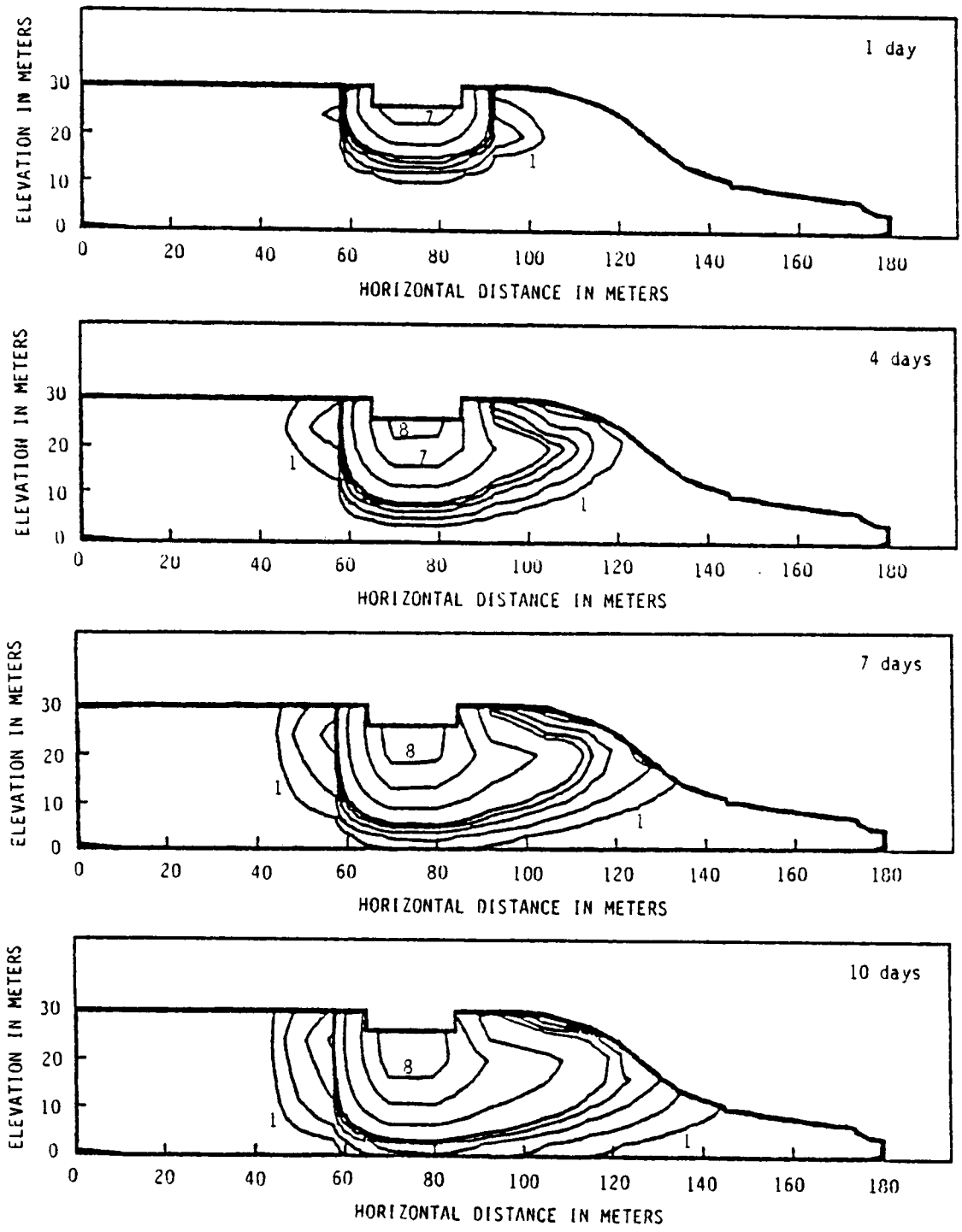

Figure 3.7. Time-Dependent Tritium Concentration Distributions for Simulation Example 3.

CHAPTER IV

SENSITIVITY THEORY AND UNCERTAINTY ANALYSIS FOR THE RADIONUCLIDE TRANSPORT EQUATION

In this chapter, we derive the adjoint equation for the radionuclide transport equation, formulate the sensitivity coefficients, and describe the methodology for the sensitivity and uncertainty analyses.

A. Responses of Interest

In almost all the simulations of the transient radionuclide transport in groundwater flow problems, the end result of the simulations is the time-dependent, spatial radionuclide concentration distributions (fields). This is unlike the case in the nuclear reactor calculations where the desired end results would be estimated values of reactor performance parameters such as the reaction rate in a detector, the final fissile mass in the core in the depletion analysis, etc.. Such a performance parameter is usually called a "response of interest." In order to perform the sensitivity analysis for the radionuclide transport problem, we define the response of interest to be an estimated value which can characterize the simulation of the radionuclide transport by groundwater flow. Two types of responses of interest are considered in this study. They are defined as follows.

(1) Space-average concentraton in a specified region:

The first type of response of interest is the spatially averaged radionuclide concentration in a specified region (area in 2-D

calculation) at a specified observation time t_f (final time). That is,

$$R_{\bar{C}} = \frac{1}{A}\int\int_A C(x,z,t_f)dxdz \tag{4.1}$$

where A represents the area of a specified two-dimensional region. Equation 4.1 can also be written as

$$R_{\bar{C}} = \left[\frac{1}{A} C(x,z,t_f)\,\delta(x,z;A)\right]_{x,z} \tag{4.2}$$

where

$$\delta(x,z;A) = \begin{cases} 1, \text{ if } (x,z) \text{ is in } A \\ 0, \text{ otherwise} \end{cases} \tag{4.3}$$

and the square brackets represent the integration over the subscripted variables. For example, if one wishes to determine the spatially averaged tritium concentration in the saturated zone of a groundwater flow system SZ ten days after the start of H-3 leaching into the porous medium, the response of interest would be

$$R_{\bar{C}} = \frac{1}{A_{SZ}}\int\int_{A_{SZ}} C(x,z,t=10)dxdz \ . \tag{4.4}$$

This kind of response of interest can also be a radionuclide concentration at a specified location. This will be the limiting case for Equation 4.1 when the area of the region containing that location shrinks to a point. In the discrete-element formulation, the response of interest would be the mean concentration in a specified discrete element.

(2) Radionuclide mass flow rate crossing the outflow boundary:

The second type of response of interest considered in this study is the toal radionuclide mass flow rate (discharge rate) passing through the outflow boundary surface and discharging into the biosphere at a specified final time t_f, i.e.,

$$R_J = \iint_{OB} \hat{n}\cdot\bar{v}(x,z)C(x,z,t_f)dxdz \tag{4.5}$$

where OB represents the outflow boundary. Equation 4.5 can be written as

$$R_J = [\hat{n} \cdot \bar{v}(x,z)C(x,z,t_f)\delta(x,z;OB)]_{x,z} \tag{4.6}$$

where

$$\delta(x,z;OB) = \begin{cases} 1, \text{ if } (x,z) \text{ is on OB} \\ 0, \text{ otherwise} \end{cases} \tag{4.7}$$

The radionuclide mass flow rate is a very important response of interest in the assessment of the environmental impact from the radioactive wastes disposal because it, in conjunction with dose conversion factors, can be used to calculate the radiological dose to man.

The responses of interest considered so far are all final-time responses and are explicit functions of the radionuclide concentration field. We only considered final-time responses of interest for the sensitivity and uncertainty analyses in this study.

B. Input Parameters

We next describe the input parameters to which the sensitivity analysis will be addressed. Five input parameters were considered. They are:

(1) Longitudinal dispersivity a_L,

(2) Transverse dispersivity a_T,

(3) Retardation factor R_d,

(4) Steady-state water content field $\theta(x,z)$,

(5) Radionuclide decay constant λ.

The first two parameters a_L, a_T are concerned with the hydrodynamic dispersion of the radionuclide in the porous medium and can be space-dependent, because a_L, a_T vary in different porous media. Retardation factor R_d is an important input parameter which measures the adsorption ability of the porous medium to the specified radionuclide. As was described in Chapter II, R_d is related to both radionuclide and porous medium. We used a fixed value for R_d throughout the system region, though it could be space-dependent. The steady-state water content field $\theta(x,z)$ was computed from the steady-state groundwater flow transport model, as was described in Chapter III. Although it is a function of space, the water content at any point in space cannot vary independently. It is because the water content is a part of the steady-state groundwater flow system, which, when combined with the Darcian velocity field, defines the hydraulic velocity field. In order to maintain the mass conservation of groundwater flow, the water content field must vary at the same proportion everywhere. The radioactive decay

constant for the specified radionuclide is a fixed-value parameter in the radionuclide transport simulation.

C. Derivation of the Adjoint Transport Equation

Designate R as any arbitrary response of interest previously described and α as any one of the input parameters. The goal of sensitivity analysis for the radionuclide transport problem is to find the effect that perturbing the input parameter α will have on the response of interest R. This can be accomplished by defining the "relative sensitivity coefficient" of the response of interest R to the specified input parameter α, which relates the percent change in R to the percent change in α.

R is an explicit functional of the radionuclide concentration field C and an implicit functional of input parameter α. That is,

$$R = R[\alpha(x,z),\ C(x,z,t)] \ . \tag{4.8}$$

C(x,z,t) is the solution to the time-dependent, two-dimensional radionuclide transport equation along with appropriate initial and boundary conditions, i.e.,

$$L[\alpha(x,z)]C(x,z,t) = 0 \tag{4.9}$$

where $L[\alpha(x,z)]$ is a linear operator and takes the form of

$$L[\alpha(x,z)] = - R_d\theta(x,z)\frac{\partial}{\partial t} + \nabla \cdot \overline{\overline{D}}(x,z)\nabla - \nabla \cdot \overline{v}(x,z) - R_d\theta(x,z)\lambda \ . \tag{4.10}$$

A change in the value of α will perturb the solution C because α is an explicit parameter in operator L. We wish to express the variation of the response R to be first order in parameter variation, but insensitive to first-order errors in the variation of the radionuclide concentration field C. That is,

$$\delta R = [a\,\delta\alpha(x,z) + b\,\delta C^2(x,z,t) + \text{higher order terms}]_{x,z,t}. \qquad (4.11)$$

After some manipulations, Equation 4.11 can be put in the form

$$\frac{\delta R}{R} = \left[S(x,z)\,\frac{\delta\alpha(x,z)}{\alpha(x,z)}\right]_{x,z} + \text{second and higher order terms.} \qquad (4.12)$$

For a small parameter variation $\delta\alpha(x,z)$, first order approximation of Equation 4.12 yields the linear relation between the percent change in the response $\delta R/R$ to the percent change in the parameter $\delta\alpha/\alpha$, with $S(x,z)$ serving as the relative sensitivity coefficient at space point (x,z), that is,

$$\frac{\delta R}{R} = \left[S(x,z)\,\frac{\delta\alpha(x,z)}{\alpha(x,z)}\right]_{x,z} \qquad (4.13)$$

where $S(x,z)$ has the significance of the percent change in R due to the percent change in α at space point (x,z).

We now employ generalized perturbation theory using the variational principle approach, formulated by Pomraning[39] and Stacey,[40] to formulate the relative sensitivity coefficient field $S(x,z)$.

Define a new response functional K which is equal to the response of interest defined in Equation 4.9 appended by another term with the

radionuclide transport equation (Equation 4.10) as a constraint condition, i.e.,

$$K[\alpha,C,\psi^*] = R[\alpha,C] + [\psi^* L(\alpha)C]_{x,z,t} \tag{4.14}$$

where ψ^* is an unspecified Lagrangian multiplier. If the input parameters are at the unperturbed state (reference state), $C(x,z,t)$ will be the exact solution (reference-state solution) to Equation 4.9. Then we have

$$K[\alpha,C,\psi^*] = R[\alpha,C]. \tag{4.15}$$

That is to say, the response functional K is equal to the response of interest at the reference state.

If the input parameter α is perturbed from the reference state to a perturbed state α', this perturbation in α will result in a new response functional at the perturbed state of the input data.

$$K'[\alpha',C',\psi^*] = R'[\alpha',C'] + [\psi^* L'(\alpha')C']_{x,z,t} \, . \tag{4.16}$$

Since $C'(x,z,t)$ is the perturbed-state solution satisfying the new radionuclide transport equation

$$L'[\alpha'(x,z)]C'(x,z,t) = 0. \tag{4.17}$$

With the same initial and boundary conditions, Equation 4.16 is reduced to

$$K'[\alpha',C',\psi^*] = R'[\alpha',C']. \tag{4.18}$$

Note that the unspecified Lagrangian multiplier ψ^* remains unchanged.

Expanding the functional K' in a Taylor series about the unperturbed state to obtain

$$K' = K + \left[\left(\frac{\partial K}{\partial \alpha}\right)_{ref} \delta\alpha + \left(\frac{\partial K}{\partial C}\right)_{ref} \delta C + \left(\frac{\partial K}{\partial \psi^*}\right)_{ref} \delta\psi^*\right]_{x,z,t}$$

$$+ \text{second and higher order terms in } \delta\alpha, \delta C, \text{ and } \delta\psi^*, \qquad (4.19)$$

where the subscript "ref" represents that the term in the parentheses is to be evaluated at the reference state. Neglecting second and higher order terms, we have

$$K' = K + \left[\left(\frac{\partial K}{\partial \alpha}\right)_{ref} \delta\alpha + \left(\frac{\partial K}{\partial C}\right)_{ref} \delta C + \left(\frac{\partial K}{\partial \psi^*}\right)_{ref} \delta\psi^*\right]_{x,z,t}. \qquad (4.20)$$

If we make the quantities $(\partial K/\partial C)_{ref}$, $(\partial k/\partial \psi^*)_{ref}$ vanish, then using Equations 4.15, 4.18 and 4.20, we have

$$\delta R = R' - R$$

$$= \left[\left(\frac{\partial K}{\partial \alpha}\right)_{ref} \delta\alpha\right]_{x,z,t} . \qquad (4.21)$$

Dividing each side of Equation 4.21 by R and multiplying and dividing the term inside the square brackets on the right-hand side of Equation 4.21 by $\alpha(x,z)$, we obtain

$$\frac{\delta R}{R} = \left[\frac{\alpha(x,z)}{R} \left(\frac{\partial K}{\partial \alpha}\right)_{ref} \frac{\delta\alpha(x,z)}{\alpha(x,z)}\right]_{x,z,t} . \qquad (4.22)$$

Since we have assumed that the parameter $\alpha(x,z)$ is independent of time in our study, we can move the time integral inside to operate on the derivative of K with respect to α evaluated at the reference state, i.e., $(\partial K/\partial \alpha)_{ref}$. Now Equation 4.22 can be written as

$$\frac{\delta R}{R} = \left[\frac{\alpha(x,z)}{R} \left[\left(\frac{\partial K}{\partial \alpha}\right)_{ref}\right]_t \frac{\delta \alpha(x,z)}{\alpha(x,z)} \right]_{x,z} . \qquad (4.23)$$

Comparing Equations 4.23 and 4.13, it is obvious that the relative sensitivity coefficient field (function of 2-D space) of R to α is equal to

$$S_\alpha(x,z) = \frac{\alpha(x,z)}{R} \left[\left(\frac{\partial K}{\partial \alpha}\right)_{ref}\right]_t . \qquad (4.24)$$

Equation 4.24 is the basic equation for the formulation of the relative sensitivity coefficient field $S_\alpha(x,z)$.

Forcing the quantities $(\partial K/\partial C)_{ref}$, $(\partial K/\partial \psi^*)_{ref}$ to vanish is equivalent to making the response functional K "stationary" with respect to the arbitrary variations of the function C and ψ^* about the reference state. We determined the appropriate stationary conditions to make the first-order variations of K with respect to the variations in C and ψ^* to vanish. One of the required Euler equations corresponds to the adjoint equation for the radionuclide transport equation.

The stationarity of the functional K with respect to the arbitrary variation in the function ψ^* yields the expected Euler condition which is the unperturbed radionuclide transport equation, namely Equation 4.9. Taking the variation of K with respect to the variation of C gives

$$\delta K_C = (\partial K/\partial C)_{ref} \, \delta C . \qquad (4.25)$$

Substituting Equation 4.14 into Equation 4.25, we have

$$\delta K_C = \delta R_C + [\psi^* L \delta C]_{x,z,t} \cdot \tag{4.26}$$

Equation 4.26 becomes (see Appendix for detailed derivation)

$$\delta K_C = \delta R_C + [\delta C L^* \psi^*]_{x,z,t} + [R_d \theta \psi^* \delta C]_{x,z,t=0}$$

$$- [R_d \theta \psi^* \delta C]_{x,z,t=t_f}$$

$$+ \int_0^{t_f} \iint_{BS} \hat{n} \cdot (\psi^* \bar{\bar{D}} \nabla \delta C - \delta C \bar{\bar{D}}^+ \nabla \psi^* - \bar{v} \psi^* \delta C) dx dz dt \ , \tag{4.27}$$

where L^* is the adjoint operator corresponding to the linear radionuclide transport operator in Equation 4.10, and has the form

$$L^* = R_d \theta \frac{\partial}{\partial t} + \nabla \cdot \bar{\bar{D}}^+ \nabla + \bar{v} \cdot \nabla - R_d \theta \lambda \ , \tag{4.28}$$

and $\bar{\bar{D}}^+$ is the transposed hydrodynamic dispersion coefficient tensor of $\bar{\bar{D}}$. The third and fourth terms on the right-hand side of Equation 4.27 are the initial and final terms resulting from the commutative operation, and the last term is the boundary term. Note that the spatial integration of the boundary term is over the boundary surface of the system region (boundary line for 2-D problem).

We next wish to make the variation of K stationary with respect to the variation in C. This will lead to the adjoint equation as the Euler condition corresponding to a variation in C. For the second term of Equation 4.27 to vanish with respect to the arbitrary variation δC, we must set

$$L^* \psi^* = 0 \tag{4.29}$$

for every point in phase space (x,z,t). The adjoint equation for the radionuclide transport can be written as

$$R_d \theta \frac{\partial \psi^*}{\partial t} = - \nabla \cdot \bar{D}^+ \nabla \psi^* - \bar{v} \cdot \nabla \psi^* + R_d \theta \lambda \psi^* \ . \qquad (4.30)$$

This equation will also be referred to as the adjoint transport equation because the adjoint function ψ^*, like the radionuclide concentration, is also transported in the porous medium by the groundwater flow in an "adjoint" sense. The solution of the adjoint transport equation and the interpretation of the adjoint will be given in Chapter V.

Next we consider the necessary boundary conditions for the adjoint transport equation. The boundary conditions for the adjoint transport equation are dependent on the boundary conditions for the radionuclide forward equation. The boundary conditions for the adjoint equation are selected to eliminate the last term on the right-hand side of Equation 4.27. Three types of boundary were considered for the adjoint transport equation.

(a) Close boundary: The close boundary is also called impermeable boundary. On the impermeable boundary of a groundwater flow system, the convective and dispersive transport flows normal to the boundary are both zero. We chose close boundary condition to eliminate the boundary term (the last term of Equation 4.27).

(b) Inflow boundary: As will be seen in the next chapter, the groundwater flow direction will be reversed when we switch from the forward problem (radionuclide transport problem) to the adjoint problem (adjoint transport problem). Therefore, the inflow boundary in the forward problem will become the outflow boundary in the adjoint problem.

In the upwind differencing method, the boundary condition is not necessary on the outflow boundary for the convective transport term calculation as previously mentioned in Chapter II. However, we specify the boundary condition to be

$$\bar{\psi}^{*}_{i,k+1/2} = 0 \tag{4.31}$$

on the inflow boundary of the forward problem in order to eliminate the boundary term, where the inflow boundary coincides with the enclosure (i,k+1/2). The "upstream" radionuclide concentration $\bar{C}_{i,k+1}$, which determines the boundary condition $\bar{C}_{i,k+1/2}$, in the upwind differencing formulation, does not vary due to the variation of the parameter in the system region. Therefore, we have $\delta C=0$ on the inflow boundary. Then, the boundary term goes away.

(c) Outflow boundary: The boundary condition for the forward transport problem was specified to be zero radionuclide dispersive flux on the outflow boundary in Chapter II, which is equivalent to zero concentration gradient in both x and z directions i.e., $\frac{\partial C}{\partial x} = 0$, $\frac{\partial C}{\partial z} = 0$. The gradient of the variation in concentration due to the change in α is equal to the variation of the concentration gradient, that is,

$$\nabla \delta C = \delta \nabla C \ . \tag{4.32}$$

And,

$$\iint_{BS} \hat{n} \cdot (\psi^{*} \bar{\bar{D}} \nabla \delta C) dx dz = \iint_{BS} \hat{n} \cdot (\psi^{*} \bar{\bar{D}} \delta \nabla C) dx dz = 0 \ . \tag{4.33}$$

We have two terms left in the boundary term . In order to eliminate the boundary term, we chose zero adjoint flux on the outflow boundary for an arbitrary variation in C, i.e.,

$$\hat{n}\cdot(\bar{v}\psi^* + \bar{\bar{D}}^+\nabla\psi^*) = 0 \qquad (4.34)$$

on the ouflow boundary. The adjoint flux consists of adjoint convective and dispersive terms. Equation 4.34 indicates that the outflow boundary in the forward problem becomes a close boundary (impermeable boundary) in the adjoint transport problem.

In summary, the boundary conditions for both the radionuclide and adjoint transport problems are listed in Table 4.1.

Table 4.1. Boundary Conditions for the Radionuclide and Adjoint Transport Problems

Radionuclide transport problem	Adjoint transport problem
a) Close boundary: zero radionuclide flux	a) Close boundary: zero adjoint flux
b) Inflow boundary: specified concentration	b) Outflow boundary: zero adjoint value
c) Outflow boundary: zero concentration gradient	c) Close boundary: zero adjoint flux

Next consider the appropriate final-time condition for the adjoint transport equation. First examine the third term on the right-hand side of Equation 4.27. Since the initial condition for the radionuclide transport equation (e.g., zero concentration field) will not be altered by any change of the input parameters in the system region, the variation of the initial condition on C with respect to the variation in α is zero, that is,

$$[R_d \theta \psi^* \delta C]_{x,z,t=0} = 0 \ . \tag{4.35}$$

We are left with the first and the third terms on the right-hand side of Equation 4.27. The variation of K will be stationary with respect to the variation of C if the following condition is met.

$$[R_d \theta \psi^* \delta C]_{x,z,t=t_f} = \delta R_C \ . \tag{4.36}$$

The response of interest R considered in this study is exclusively the "final-time functional," that is, a functional of the radionuclide concentration field evaluated at the final time t_f. Furthermore, the left-hand side term of Equation 4.36 is a spatial integral evaluated at the final time t_f. Therefore, Equation 4.36 can provide us with the "final-time condition" for the adjoint transport problem. From Equations 4.2 and 4.6, the response of interest can be represented as the spatial integration of a generalized final-time functional F over the system region, that is,

$$R = \int_V F(x,z,t_f)dxdz = [F(x,z,t)\,\delta(t-t_f)]_{x,z,t} \tag{4.37}$$

where V represents the entire system region, and $\delta(t-t_f)$ is the Dirac-delta function of time at t_f. From Equation 4.37, the variation of R with respect to the variation of C becomes

$$\delta R_C = [(\partial F/\partial C)\,\delta(t-t_f)\,\delta C]_{x,z,t} \cdot \tag{4.38}$$

The final condition for the adjoint transport equation (Equation 4.30) will be specified for the two types of response of interest described previously in this chapter.

(1) Space-average concentration in a specified region A:

Equation 4.2 can be written as

$$R_C = [\frac{1}{A}\, C(x,z,t)\,\delta(x,z;A)\,\delta(t-t_f)]_{x,z,t} \cdot \tag{4.39}$$

Comparing Equations 4.39 and 4.37, we obtain

$$F(x,z,t) = \frac{1}{A}\, C(x,z,t)\,\delta(x,z;A) \cdot \tag{4.40}$$

The derivative of F with respect to C gives

$$\frac{\partial F(x,z,t)}{\partial C(x,z,t)} = \frac{1}{A}\,\delta(x,z;A) \cdot \tag{4.41}$$

Equation 4.36 can be written as

$$[R_d\,\theta\psi^*\,\delta(t-t_f)\,\delta C]_{x,z,t} - \delta R_C = 0 \cdot \tag{4.42}$$

Substituting Equations 4.41 into 4.38, then into 4.42, we have

$$[(R_d\,\theta(x,z)\,\psi^*(x,z,t) - \frac{1}{A}\,\delta(x,z;A))\,\delta(t-t_f)\,\delta C(x,z,t)]_{x,z,t} = 0 \,, \tag{4.43}$$

or

$$[(R_d\theta(x,z)\psi^*(x,z,t_f) - \frac{1}{A}\,\delta(x,z;A))\delta C(x,z,t_f)]_{x,z} = 0 \ . \qquad (4.44)$$

For arbitrary variation of C, Equation 4.44 leads to the final condition for the adjoint transport equation

$$\psi^*(x,z,t_f) = \frac{\delta(x,z;A)}{R_d\theta(x,z)A} \qquad (4.45)$$

where $\delta(x,z;A)$ was defined by Equation 4.3. In the FLIDE mathematical formulation, the final condition for the adjoint transport equation defined in Equation 4.45 is implemented to be

$$\psi^*_{i,k}(t_f) = \begin{cases} \dfrac{1}{R_d\theta_{i,k}A_r} & \text{, for discrete-element } (i,k) \text{ in } A \\ 0 & \text{, otherwise} \end{cases} \qquad (4.46)$$

where A_r is the area of the specified response region.

(2) Radionuclide mass flow rate through the outflow boundary:

From Equation 4.6,

$$R_J = [\hat{n}\cdot\bar{v}(x,z)C(x,z,t)\,\delta(x,z;OB)\,\delta(t-t_f)]_{x,z,t} \ . \qquad (4.47)$$

Comparing Equations 4.47 and 4.37, we have

$$F(x,z,t) = v_n(x,z)C(x,z,t)\,\delta(x,z;OB) \qquad (4.48)$$

where $v_n(x,z)$ is the normal component of Darcian velocity at the point (x,z) in space.

The derivative of F with respect to C is

$$\frac{\partial F(x,z,t)}{\partial C(x,z,t)} = v_n(x,z)\,\delta(x,z;OB) \ . \qquad (4.49)$$

After combining Equations 4.36, 4.38, and 4.49, we obtain

$$[(R_d\theta(x,z)\psi^*(x,z,t_f) - v_n(x,z)\delta(x,z;OB))\delta C(x,z,t_f)]_{x,z} = 0 \ . \quad (4.50)$$

For an arbitrary variation of C, Equation 4.50 leads to

$$\psi^*(x,z,t_f) = \frac{v_n(x,z)\delta(x,z;OB)}{R_d\theta(x,z)} \quad (4.51)$$

where $\delta(x,z;OB)$ was defined by Equation 4.7. In the discrete-element mathematical formulation, we implement Equation 4.51 to be

$$\psi^*_{i,k}(t_f) = \frac{G_{x_{i,k}} + G_{z_{i,k}}}{R_d\theta_{i,k}A_{i,k}} \quad (4.52)$$

for the discrete-element (i,k) on the outflow boundary, where $G_{x_{i,k}}$, $G_{z_{i,k}}$ are the groundwater flow rates in x and z directions on the boundary enclosures of element (i,k) and $A_{i,k}$ is the area of this boundary element (on x-z plane).

We have completed the derivation of the adjoint transport equation by considering the stationarity of the variation of K with respect to the variation of C. In summary, the adjoint transport problem which corresponds to the radionuclide transport problem is completely specified by the adjoint transport equation (Equation 4.30), the boundary conditions listed in Table 4.1, and the final conditions defined by Equations 4.46 and 4.52 for two types of response of interest. Note that the adjoint transport problem can be characterized as a "final-value problem" just as the radionuclide transport problem was characterized as an "initial-value problem." This adjoint transport problem at the reference state of the input parameters will

be solved in Chapter V. The solutions of the adjoint transport problem (i.e., time-dependent adjoint fields) will be used in conjunction with the time-dependent concentration fields to produce relative sensitivity coefficient fields.

D. Relative Sensitivity Coefficient Fields

Consider Equation 4.24 to formulate the relative sensitivity coefficient field of response of interest R to input parameter $\alpha(x,z)$. We take a partial derivative of the functional K defined in Equation 4.14 with respect to the parameter α.

$$\frac{\partial K}{\partial \alpha} = \frac{\partial R}{\partial \alpha} + \left[\psi^* \frac{\partial L(\alpha)}{\partial \alpha} C\right]_{x,z,t} . \tag{4.53}$$

Since the responses of interest considered in this dissertation are not explicit functions of any input parameter, we have

$$\frac{\partial R}{\partial \alpha} = 0 . \tag{4.54}$$

Substituting Equations 4.54 into 4.53, then into 4.24, and writing out the system variables x,z,t explicitly, the relative sensitivity coefficient field of the response R to the input parameter α at the phase space point (x,z,t) becomes

$$S_\alpha(x,z) = \frac{\alpha(x,z)}{R} \left[\psi^*(x',z',t') \frac{\partial L[\alpha(x',z',t')]}{\partial \alpha(x,z,t)} C(x',z',t')\right]_{x',z',t',t} . \tag{4.55}$$

The derivative of the radionuclide transport operator L with the parameter α in phase space (x',z',t') with respect to α in phase space

(x,z,t) generates a time Dirac-delta function of t' at t because the parameters at phase space points (x',z',t') and (x,z,t) are independent of each other. That is,

$$\frac{\partial L[\alpha(x',z',t')]}{\partial \alpha(x,z,t)} = \frac{\partial L[\alpha(x',z')]}{\partial \alpha(x,z)} \delta(t'-t) \ . \tag{4.56}$$

Substituting Equations 4.56 into 4.55, carrying out the time integration over t', we obtain the relative sensitivity coefficient field in integral form as

$$S_\alpha(x,z) = \frac{\alpha(x,z)}{R} \int_0^{t_f} \iint_V \psi^*(x',z',t) \frac{\partial L[\alpha(x',z')]}{\partial \alpha(x,z)} C(x',z',t)dx'dz'dt \ , \tag{4.57}$$

where V represents the entire system region.

Equation 4.57 is the basis for the calculations of the relative sensitivity coefficients to be presented in Chapter VI.

The relative sensitivity coefficient $S_\alpha(x,z)$ can be interpreted as the sensitivity of the radionuclide transportive flow rate at space (x',z') with respect to the variation of parameter α at (x,z) (i.e., $\partial LC/\partial\alpha(x,z)$) weighted by the adjoint value ψ^* at (x',z') (importance to the response R) and integrated over all space and time. The numerical implementation of Equation 4.57 in the FLIDE formulation and the numerical demonstration on the hypothetical sample problem will be presented in Chapter VI.

The calculations of the relative sensitivity coefficient fields of the response R to the parameter α will be performed as follows:

(i) Solve the radionuclide transport problem at the reference state of the input data (as was done in Chapter III), store the time-dependent radionuclide concentration fields from time zero to time t_f in the magnetic disk;

(ii) Solve the adjoint transport problem at the reference state of the input data and store the time-dependent adjoint fields from time t_f back to time zero in the magnetic disk (will be done in Chapter V);

(iii) Retrieve the radionuclide concentration fields and the corresponding adjoint fields from time zero to the final time t_f, and "fold" them together by using Equation 4.57 to obtain the relative sensitivity coefficient field $S_\alpha(x,z)$.

E. Uncertainty Analysis

Having the capability of determining the relative sensitivity coefficients, we now develop the uncertainty in response due to the uncertainties in the input parameter data by employing the relative sensitivity coefficient fields in conjunction with the uncertainty files of the input parameter data.

Consider the uncertainty in the response due to a small perturbation (uncertainty) of any parameter from its reference-state value. Let $\alpha'(x,z)$ represent the perturbed value of the parameter α at location (x,z). The uncertainty of α at (x,z) is defined as

$$\delta\alpha(x,z) = \alpha'(x,z) - \alpha(x,z) \ . \qquad (4.58)$$

Let R' represent the response of interest corresponding to the parameter α' at the perturbed state. From Equations 4.23, 4.24, and 4.58, the percent change in R for a small uncertainty in $\alpha(x,z)$ (such that the generalized perturbation theory is valid) is

$$\frac{R' - R}{R} = \frac{\delta R}{R} = \left[S_\alpha(x,z) \frac{\alpha'(x,z) - \alpha(x,z)}{\alpha(x,z)}\right]_{x,z} . \tag{4.59}$$

Equation 4.59 states that the percent uncertainty in the response due to the uncertainty in the parameter can be calculated by integrating the relative sensitivity coefficient field times the percent change in $\alpha(x,z)$ over the system region. For the case of a space-independent parameter α, Equation 4.59 can be simplified to be

$$\frac{R' - R}{R} = \left[S_\alpha(x,z)\right]_{x,z} \frac{\alpha' - \alpha}{\alpha} . \tag{4.60}$$

Define the total relative sensitivity coefficient of R to the fixed-value parameter α to be the space integral of the relative sensitivity coefficient field over the entire system region, i.e.,

$$P_\alpha = \left[S_\alpha(x,z)\right]_{x,z} . \tag{4.61}$$

In the FLIDE formulation, P_α become

$$P_\alpha = \sum_{(i,k)} S_{\alpha_{i,k}} A_{i,k} \tag{4.62}$$

for all element (i,k) in the system region, where $S_{\alpha_{i,k}}$ is the relative sensitivity coefficient in element (i,k), $A_{i,k}$ is the area of that

element. Now the percent change in R due to the percent change in α will be calculated by the equation

$$\frac{\Delta R}{R} = P_{\alpha} \frac{\Delta \alpha}{\alpha} . \tag{4.63}$$

So far what has been done regarding the uncertainty analysis is the estimation of the uncertainty in the response of interest due to the deviation of a single input parameter from its reference value. We now explore the uncertainty analysis for the radionuclide transport calculations, which can be used to determine the standard deviations of the responses of interest due to the uncertainties in data collection of all the input parameters. This uncertainty analysis can be done by utilizing the sensitivity coefficients previously presented in conjunction with the covariance file for the basic hydrogeological data to determine uncertainties in responses of interest.

Suppose there are M parameters in the input data to be addressed in the uncertainty analysis designated as $\alpha_1, \alpha_2, \ldots, \alpha_M$. Each of the parameters contains a collection of N different values, e.g., $\alpha_{m1}, \alpha_{m2}, \ldots, \alpha_{mN}$ for m^{th} parameter. For example, dispersivities and retardation factor may have different values obtained from laboratory or field measurements. Let the parameter data of each collection form a "data vector" $\underline{Q}(\alpha)$. For i^{th} collection, we have the i^{th} data vector

$$\underline{Q}_i(\alpha) = (\alpha_{1i}, \alpha_{2i}, \ldots, \alpha_{Mi}) . \tag{4.64}$$

By summing N values of each parameter and dividing by N, we obtain the mean data vector

$$\bar{\underline{Q}}(\alpha) = (\bar{\alpha}_1, \bar{\alpha}_2, \ldots, \bar{\alpha}_M) \tag{4.65}$$

with the m^{th} component calculated by

$$\bar{\alpha}_m = \frac{1}{N} \sum_{i=1}^{N} \alpha_{mi} \cdot \tag{4.66}$$

With this mean data vector as the input parameter data, the expected value of the response is calculated to be R. Corresponding to each data vector $\underline{Q}_i$, the response R_i can be calculated. Then the statistical distribution of all such possible calculated response values due to the distribution of the collection of N data vectors is described by the response variance given by

$$V = \frac{1}{N} \sum_{i=1}^{N} (R_i - R)^2 \cdot \tag{4.67}$$

Expanding R_i in a first-order Taylor series about the expectation value R yields

$$R_i = R + \left[\left(\frac{\partial R}{\partial \underline{Q}(x,z)} \right)^T \Delta \underline{Q}_i(x,z) \right]_{x,z} \cdot \tag{4.68}$$

Substituting Equation 4.68 into Equation 4.67 results in

$$V = \frac{1}{N} \sum_{i=1}^{N} \left(\left[\frac{\partial R^T}{\partial \underline{Q}} \Delta \underline{Q}_i \right]_{x,z} \right)^2 \cdot \tag{4.69}$$

We define a diagonal matrix of the form

$$\underline{\underline{D}} = \begin{bmatrix} \bar{\alpha}_1 & 0 & \cdots & 0 \\ 0 & \bar{\alpha}_2 & \cdots & 0 \\ \vdots & & & \\ 0 & 0 & \cdots & \bar{\alpha}_M \end{bmatrix} \tag{4.70}$$

where $\bar{\alpha}_1$, $\bar{\alpha}_2$, ..., $\bar{\alpha}_M$ are the components of the mean data vector $\bar{\underline{Q}}(\alpha)$. Now Equation 4.69 can be put in another form

$$V = \left[\frac{1}{N} \sum_{i=1}^{N} \left(\frac{\partial R^T}{\partial \underline{Q}} \underline{\underline{D}} \, \underline{\underline{D}}^{-1} \, \Delta \underline{Q}_i \right)^2 \right]_{x,z} , \tag{4.71}$$

or

$$V = R^2 \left[\frac{1}{N} \sum_{i=1}^{N} \left(\frac{\underline{\underline{D}}}{R} \frac{\partial R}{\partial \underline{Q}} \right)^T \left(\underline{\underline{D}}^{-1} \Delta \underline{Q}_i \, \Delta \underline{Q}_i^T \underline{\underline{D}}^{-1} \right) \left(\frac{\underline{\underline{D}}}{R} \frac{\partial R}{\partial \underline{Q}} \right) \right]_{x,z} . \tag{4.72}$$

Finally, the relative response variance is defined to be

$$\frac{V}{R^2} = \left[\underline{P}^T(x,z) \underline{\underline{C}}(x,z) \underline{P}(x,z) \right]_{x,z} \tag{4.73}$$

where

$$\underline{P}(x,z) = \frac{\underline{\underline{D}}(x,z)}{R} \frac{\partial R}{\partial \underline{Q}(x,z)} , \tag{4.74}$$

$$\underline{\underline{C}}(x,z) = \frac{1}{N} \sum_{i=1}^{N} \left(\underline{\underline{D}}^{-1}(x,z) \Delta \underline{Q}_i(x,z) \Delta \underline{Q}_i^T(x,z) \underline{\underline{D}}^{-1}(x,z) \right) . \tag{4.75}$$

The vector $\underline{P}(x,z)$ is called the "relative sensitivity coefficient vector," whose components consist of the relative sensitivity

coefficient fields of R to the components of the mean data vector. And the matrix $\underline{\underline{C}}(x,z)$ is called the "relative data covariance matrix," which is the mean matrix of these N data matrices of the form

$$\underline{\underline{C}}_i = \underline{\underline{D}}^{-1} \Delta\underline{Q}_i \Delta\underline{Q}_i^T \underline{\underline{D}}^{-1}$$

$$= \begin{bmatrix} \left(\frac{\alpha_{1i} - \bar{\alpha}_1}{\bar{\alpha}_1}\right)^2 & \left(\frac{\alpha_{1i} - \bar{\alpha}_1}{\bar{\alpha}_1}\right)\left(\frac{\alpha_{2i} - \bar{\alpha}_2}{\bar{\alpha}_2}\right) & \cdots \\ \left(\frac{\alpha_{2i} - \bar{\alpha}_2}{\bar{\alpha}_2}\right)\left(\frac{\alpha_{1i} - \bar{\alpha}_1}{\bar{\alpha}_1}\right) & \left(\frac{\alpha_{2i} - \bar{\alpha}_2}{\bar{\alpha}_2}\right)^2 & \\ \vdots & & \end{bmatrix}. \qquad (4.76)$$

The off-diagonal elements of $\underline{\underline{C}}$ account for cross-correlations in data uncertainties between different parameters. Each element of $\underline{\underline{C}}$ is generally space-dependent. Notice that there are only correlations between any two parameters corresponding to the same space point (x,z).

In summary, the uncertainty analysis for the radionuclide transport by groundwater flow is performed by the following steps:

(i) Collect all the input parameter data required by the radionuclide transport calculations;

(ii) Calculate the mean values for all the parameters by Equation 4.66;

(iii) Calculate the expectation value of the response of interest from the radionuclide transport calculation with the mean parameter data determined in step (ii);

(iv) Compute the relative sensitivity coefficient fields for all the parameters at the reference state (i.e., mean parameter data), and form the relative sensitivity coefficient vector by Equation 4.74;

(v) Construct data covariance fields from the uncertainty data and the mean data using Equations 4.75 and 4.76;

(vi) Compute the relative response variance from Equation 4.73. Then the relative standard deviation of the response is calculated by

$$\sigma_R = (V/R^2)^{1/2} \ . \qquad (4.77)$$

CHAPTER V

SOLUTION AND INTERPRETATION OF THE ADJOINT TRANSPORT EQUATION

In this chapter we will discuss the methodology developed for solving the adjoint transport equation derived in the last chapter. The solution of the adjoint transport equation and the physical interpretation of the adjoint functions for the hypothetical sample problem in Chapter III will also be presented in this chapter.

The adjoint transport equation derived for the radionuclide transport equation is rewritten here for convenience,

$$R_d \theta \frac{\partial \psi^*}{\partial t} = -\nabla \cdot \bar{\bar{D}} \nabla \psi^* - \bar{v} \cdot \nabla \psi^* + R_d \theta \lambda \psi^*. \qquad (5.1)$$

As previously discussed, Equation 5.1 together with the appropriate boundary and final conditions for the specified responses of interest formulated in Chaper IV constitutes a complete final-value adjoint transport problem. This final-value problem can be solved with minimal difficulty by utilizing the same computer program used for solving the radionuclide transport equation. However, some modifications in the adjoint transport equation need to be made in order to perform the adjoint calculation properly. Equation 5.1 will be transformed to a form compatible with that of the radionuclide transport equation so that the computer program developed for the radionuclide transport simulation (i.e., computer code RADMIG) can be utilized to solve the adjoint transport equation.

First, we note that the convective term in the adjoint transport equation (Equation 5.1) is the vector product of the Darcian velocity vector and the gradient of the adjoint function, i.e., $\bar{v}\cdot\nabla\psi^*$, instead of the divergence of the product of the velocity vector and the adjoint function $\nabla\cdot\bar{v}\psi^*$. However, these two terms are related to each other by the following equation from the vector calculus.

$$\bar{v}\cdot\nabla\psi^* = \nabla\cdot\bar{v}\psi^* - \psi^*\nabla\cdot\bar{v} \ . \tag{5.2}$$

Substituting Equation 5.2 into the second term on the right-hand side of Equation 5.1 yields

$$R_d\theta\frac{\partial\psi^*}{\partial t} = -\nabla\cdot\bar{\bar{D}}\nabla\psi^* - \nabla\cdot\bar{v}\psi^* + R_d\theta\lambda\psi^* + \psi^*\nabla\cdot\bar{v} \ . \tag{5.3}$$

As a result, Equation 5.3 has the addition of the term $\psi^*\nabla\cdot\bar{v}$ on its right-hand side, which accounts for the divergence of the velocity field $\nabla\cdot\bar{v}$. For an incompressible steady-state goundwater flow, the term $\nabla\cdot\bar{v}$ vanishes from the continuity equation.

$$\nabla\cdot\bar{v} = -\frac{\partial\rho}{\partial t} = 0, \tag{5.4}$$

where ρ is the water density. In our study it is assumed that a steady-state groundwater flow has developed before radionuclides begin to transport in the groundwater flow system. Therefore, theoretically speaking, $\nabla\cdot\bar{v}$ should be zero. But in a practical situation, this term does not necessarily vanish because the numerical model used for solving the steady-state groundwater flow transport problem may not be very accurate. If we examine the groundwater flow rate data in the discrete elements, which were obtained by bilinearly interpolating the Darcian

velocities from the finite-element grid system to the discrete-element grid system, we would find mass conservation errors in the groundwater flow in some discrete elements. Therefore, this term should be kept in the adjoint transport equation and implemented in the numerical solution.

Further comparison between Equation 5.3 and the radionuclide transport equation (Equation 2.8) indicates that signs of the dispersive term and the radioactive decay loss term (the first and the third terms) are different. The sign reversal of the time derivative term in both the forward and adjoint equations implies that the forward equation is to be solved by advancing time in a forward manner (same as the real time) from the initial time to the final time, while the adjoint equation is to be solved by marching the time in a backward manner from the final time back to the initial time. Therefore, the adjoint transport problem can be characterized as a final-value problem just as the radionuclide transport problem is characterized as an initial-valve problem. We now solve the adjoint final-value problem by first reversing the sign of the time variable in the adjoint transport equation and then using the same computational technique developed for solving the radionuclide transport problem.

The reversal of the time variable sign can be accomplished by change of variable in time. From Equation 5.3 the time-dependent adjoint transport equation becomes

$$R_d \theta \frac{\partial \psi^*(t)}{\partial t} = -\nabla \cdot \bar{D}^+ \nabla \psi^*(t) - \nabla \cdot \bar{v} \psi^*(t) + R_d \theta \lambda \psi^*(t) + \psi^*(t) \nabla \cdot \bar{v}, \quad (5.5)$$

$$0 \leq t < t_f .$$

The final-time condition $\psi^*(t=t_f)$ can be determined for the specified response of interest. Making a change of variable in t by defining

$$\tau = t_f - t, \tag{5.6}$$

$$\frac{d}{d\tau} = -\frac{d}{dt}, \tag{5.7}$$

and $$\psi^*(\tau=0) = \psi^*(t=t_f) . \tag{5.8}$$

Then the adjoint transport problem becomes

$$R_d\theta \frac{\partial\psi^*(\tau)}{\partial\tau} = \nabla\cdot\bar{\bar{D}}^+\nabla\psi^*(\tau) + \nabla\cdot\bar{v}\psi^*(\tau) - R_d\theta\lambda\psi^*(\tau) - \psi^*(\tau)\nabla\cdot\bar{v} , \tag{5.9}$$

$$0 < \tau \leq t_f$$

with $\psi^*(\tau=0) = \psi^*(t=t_f)$ as the initial condition for the "time-reversed" adjoint equation. This "time-reversed" adjoint transport problem can be solved in the same manner as was the radionuclide transport problem by marching the time variable forward form $\tau=0$ to $\tau=t_f$.

Comparing Equation 5.9 with Equation 2.8 we observe that the sign of the second term on the right-hand side of Equation 5.9, namely, the convective term, is different. Roache[30] pointed out that the solution of the mass transport equation of the form

$$\frac{\partial\xi}{\partial t} = D\frac{\partial^2\xi}{\partial x^2} + v\frac{\partial\xi}{\partial x}$$

is unstable. Whereas the solution of the differential equation

$$\frac{\partial\xi}{\partial t} = D\frac{\partial^2\xi}{\partial x^2} - v\frac{\partial\xi}{\partial x}$$

is stable. In order to have a stable solution and make Equation 5.9 compatible in form with the radionuclide transport equation, the sign of

the convective term must be reversed. This is accomplished by defining a reverse Darcian velocity vector

$$\bar{v}_r = -\bar{v}. \tag{5.10}$$

Then Equation 5.9 can be written as

$$R_d\theta \frac{\partial \psi^*}{\partial \tau} = \nabla\cdot\bar{\bar{D}}^+\nabla\psi^* - \nabla\cdot\bar{v}_r\psi^* - R_d\theta\lambda\psi^* + \psi^*\nabla\cdot\bar{v}_r. \tag{5.11}$$

It is obvious that negating the velocity vector field has the same effect as reversing the groundwater flow directions.

The sign of the dispersive term in Equation 5.11 (the first term on the right-hand side) remains unchanged after the reversal of the groundwater flow directions. It is because the elements in the hydrodynamic dispersion coefficient tensor $\bar{\bar{D}}$ depend only on the magnitudes of the velocity components, not on the velocity directions (see Equation 2.7). In our case the off-diagonal elements of the dispersion coefficient tensor are zero, therefore, $\bar{\bar{D}}^+ = \bar{\bar{D}}$. The modified adjoint transport equation (Equation 5.11) has the same form as the forward radionuclide transport equation (Equation 2.8) with the exception of the addition of the "convection-defect" term $\psi^*\nabla\cdot\bar{v}_r$.

We now summarize the method for solving the adjoint transport problem based on the investigations in Chapter IV and this chapter as follows:

(i) Reverse the time coordinate so that the final-value adjoint problem becomes the "initial-value adjoint problem" with the initial conditions defined by Equations 5.8, 4.46, and 4.52;

(ii) Reverse the directions of the groundwater flow field (i.e.,

negate the groundwater flow rates, Darcian velocity components throughout the flow system region);

(iii) Modify the radionuclide transport simulation code RADMIG by implementing the changes made in steps (i) and (ii), and adding the discrete-element formulation of the convection-defect term $\psi^* \nabla \cdot \overline{v}_r$ into the program module CONVEC. The adjoint transport simulation computer code ADJMIG (ADJoint MIGration) was developed;

(iv) Employ computer code ADJMIG to solve the adjoint transport problem which is composed of Equation 5.11, boundary conditions listed in Table 4.1 (p. 73), and initial conditions previously mentioned. The adjoint function fields are computed by marching the time from final time $t=t_f$ ($\tau=0$) to initial time $t=0$ ($\tau=t_f$) with the same time-step size Δt as was used in the radionuclide transport simulation;

(v) Store the computed adjoint fields in magnetic disk for the use of the sensitivity calculation.

We now present the solution of the adjoint transport equation and the physical interpretation of the adjoint function for the sample problem used in Chapter III to (a) illustrate the properties of the adjoint function, and (b) demonstrate the usefulness of the adjoint approach in the radionuclide transport sensitivity analysis. We first consider the physical significance that the adjoint function has from the point of view of its mathematical derivation. Recall from Chapter IV that the adjoint function is incorporated together with the radionuclide transport term to produce the relative sensitivity coefficient (see Equation 4.57). The adjoint function $\psi^*(x,z,t)$ can be interpreted as being the "response-importance" because it is used as the

"weighting-function" to evaluate the variation in the specified response of interest. The adjoint function have the following definition:

$\psi^*(x,z,t)$ = importance of the radionuclide concentration $C(x,z,t)$ at space (x,z) and time t to the response of interest at time t_f.

= probability at space (x,z) and time t per unit area that the radionuclide concentration at space (x,z) and time t will contribute to the response of interest at final time t_f.

We now examine the transport of these "adjoints" in space and time imagining that these adjoint function values, like radionuclides, can move in the groundwater flow system through the mechanisms of dispersion, convection, and can also suffer "radioactive decay." As previously discussed, the adjoint transport problem can be characterized as a final-value problem. In other words, the adjoint field at final time t_f (i.e., final conditions) must first be known, then the solutions (adjoint fields) prior to t_f can be determined from these final conditions. The final conditions are related to the specified response of interest by being the importance-values to that response. We observe that there is no internal source at all time in both the forward and adjoint equation (i.e., both differential equations are homogeneous). Therefore, the final conditions serve as the only adjoint source (only at time t_f) to the adjoint transport equation. For example, suppose the response of interest for a radionuclide transport problem is the space-average radionuclide concentration in a discrete-element located downstream of the groundwater flow near the outflow boundary at final

time t_f. Then the final conditions for the adjoint function are specified according to Equation 4.46 such that the adjoint field at time t_f is everywhere zero except at the specified discrete element where the adjoint value has probability (importance) of unity in contributing to the response of interest with the computed concentration field at t_f.

We now look at two numerical examples. For the case of radionuclide transport problem, the concentration fields correspond only to the specific input parameter values because the initial conditions are independently specified. But in the case of adjoint transport calculations, we have different time-dependent adjoint fields determined by different final conditions which in turn are based on the specified response of interest, even though the same input parameter values are used. The same set of input parameter data was used for the adjoint transport calculations as was used in Chapter III for the radionuclide transport simulations, that is, radionuclide = H-3, a_L = 10m, a_T = 5m, R_d = 1, Darcian velocity field and water content field were taken from Chapter III. The adjoint transport calculations were made for two different responses of interest. Two-dimensional contour plots of the time-dependent adjoint fields were presented for each response case.

Simulation Case 1

The response of interest in the first case of adjoint transport calculation is the space-average tritium concentration in region ZONE-1 as shown in Figure 5.1 at the final time of 10 days. The final conditions were zero everywhere except in the region ZONE-1 where the adjoint values were determined by Equation 4.46. The transient

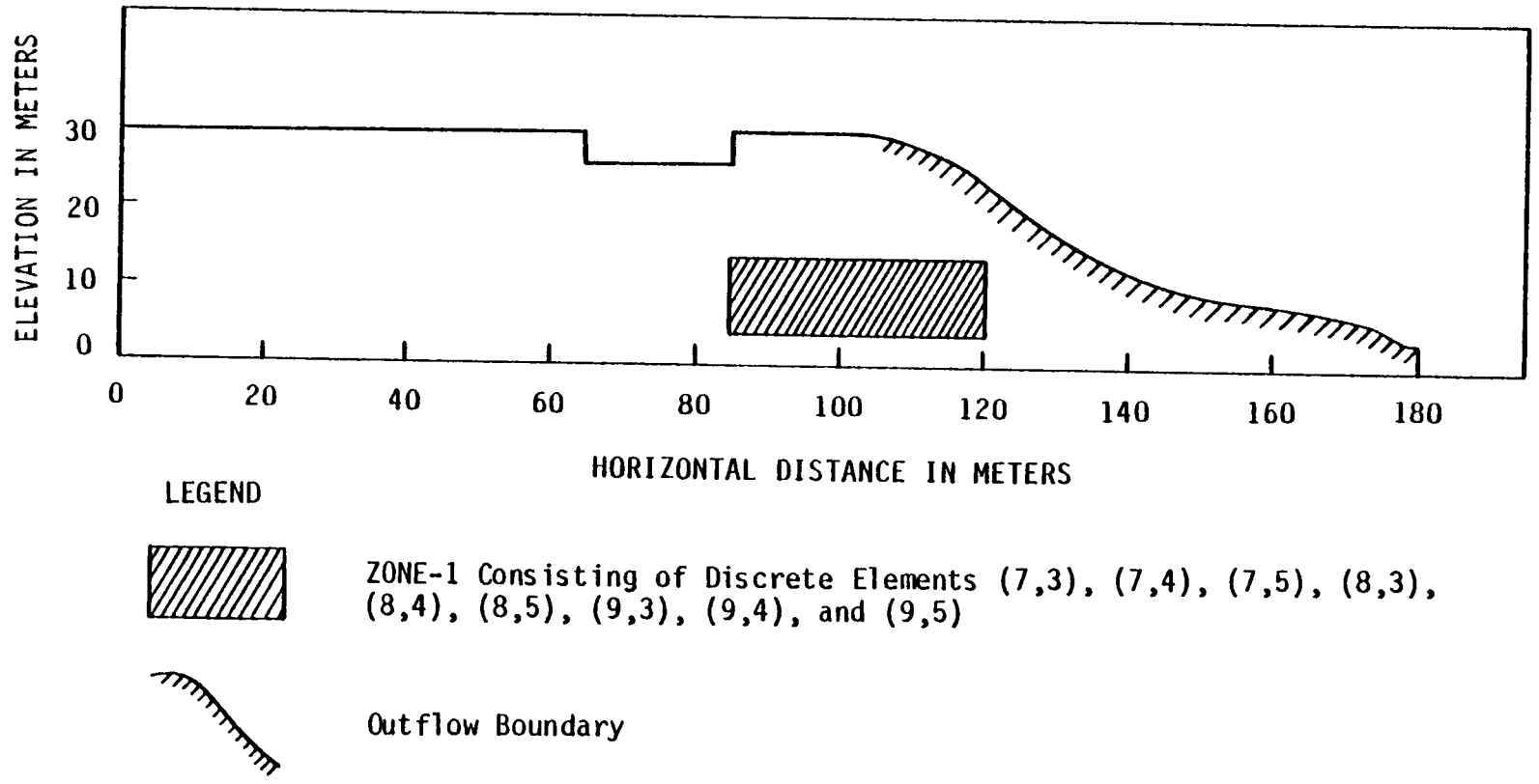

Figure 5.1. Schematic Representation of the Response Regions for the Adjoint Transport Calculation.

adjoint fields from t = 0 to t = 9 days (in real-time coordinate) were illustrated in 2-D contour plots as shown in Figure 5.2. Note that the adjoint values have the unit of $1/m^2$ (for 2-D geometry). Since the adjoint transport is a final-value problem, the simulation begins with final conditions at t = 10 days (because the response of interest was specified at t = 10 days) and proceeds backward in time to t = 0. One should examine these graphs in reverse-time sequence, that is, from t = 9 days to t = 0. We see that the adjoint value interpreted as the importance to the response is highest in the response region and decreases as we go out away from that region. As "adjoint" time goes by, (or real-time shortens) the adjoint contours (i.e., isoadjoint lines) disperse out in both upstream and downstream directions. We can also see that the adjoint value dilutes with the decrease in real time. This is why some inner contours shrink and then disappear. We also notice that same adjoint contours tend to move toward the bottom of the trench. This phenomenon is due to convection because the groundwater flow directions were reversed in the adjoint calculation. The convective transport of the adjoint values in reversed groundwater flow directions is not so obvious because the dispersion effect is large due to large dispersivity values used. The dilution of the adjoint values (due to dispersion) results from the fact that there is no adjoint source in the system except the final conditions.

We can also view the adjoint transport in real time coordinate as follows. At t = 0, the predicted adjoint field (in adjoint time sense) portrays the potential (importance) that the radionuclide concentration field at this time would contribute to the response at t = 10 days.

Isoadjoint Contours 1-7 at Values of 0.0001, 0.00025, 0.0005, 0.00075, 0.001, 0.0025, and 0.005 $1/m^2$

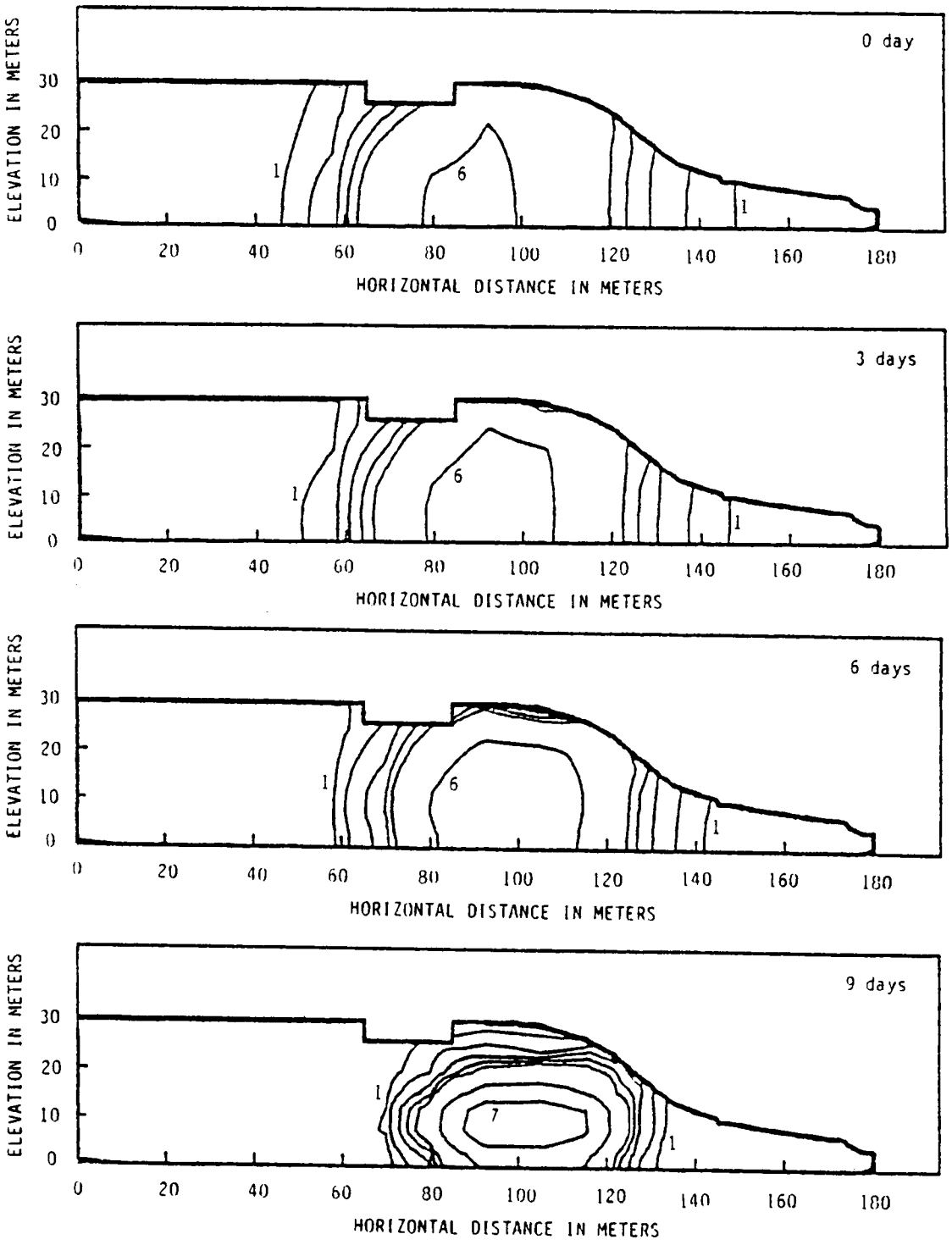

Figure 5.2. Time-Dependent Adjoint Fields for Adjoint Calculation Case 1.

Then the adjoint values are concentrating toward the response region ZONE-1 with respect to time. That is, the potential increases and becomes more concentrated around the response region. Finally, the final conditions at t = 10 days will be reached when only the concentrations within the response region contribute to the response of interest.

Simulation Case 2

We next consider the tritium discharge rate (Ci/day) on the outflow boundary at t = 10 days as the second response of interest (see Figure 5.1). The final-time conditions were everywhere zero except on the outflow boundary where the adjoint values were specified according to Equation 4.52 and have the unit of m/day. The description of the adjoint transport in the present case is similar to that in the first case except that the adjoint-value contours always move upstream from the outflow boundary toward the source boundary (bottom of the burial trench). As can be seen from the adjoint plots depicted in Figure 5.3, the adjoint values at t = 9 days were concentrated near the outflow boundary with the middle part of the boundary having the highest values (due to the high outgoint groundwater flow velocity). As the adjoint time increases, the adjoint values convect, disperse toward the central part of the system region. That is, the adjoint values are essentially moving from the outflow boundary to the left, because the groundwater is mainly flowing from the central part (beneath the trench bottom) to the right. The dilution effect can be seen from the increasing separation between contours with the increase in the adjoint time.

Isoadjoint Contours 1-8 at Values of 0.001, 0.0025, 0.005, 0.0075, 0.01, 0.025, 0.05, and 0.075 m/day

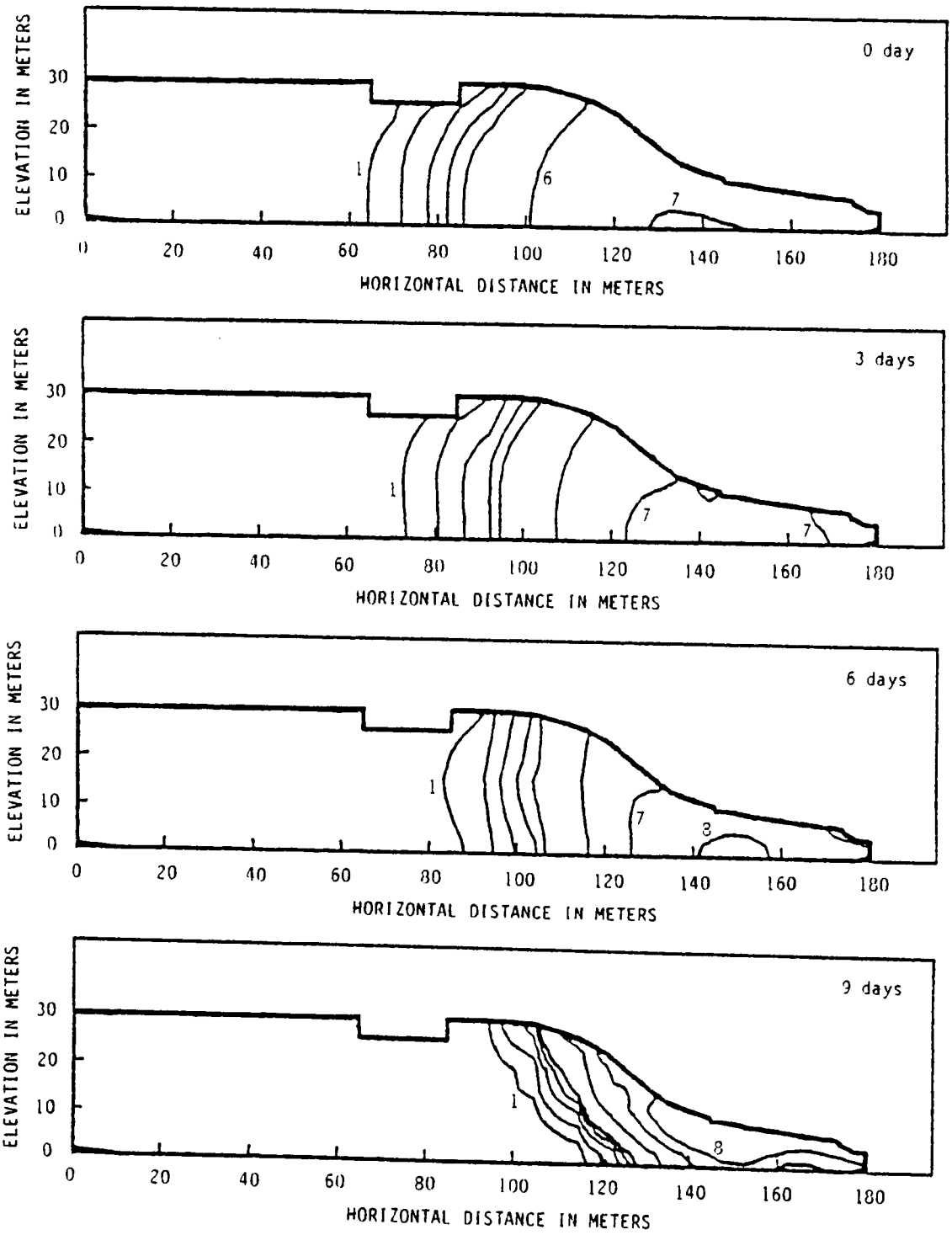

Figure 5.3. Time-Dependent Adjoint Fields for Adjoint Calculation Case 2.

CHAPTER VI

CALCULATIONS OF RELATIVE SENSITIVITY COEFFICIENTS

The relative sensitivity coefficients of the response of interest to each associated input parameter will be formulated from the sensitivity coefficient equation derived in Chapter IV and implemented into the FLIDE numerical formulation in this chapter. The spatial distributions (fields) of the relative sensitivity coefficients will be computed by combining the time-dependent radionuclide concentration and adjoint fields together in the discrete-element grid system for the sample problem given in Chapter III. The relative sensitivity coefficient fields will be presented and followed by physical interpretations and discussions. Procedures for performing the sensitivity coefficient calculations will also be given.

A. Sensitivity Coefficients Formulation

Formulate the relative sensitivity coefficients in the discrete-element numerical formulation based on the sensitivity coefficient equation, Equation 4.57, which is rewritten here for convenience.

$$S_{\alpha}(\bar{r}) = \frac{\alpha(\bar{r})}{R} \int_0^{t_f} \left[\int_V \psi^*(\bar{r}',t) \frac{\partial L[\alpha(\bar{r}')]}{\partial \alpha(\bar{r})} C(\bar{r}',t)\, d\bar{r}' \right] dt \qquad (6.1)$$

where R is a final-time response of interest, $\alpha(\bar{r})$ is a specified parameter at space point $\bar{r}$ and is independent of time. Recall from

Chapter IV that the input parameter α can be any one of five parameters. They are longitudinal dispersivity a_L, transverse dispersivity a_T, retardation factor R_d, water content field $\theta(\bar{r})$, and radionuclide decay constant λ. L is the linear differential operator for the radionuclide transport by groundwater flow. The operator L contains the addressed input parameters and has the form shown in Equation 4.10. $C(\bar{r},t)$ and $\psi^*(\bar{r},t)$ are the time-dependent solutions of the radionuclide transport equation and the adjoint transport equation, respectively.

Sensitivity Coefficients to Longitudinal and Transverse Dispersivities

First consider the sensitivity coefficients of the response of interest with respect to the parameters of longitudinal dispersivity a_L and transverse dispersivity a_T. These two parameters are only concerned with the dispersive term in the radionuclide transport equation. Let $a(\bar{r})$ represent the parameter of either a_L or a_T at space point $\bar{r}$. The partial derivative of the radionuclide transport expression $L[a(\bar{r}')]\,C(\bar{r}',t)$ with respect to $a(\bar{r})$ involves the dispersive term, i.e.,

$$\frac{\partial}{\partial a(\bar{r})} L[a(\bar{r}')]C(\bar{r}',t) = \frac{\partial}{\partial a(\bar{r})} \nabla\cdot\bar{\bar{D}}[a(\bar{r}')]\nabla C(\bar{r}',t) \qquad (6.2)$$

$$= \nabla\cdot\bar{\bar{D}}'_a[a(\bar{r}')]\nabla C(\bar{r}',t)$$

where $\bar{\bar{D}}'_a[(\bar{r}')]$ is the derivative of the dispersion coefficient $\bar{\bar{D}}[a(\bar{r}',t)]$ with respect to $a(\bar{r})$. Equation 6.2 is the sensitivity of the dispersive transport flow rate in a differential volume at location $\bar{r}'$ with respect to the parameter a at location $\bar{r}$.

The dispersion coefficient tensor at location $\bar{r}'$ has the form of

$$\bar{\bar{D}}(\bar{r}') = \begin{bmatrix} (a_L(\bar{r}')v_x^2(\bar{r}') + a_T(\bar{r}')v_z^2(\bar{r}'))/v(\bar{r}') & 0 \\ 0 & (a_T(\bar{r}')v_x^2(\bar{r}') + a_L(\bar{r}')v_z^2(\bar{r}'))/v(\bar{r}') \end{bmatrix} \tag{6.3}$$

where $v_x(\bar{r}')$, $v_z(\bar{r}')$, and $v(\bar{r}')$ are x, z components, and the magnitude of the Darcian velocity vector at location $\bar{r}'$ respectively. The partial derivative of the dispersion coefficient tensor $\bar{\bar{D}}(\bar{r}')$ with respect to longitudinal dispersivity $a_L(\bar{r})$ at $\bar{r}$ is

$$\bar{\bar{D}}'_{a_L}(\bar{r}';\bar{r}) = \frac{\partial \bar{\bar{D}}(\bar{r}')}{\partial a_L(\bar{r})}$$

$$= \begin{bmatrix} \left(\frac{\partial a_L(\bar{r}')}{\partial a_L(\bar{r})} v_x^2(\bar{r}') + \frac{\partial a_T(\bar{r}')}{\partial a_L(\bar{r})} v_z^2(\bar{r}') \right)/v(\bar{r}') & 0 \\ 0 & \left(\frac{\partial a_T(\bar{r}')}{\partial a_L(\bar{r})} v_x^2(\bar{r}') + \frac{\partial a_L(\bar{r}')}{\partial a_L(\bar{r})} v_z^2(\bar{r}') \right)/v(\bar{r}') \end{bmatrix}$$

$$= \begin{bmatrix} v_x^2(\bar{r}')\,\delta(\bar{r}'-\bar{r})/v(\bar{r}') & 0 \\ 0 & v_z^2(\bar{r}')\,\delta(\bar{r}'-\bar{r})/v(\bar{r}') \end{bmatrix} \tag{6.4}$$

where $\delta(\bar{r}'-\bar{r})$ is a space delta function defined as

$$\delta(\bar{r}'-\bar{r}) = \begin{cases} 1 & , \text{ if } \bar{r}'=\bar{r} \\ 0 & , \text{ otherwise.} \end{cases} \tag{6.5}$$

The partial derivative of $a_L(\bar{r}')$ with respect to $a_L(\bar{r})$ gives this space delta function because a change of a parameter value at a space point $\bar{r}$ does not alter the parameter value at any location but $\bar{r}$. In actuality the parameter value is always defined in a finite differential volume at location $\bar{r}$, $\delta V(\bar{r})$ in any finite-differencing numerical method. Therefore, $\delta(\bar{r}'-\bar{r})$ can be defined as follows.

$$\delta(\bar{r}'-\bar{r}) = \begin{cases} 1 & \text{, if } \bar{r}' \text{ is inside } \delta V(\bar{r}) \\ 0 & \text{, otherwise.} \end{cases} \tag{6.6}$$

The partial derivative of dispersion coefficient tensor $\bar{\bar{D}}(\bar{r}')$ with respect to transverse dispersivity $a_T(\bar{r})$ in a differential volume $\delta V(\bar{r})$ at $\bar{r}$ is

$$\bar{\bar{D}}'_{a_T}(\bar{r}';\bar{r}) = \frac{\partial \bar{\bar{D}}(\bar{r}')}{\partial a_T(\bar{r})}$$

$$= \begin{bmatrix} v_z^2(\bar{r}')\,\delta(\bar{r}'-\bar{r})/v(\bar{r}') & 0 \\ 0 & v_x^2(\bar{r}')\,\delta(\bar{r}'-\bar{r})/v(\bar{r}') \end{bmatrix} . \tag{6.7}$$

The relative sensitivity coefficient field $S_a(\bar{r})$ of the response R to the dispersivity a (a_L or a_T) now becomes (from Equation 6.1 and 4.57)

$$S_a(\bar{r}) = \frac{a(\bar{r})}{R} \int_0^{t_f} \left[\int_V \psi^*(\bar{r}',t)\, \nabla\cdot\bar{\bar{D}}'_a(\bar{r}';\bar{r})\, \nabla C(\bar{r}',t)\, d\bar{r}' \right] dt . \tag{6.8}$$

Note $\bar{\bar{D}}'_a(\bar{r}';\bar{r})$ can be written as

$$\bar{\bar{D}}'_a(\bar{r}';\bar{r}) = \bar{\bar{D}}'_a(\bar{r}')\,\delta(\bar{r}'-\bar{r}) \tag{6.9}$$

where $\overline{\overline{D}}'_a(\bar{r})$ is either $\overline{\overline{D}}'_{aL}(\bar{r};\bar{r})$ for $a = a_L$ or $\overline{\overline{D}}'_{aT}(\bar{r};\bar{r})$ for $a = a_T$, defined by Equations 6.4, 6.5, and 6.7. The volume integral over the system region V can be reduced to the volume integral over the differential volume $\delta V(\bar{r})$ about $\bar{r}$ using the definition of $\delta(\bar{r}'-\bar{r})$ in Equation 6.6, i.e.,

$$S_a(\bar{r}) = \frac{a(\bar{r})}{R} \int_0^{t_f} \left[\int_{\delta V(\bar{r})} \psi^*(\bar{r}',t)\, \nabla\cdot\overline{\overline{D}}'_a(\bar{r}')\, \nabla C(\bar{r}',t)\, d\bar{r}' \right] dt. \qquad (6.10)$$

Equation (6.10) will be converted into finite-differencing form in the two-dimensional discrete-element numerical formulation. We operate the dispersion coefficient derivative tensor $\overline{\overline{D}}'_{aL}(\bar{r})$ on the gradient of concentration $\nabla C(\bar{r},t)$ in the two dimensional (x,z) coordinate system to get

$$\overline{\overline{D}}'_{aL}(\bar{r})\, \nabla C(\bar{r},t) = \begin{bmatrix} v_x^2/v & 0 \\ 0 & v_z^2/v \end{bmatrix} \begin{bmatrix} \frac{\partial C}{\partial x} \\ \frac{\partial C}{\partial z} \end{bmatrix}$$

$$= \frac{v_x^2}{v} \frac{\partial C}{\partial x}\, \hat{i} + \frac{v_z^2}{v} \frac{\partial C}{\partial z}\, \hat{k}. \qquad (6.11)$$

Note that the left-hand side of Equation 6.11 is to be evaluated at space $\bar{r}$ and time t. Taking divergence on Equation 6.11, we get

$$\nabla\cdot\overline{\overline{D}}'_{aL}\, \nabla C = \frac{\partial}{\partial x} \left(\frac{v_x^2}{v} \frac{\partial C}{\partial x}\right) + \frac{\partial}{\partial z} \left(\frac{v_z^2}{v} \frac{\partial C}{\partial z}\right) \qquad (6.12)$$

which is a scalar and is to be evaluated at location $\bar{r}$ and time t.

In the discrete-element grid system, let the differential volume $\delta V(\bar{r})$ be the discrete element (i,k) and $\bar{r}$ be located at the center of the element. Then the right-hand side of Equation 6.10 is approximated to be the net flow rate of the term $\bar{\bar{D}}_a' \nabla C$ through the four enclosures of the discrete element (i,k), multiplied by the mean adjoint value of the element $\psi^*_{i,k}$.

The relative sensitivity coefficient of the response R to the input parameter a_L at the discrete element (i,k) was formulated to be

$$S_{a_L}(i,k) = \frac{a_L(i,k)}{R} \int_0^{t_f} \psi^*_{i,k} \left[\left(-\frac{v_x^2}{v} \frac{\partial C}{\partial x} \Delta z \right) \Bigg|_{i-1/2,k} - \left(-\frac{v_x^2}{v} \frac{\partial C}{\partial x} \Delta z \right) \Bigg|_{i+1/2,k} \right.$$

$$\left. + \left(-\frac{v_z^2}{v} \frac{\partial C}{\partial z} \Delta x \right) \Bigg|_{i,k-1/2} - \left(-\frac{v_z^2}{v} \frac{\partial C}{\partial z} \Delta x \right) \Bigg|_{i,k+1/2} \right] dt \, . \qquad (6.13)$$

The relative sensitivity coefficient of the response R to the transverse dispersivity a_T at the discrete element (i,k) was derived to be

$$S_{a_T}(i,k) = \frac{a_T(i,k)}{R} \int_0^{t_f} \psi^*_{i,k} \left[\left(-\frac{v_z^2}{v} \frac{\partial C}{\partial x} \Delta z \right) \Bigg|_{i-1/2,k} - \left(-\frac{v_z^2}{v} \frac{\partial C}{\partial x} \Delta z \right) \Bigg|_{i+1/2,k} \right.$$

$$\left. + \left(-\frac{v_x^2}{v} \frac{\partial C}{\partial z} \Delta x \right) \Bigg|_{i,k-1/2} - \left(-\frac{v_x^2}{v} \frac{\partial C}{\partial z} \Delta x \right) \Bigg|_{i,k+1/2} \right] dt. \qquad (6.14)$$

The notations $\left(\quad \right|_{i\pm1/2,k}$ and $\left(\quad \right|_{i,k\pm1/2}$ indicate that the terms between the left parentheses and the vertical bars are to be evaluated at the centers of the four enclosures $(i\pm1/2,k)$, $(i,k\pm1/2)$ of the

discrete element (i,k) respectively. Equations 6.13 and 6.14 can be expressed in terms of the values of v_x, v_z, v, and C at the centers of discrete elements by using the following equations.

$$v_{i\pm1/2,k} = \frac{1}{2}\,(v_{i\pm1,k} + v_{i,k}) \,, \tag{6.15}$$

$$v_{i,k\pm1/2} = \frac{1}{2}\,(v_{i,k\pm1} + v_{i,k}) \,, \tag{6.16}$$

$$\left.\frac{\partial C}{\partial x}\right|_{i-1/2,k} = \frac{C_{i,k} - C_{i-1,k}}{\Delta x_{i-1/2,k}} \,, \tag{6.17}$$

$$\left.\frac{\partial C}{\partial x}\right|_{i+1/2,k} = \frac{C_{i+1,k} - C_{i,k}}{\Delta x_{i+1/2,k}} \,, \tag{6.18}$$

$$\left.\frac{\partial C}{\partial z}\right|_{i,k-1/2} = \frac{C_{i,k} - C_{i,k-1}}{\Delta z_{i,k-1/2}} \,, \tag{6.19}$$

$$\left.\frac{\partial C}{\partial z}\right|_{i,k+1/2} = \frac{C_{i,k+1} - C_{i,k}}{\Delta z_{i,k+1/2}} \,, \tag{6.20}$$

where

$$\Delta x_{i\pm1/2,k} = \frac{1}{2}\,(\Delta x_{i\pm1,k} + \Delta x_{i,k}) \,, \tag{6.21}$$

$$\Delta z_{i,k\pm1/2} = \frac{1}{2}\,(\Delta z_{i,k\pm1} + \Delta z_{i,k}) \,. \tag{6.22}$$

The half-point values of v_x, v_z can be evaluated using Equations 6.15, 6.16. The time variable was dropped from C and ψ^* for notation simplicity.

Sensitivity Coefficients to Water Content Field and Retardation Factor

We now formulate the relative sensitivity coefficient fields of the response R to water content field $\theta(x,z)$ and retardation factor R_d. Sensitivity coefficients of responses to water content field and retardation factor are expected to have the same expression because these two parameters are always tied together in the radionuclide transport equation. Both parameters are in general space-dependent.

The relative sensitivity coefficient of response R to water content value at location $\bar{r}$ is

$$S_{\theta}(\bar{r}) = \frac{\theta(\bar{r})}{R} \int_0^{t_f} \left[\int_V \psi^*(\bar{r}',t) \frac{\partial L[\theta(\bar{r}')]}{\partial \theta(\bar{r})} C(\bar{r}',t) d\bar{r}' \right] dt \ . \qquad (6.23)$$

After differentiating the transport operator L with respect to $\theta(\bar{r})$ and utilizing the "local effect" property of the parameters (i.e., $\partial\theta(\bar{r}')/\partial\theta(\bar{r}) = \delta(\bar{r}'-\bar{r})$ as defined by Equation 6.6), we come up with

$$S_{\theta}(\bar{r}) = -\frac{\theta(\bar{r})}{R} \int_0^{t_f} \left[\int_{\delta V(\bar{r})} \psi^*(\bar{r}',t) R_d \left(\lambda + \frac{\partial}{\partial t}\right) C(\bar{r}',t) d\bar{r}' \right] dt \ . \qquad (6.24)$$

Similarly after the same manipulation, the relative sensitivity coefficient of response R to the ratardation factor R at location $\bar{r}$ is

$$S_{R_d}(\bar{r}) = -\frac{R_d}{R} \int_0^{t_f} \left[\int_{\delta V(\bar{r})} \psi^*(\bar{r}',t)\, \theta(\bar{r}') \left(\lambda + \frac{\partial}{\partial t}\right) C(\bar{r}',t) d\bar{r}' \right] dt \ . \qquad (6.25)$$

If R_d and $\theta(\bar{r}')$ are factored out of the volume integrals in Equations 6.24 and 6.25 respectively (they are assumed to have constant values

in the differential volume $\delta V(\bar{r})$ at $\bar{r}$), we have the relative sensitivity coefficient field of response R to either R_d or $\theta(\bar{r})$ as

$$S_{R_d}(\bar{r}) = S_{\theta}(\bar{r}) = - \frac{R_d \theta(\bar{r})}{R} \int_0^{t_f} \left[\int_{\delta V(\bar{r})} \psi^*(\bar{r}',t)\left(\lambda + \frac{\partial}{\partial t}\right) C(\bar{r}',t) d\bar{r}' \right] dt \ . \quad (6.26)$$

Equation 6.26 can be further implemented into discrete-element form by taking the differential volume $\delta V(\bar{r})$ as the discrete element (i,k) in the two-dimensional discrete-element grid system. Then the relative sensitivity coefficient field of R to R_d or θ in the FLIDE formulation is

$$S_{R_d}(i,k) = S_{\theta}(i,k)$$

$$= - \frac{R_d \theta_{i,k}}{R} \int_0^{t_f} \left(\lambda \overset{*}{\psi}_{i,k}(t) C_{i,k}(t) + \overset{*}{\psi}_{i,k}(t) \frac{\partial C_{i,k}(t)}{\partial t} \right)$$

$$\Delta x_{i,k} \Delta z_{i,k} dt \quad (6.27)$$

for each discrete element (i,k) in the system region.

Sensitivity Coefficient to Radioactive Decay Constant

The relative sensitivity coefficient field of the response R to the radioactive decay constant λ of a specified radionuclide is

$$S_{\lambda}(\bar{r}) = - \frac{\lambda}{R} \int_0^{t_f} \left[\int_{\delta V(\bar{r})} \psi^*(\bar{r}',t) R_d \theta(\bar{r}') C(\bar{r}',t) d\bar{r}' \right] dt \ . \quad (6.28)$$

The relative sensitivity coefficient field $S_{\lambda}(r)$ in the discrete-element form becomes

$$S_\lambda(i,k) = \frac{-\lambda R_d \theta_{i,k}}{R} \int_0^{t_f} \psi^*_{i,k}(t) C_{i,k}(t) \Delta x_{i,k} \Delta z_{i,k} dt \qquad (6.29)$$

for each discrete element (i,k) in the system region.

So far we have formulated the relative sensitivity coefficients of responses of interest to five input parameters. They are longitudinal and transverse dispersivities, water content, retardation factor, and radioactive decay constant. It should be noted that the sensitivity coefficient is in general a function of space regardless of whether the parameter considered is a space-dependent function or a constant in the system region. Such space-dependent sensitivity coefficients have been called sensitivity coefficient fields. For example, suppose $S_\alpha(x,z)$ is the relative sensitivity coefficient field of response R to input parameter α. Then the value $S_\alpha(x_0,z_0)$ represents the percent change in R due to the percent change in the value of parameter α at the space location (x_0,z_0).

B. Time Integration of the Sensitivity Coefficients

In this study, the response of interest was specified to be the functional of radionuclide concentration field at the specified observation time (final time). The time-dependent radionuclide concentrations were computed by solving the transient radionuclide transport equation from initial time t_0 (usually zero) to final time t_f with a constant time-step size Δt. The number of simulation time step N_t is hence $(t_f - t_0)/\Delta t$. The adjoint fields were solved from the adjoint transport equation which was characterized as a final-value problem. The adjoint calculation was performed by reversing the time

direction from t_f to t_0 having the same number of time step N_t and the same time-step size Δt as in the concentration calculation. In both concentration and adjoint calculations, we had $N_t + 1$ concentration fields and $N_t + 1$ adjoint fields including the initial and final conditions for concentration and adjoint respectively stored.

Trapezoidal integration rule was employed to carry out the time integrations for the relative sensitivity coefficients. As a result, the time-dependent concentration and adjoint fields at any time were evaluated by linear interpolations from the $N_t + 1$ sets of concentration and adjoint data respectively, in the time integration process. For N_t time intervals, there are $N_t + 1$ point-values for concentrations $C_0, C_1, \ldots, C_{N_t}$, and $N_t + 1$ point-values for adjoints $\psi^*_0, \psi^*_1, \ldots, \psi^*_{N_t}$, where C_0 and $\psi^*_{N_t}$ are the initial and final conditions for concentration and adjoint respectively. The values of C and ψ^* at any time t within the n^{th} time interval, C(t) and $\psi^*(t)$, are assumed to be linear variations between the two consecutive values of C and ψ^* at times t_{n-1} and t_n, respectively. C(t) and $\psi^*(t)$ can be expressed as

$$C(t) = C_{n-1} + C'_n(t - t_{n-1}) \ , \tag{6.30}$$

$$\psi^*(t) = \psi^*_{n-1} + \psi^{*\prime}_n(t - t_{n-1}) \ , \tag{6.31}$$

where

$$C'_n = (C_n - C_{n-1})/\Delta t \ , \tag{6.32}$$

$$\psi^{*\prime}_n = (\psi^*_n - \psi^*_{n-1})/\Delta t \ , \tag{6.33}$$

and $t_n = t_0 + n\Delta t$, $t_f = t_0 + N_t \Delta t$, and t falls within the time interval (t_{n-1}, t_n).

We first break each one of the time integrals in Equations 6.13, 6.14, 6.27, and 6.29 into time integral terms. Then the relative sensitivity coefficient of response R to input parameter α at any discrete-element center (leaving out notations for space-dependence in discrete-element grid system) can be written as

$$S_\alpha = A \sum_{m=1}^{M} S_\alpha^m , \tag{6.34}$$

where A is the common factor independent of time, M is the number of terms inside the time integral. Let us designate functionals $F_m[\psi^*(t)]$ and $G_m[C(t)]$ to represent the associated terms pertaining to $\psi^*(t)$ and C(t) respectively in each time integral term S_α^m. $F_m[\psi^*(t)]$ may contain linear function, spatial gradient of $\psi^*(t)$. $G_m[C(t)]$ may contain linear function, spatial gradient, and time derivative of C(t). Now the time integral term S_α^m can be attributed to F_m and G_m as

$$S_\alpha^m = \int_0^{t_f} F_m[\psi^*(t)] G_m[C(t)] dt . \tag{6.35}$$

For example, the relative sensitivity coefficient of R to R_d (Equation 6.31) can be broken into two terms as $A(F_1G_1 + F_2G_2)$ with $A = -R_d \theta \Delta x \Delta z / R$ and $F_1 = \lambda\psi^*(t)$, $G_1 = C(t)$, $F_2 = \psi^*(t)$, and $G_2 = \partial C(t)/\partial t$. Now the time integral in Equation 6.35 is broken up into N_t time integrals with each integration range from the starting time to the ending time of each time interval Δt. Within each time interval, C and

ψ^* are linearly interpolated as expressed in Equations 6.30 through 6.33. Equation 6.35 is approximated by employing trapezoidal integration technique. Substituting Equations 6.30, 6.31 into Equation 6.35, we get

$$S_\alpha^m = \sum_{n=1}^{N_t} \int_{t_{n-1}}^{t_n} F_m[\psi_{n-1}^* + \psi_n^{*\prime}(t - t_{n-1})]\, G_m[C_{n-1} + C_n'(t - t_{n-1})]dt \ . \quad (6.36)$$

Using the linearity property of functional F_m and G_m and making a change of integrating variable from t to $t' = t_{n-1} + t$ for n = 1 to N_t, Equation 6.36 was reduced to

$$S_\alpha^m = \sum_{n=1}^{N_t} \int_0^{\Delta t} [F_m(\psi_{n-1}^*) + F_m(\psi_n^{*\prime})t'][G_m(C_{n-1}) + G_m(C_n')t']dt' \ . \quad (6.37)$$

Multiplying the two square-bracketed terms and carrying out the integration term by term, Equation 6.37 now becomes

$$S_\alpha^m = \sum_{n=1}^{N_t} [H_{m11}^n\, \Delta t + (H_{m12}^n + H_{m21}^n)\frac{\Delta t^2}{2} + H_{m22}^n \frac{\Delta t^3}{3}] \ , \quad (6.38)$$

where

$$H_{m11}^n = F_m(\psi_{n-1}^*)G_m(C_{n-1}) \ , \quad (6.39)$$

$$H_{m12}^n = F_m(\psi_{n-1}^*)G_m(C_n') \ , \quad (6.40)$$

$$H_{m21}^n = F_m(\psi_n^{*\prime})G_m(C_{n-1}) \ , \quad (6.41)$$

$$H_{m22}^n = F_m(\psi_n^{*\prime})G_m(C_n') \ . \quad (6.42)$$

The first term H^n_{m11} involves the "folding" between the concentration and adjoint values at $N_t + 1$ discrete times (will be called point-values). The second and third terms H^n_{m12}, H^n_{m21} involve the point-values and time-derivative values of concentrations and adjoints. And the last term H^n_{m22} accounts for the contribution from the time-derivative values of both concentrations and adjoints

C. Computational Procedure

We have completed the mathematical formulation of the relative sensitivity coefficients of the specified response of interest to each one of five input parameters. The relative sensitivity coefficient fields for these input parameters have been implemented into a computer program SENCOF (SENsitivity COefficient Field code) in the discrete-element grid system using Equations 6.13, 6.14, 6.27 and 6.29 as the sensitivity coefficient equations in the FLIDE formulation and Equations 6.34, 6.39-6.42 for the time integration.

The computational procedure for performing the sensitivity coefficient calculations is the following:

(i) Perform a reference-state radionuclide transport simulation with the reference-values of the input parameters to obtain the time-dependent radionuclid concentration fields from initial time to final time with a stable time-step size using the computer code RADMIG (see Chapter III for details);

(ii) Perform a reference-state adjoint transport simulation with the same set of input parameter values as in step (i) to obtain the time-dependent adjoint fields from final time to initial time with the

same time-step size as in step (i) using the computer code ADJMIG (see details in Chapter V). The final conditions are established on the basis of the specified response of interest;

(iii) Retrieve from magnetic disk the concentration and the corresponding adjoint fields in a real-time sequence from initial time to final time and compute the relative sensitivity coefficient fields of the specified response of interest to five input parameters considered in this study using the computer code SENCOF. Present the relative sensitivity coefficient fields in 2-D digital graphs.

D. Numerical Demonstration and Discussion

In this section two examples for the calculation of the sensitivity coefficients of the specified responses to four input parameters a_L , a_T, R_d and λ will be given and the results will be presented and discussed. Since the sensitivity coefficients for the retardation factor R_d and water content field are identical, we only discuss the sensitivity for R_d.

We will follow the computational procedure for the sensitivity coefficient calculation just outlined in the last section. The operational flow and data path of the sensitivity calculations for the two examples are illustrated in Figure 6.1. Both examples share the same set of input data (including the groundwater flow and input parameter data). Hence the radionuclide transport code RADMIG only need be run once to obtain the time-dependent concentration fields. The radionuclide transport simulation with the basic input data has been done in the first example of Chapter III. The time-dependent tritium

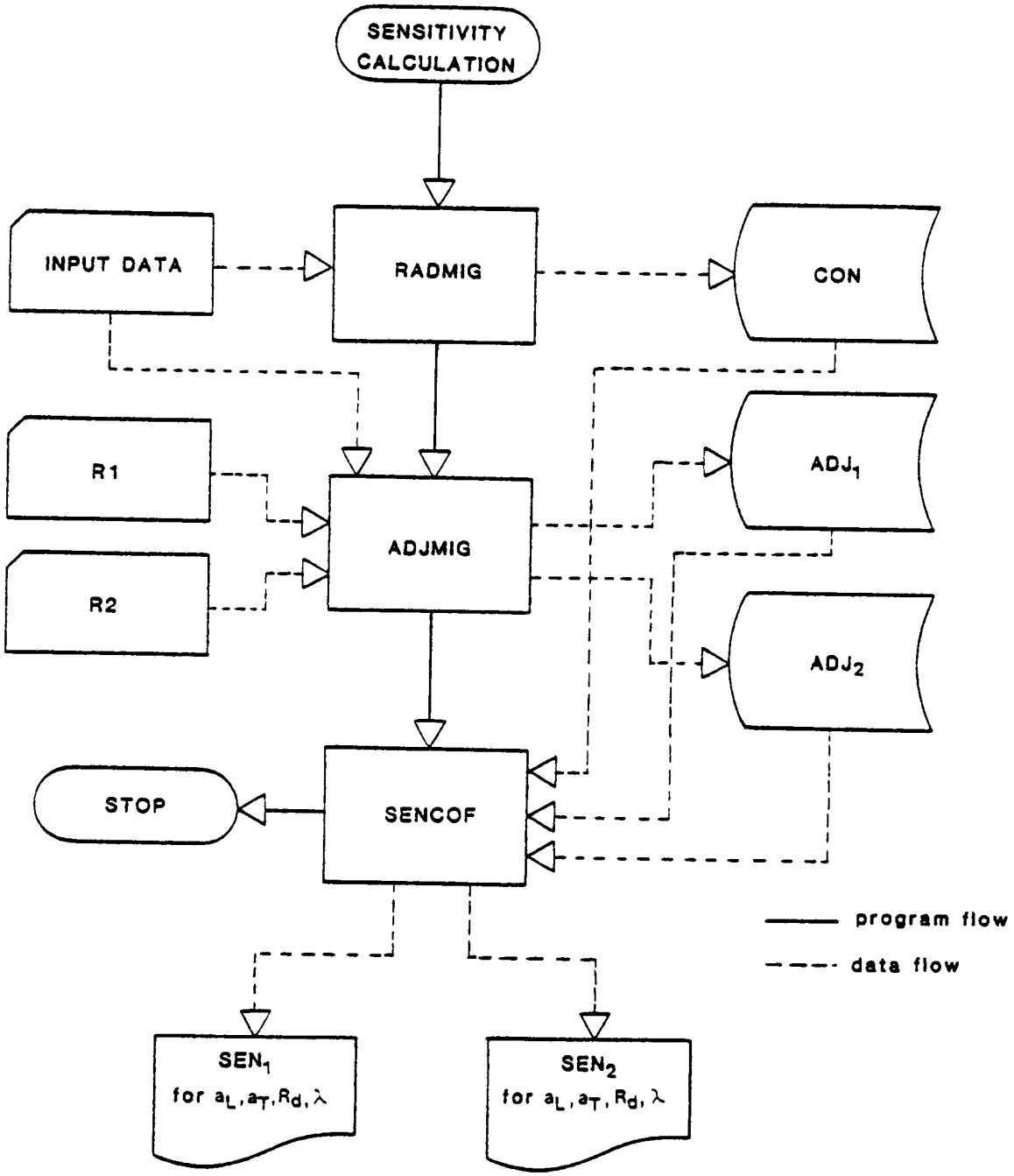

Figure 6.1. Schematic Flow-Diagram of the Radionuclide Transport Sensitivity Analysis.

concentration fields from initial time t_0 = 0 to final time t_f = 10 days with time-step size of 0.1 day were computed and stored on the magnetic disk to be used for sensitivity calculation (see Chapter III for detail).

As far as the adjoint transport calculation is concerned, each specified response of interest corresponds to one adjoint calculation and hence one set of time-dependent adjoint fields (even though the input data used are the same). It is because the final conditions for the adjoint calculation are determined by the specified response of interest. In the present case, the two sensitivity examples only differ by the response of interest. The responses of interest for these two sensitivity examples were taken from the examples of adjoint transport calculation in Chapter V. The response for the first sensitivity example is the space-average tritium concentration in region ZONE-1 (see Figure 5.1, page 95) at final time t_f = 10 days. The response for the second example is the tritium discharge rate (Ci/day) at t_f = 10 days. The adjoint transport code ADJMIG was run twice to obtain the time-dependent adjoint fields from final time t_f = 10 days back to initial time t_0 = 0 for the two responses of interest (see Chapter V). The calculated adjoint field data were also stored on the magnetic disk.

The sensitivity coefficient calculation code SENCOF was then employed to compute the sensitivity coefficients of both responses to the input parameters. The concentration fields and the adjoint fields corresponding to the first response were read from the disk to SENCOF to compute the relative sensitivity coefficient fields of the response (space-average tritium concentration in region ZONE-1 at t_f = 10 days)

to the four input parameters. The same concentration fields and the adjoint fields for the second example were read to compute the relative sensitivity coefficient fields of the second response (tritium discharge rate at t_f = 10 days) to the four input parameters. The results for both examples are presented in Figures 6.2 through 6.9. Note that each relative sensitivity coefficient field consists of the relative sensitivity coefficients at the discrete-element centers of the flow system. The relative sensitivity coefficient at each discrete-element center represents the percent change of response per percent change of the parameter in that discrete element.

In the first sensitivity example with space-average concentration in ZONE-1 at t_f = 10 days as the response of interest, we generally have higher sensitivity coefficients in the upstream region of ZONE-1, particularly near the source boundary (i.e., bottom of the burial trench), for the parameter of longitudinal dispersivity a_L. In other words, the response is more sensitive to the variation of a_L in the upstream region of ZONE-1, and also in part of ZONE-1 itself. For example, one percent increase in a_L at element (6,8) will results in 0.094% increase in the space-average tritium concentration in ZONE-1 predicted at t_f = 10 days. High longitudinal dispersivity sensitivity in the upstream region and near ZONE-1 is due to the high groundwater flow rates near the source boundary, which result in high longitudinal dispersive transport rates toward the response region. In general, the response specified in ZONE-1 would be more sensitive to the parameters in the upstream region than any other regions because any change of the parameters in the

KZ																					
9	0	0	0	0			6	0	0												
8	0	0	0	0	27	100	-9	1	0	0											
7	0	0	0	0	23	28	26	12	2	0	0										
6	0	0	0	0	42	50	39	10	10	1	0	0									
5	0	0	0	0	29	34	39	10	13	0	0	0	0	0							
4	0	0	0	0	12	13	21	5	7	0	0	0	0	0	0	0	0	0	0	0	
3	0	0	0	0	1	0	3	1	1	0	0	0	0	0	0	0	0	0	0	0	0
2	0	0	0	0	0	0	0	0	1	0	0	0	0	0	0	0	0	0	0	0	0
1	0	0	0	0	0	-1	0	0	0	0	0	0	0	0	0	0	0	0	0	0	0
IX=	1	2	3	4	5	6	7	8	9	10	11	12	13	14	15	16	17	18	19	20	21

IX = Discrete element grid number in x-direction.

KZ = Discrete element grid number in z-direction.

Response = Space-average tritium concentration in region ZONE-1 at final time t_f = 10 days.

Value 100 = 0.0741% change in response/% change in a_L.

Figure 6.2. Relative Sensitivity Coefficient Field of the First Response to Longitudinal Dispersivity.

KZ	IX= 1	2	3	4	5	6	7	8	9	10	11	12	13	14	15	16	17	18	19	20	21
9	0	0	0	0			4	0	0												
8	0	0	0	0	-8	-29	57	1	0	0											
7	0	0	0	0	-14	-54	-100	-20	-2	0	0										
6	0	0	0	0	-8	-5	-7	-23	-4	-1	0	0									
5	0	0	0	0	-1	8	18	-1	-6	0	0	0	0	0							
4	0	0	0	0	15	33	60	19	2	0	0	0	0	0	0	0	0	0	0	0	
3	0	0	0	0	3	20	36	12	3	0	0	0	0	0	0	0	0	0	0	0	0
2	0	0	0	0	2	15	32	10	3	0	0	0	0	0	0	0	0	0	0	0	0
1	0	0	0	0	1	12	25	8	2	0	0	0	0	0	0	0	0	0	0	0	0

Response = Space-average tritium concentration in ZONE-1 at final time at t_f = 10 days.

Value -100 = -0.0721% change in response/% change in a_T.

Figure 6.3. Relative Sensitivity Coefficient Field of the First Response to Transverse Dispersivity.

KZ	IX= 1	2	3	4	5	6	7	8	9	10	11	12	13	14	15	16	17	18	19	20	21
9	0	0	0	0			-4	0	0												
8	0	0	0	0	-4	-6	-17	-2	0	0											
7	0	0	0	0	-34	-69	-47	-8	-1	0	0										
6	0	0	0	0	-32	-69	-77	-25	-8	0	0	0									
5	0	0	0	0	-24	-61	-100	-35	-15	-1	0	0	0	0							
4	0	0	0	0	-12	-40	-80	-31	-13	-1	0	0	0	0	0	0	0	0	0	0	
3	0	0	0	0	-3	-11	-27	-10	-4	0	0	0	0	0	0	0	0	0	0	0	0
2	0	0	0	0	-1	-7	-18	-7	-3	0	0	0	0	0	0	0	0	0	0	0	0
1	0	0	0	0	-1	-5	-14	-6	-2	0	0	0	0	0	0	0	0	0	0	0	0

Response = Space-average tritium concentration in ZONE-1 at at t_f = 10 days.

Value -100 = -0.152% change in response/% change in R_d.

Figure 6.4. Relative Sensitivity Coefficient Field of the First Response to Retardation Factor.

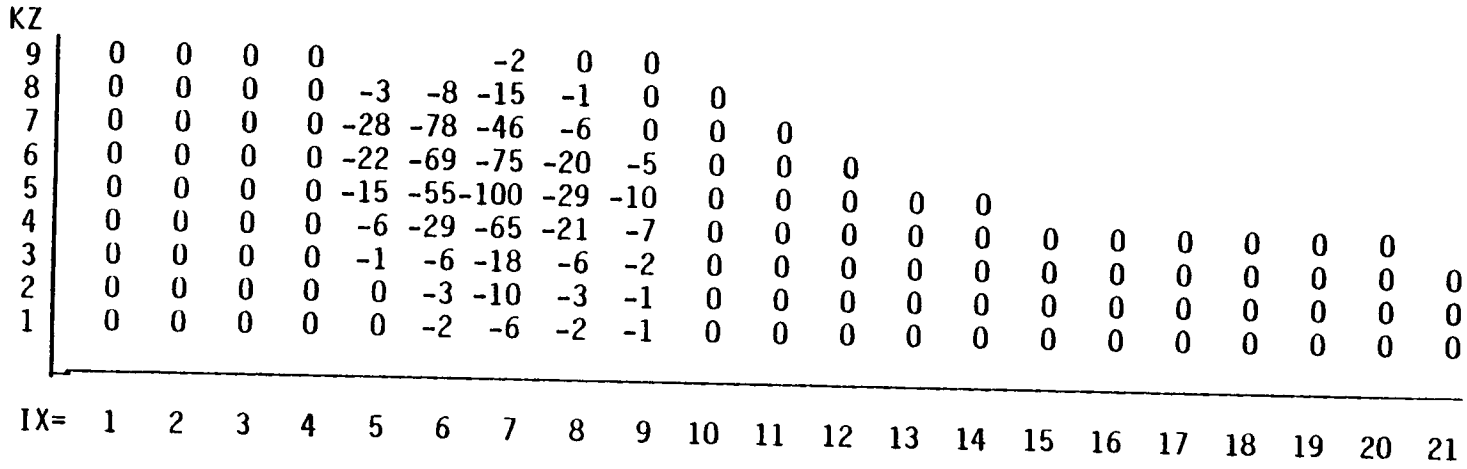

Response = Space-average tritium concentration in ZONE-1 at at t_f = 10 days.

Value -100 = -1.18×10^{-4}% change in response/% change in λ.

Figure 6.5. Relative Sensitivity Coefficient Field of the First Response to Radioactive Decay Constant.

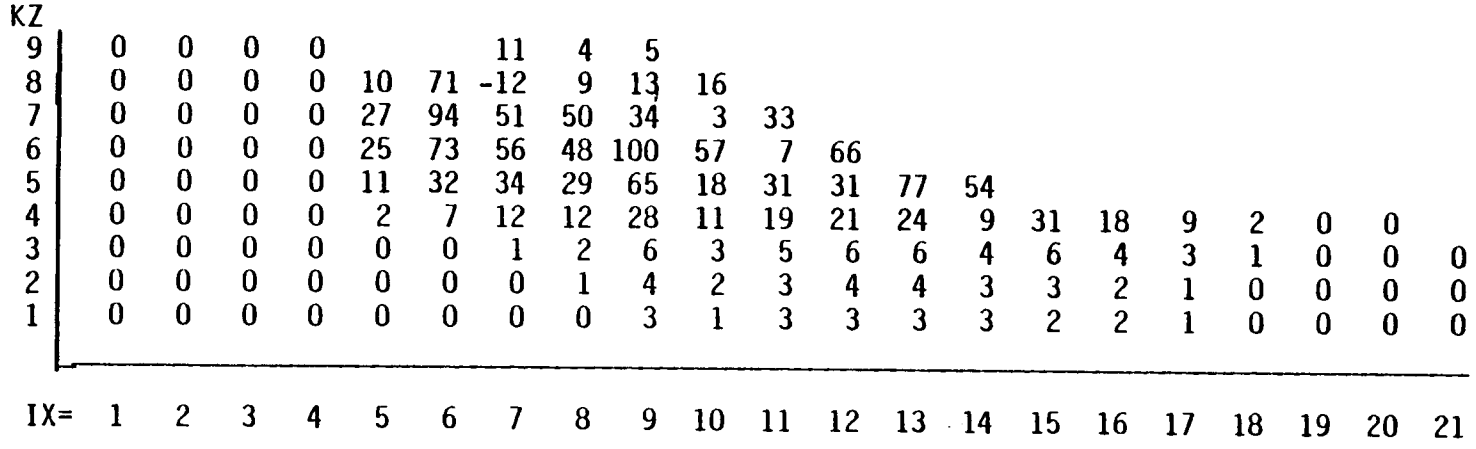

Response = Tritium discharge rate at final time t_f = 10 days.

Value 100 = 0.0903% change in response/% change in a_L.

Figure 6.6. Relative Sensitivity Coefficient Field of the Second Response to Longitudinal Dispersivity.

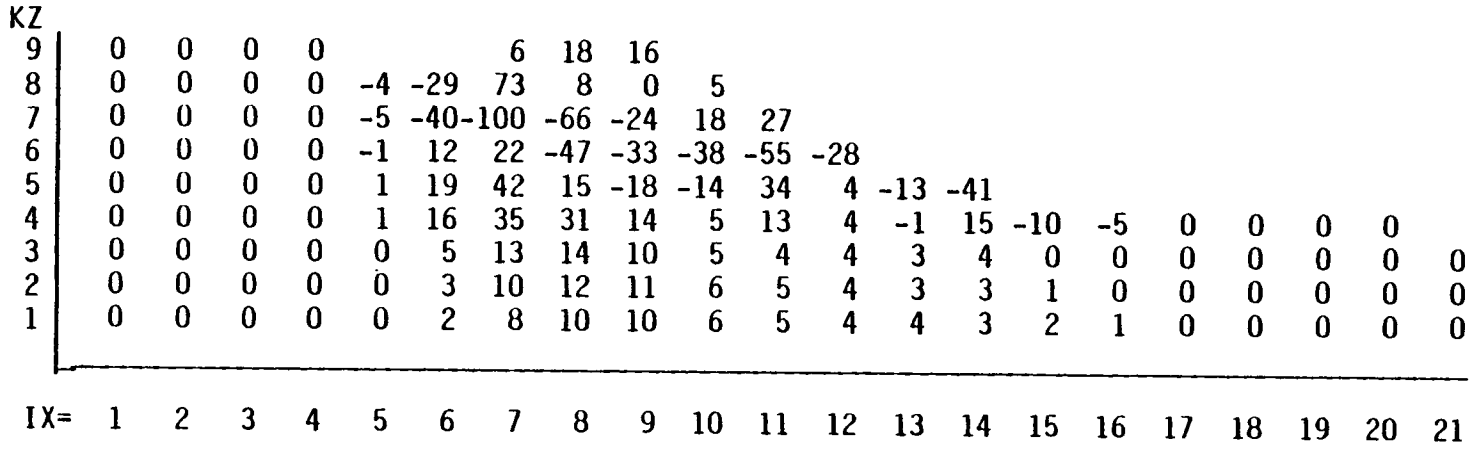

Response = Tritium discharge rate at t_f = 10 days.

Value -100 = -0.0971% change in response/% change in a_T.

Figure 6.7. Relative Sensitivity Coefficient Field of the Second Response to Transverse Dispersivity.

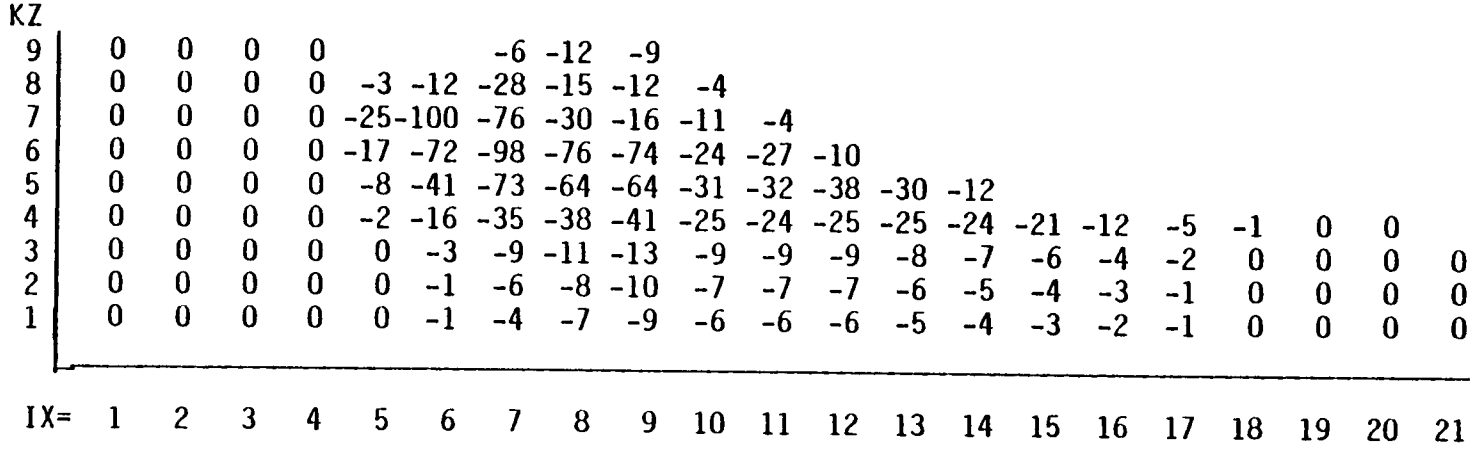

Response = Tritium discharge rate at t_f = 10 days.

Value -100 = -0.211% change in response/% change in R_d.

Figure 6.8. Relative Sensitivity Coefficient Field of the Second Response to Retardation Factor.

KZ																					
9	0	0	0	0			-6	-14	-10												
8	0	0	0	0	-3	-13	-29	-18	-15	-5											
7	0	0	0	0	-20	-100	-78	-34	-18	-14	-6										
6	0	0	0	0	-12	-64	-92	-78	-76	-27	-29	-11									
5	0	0	0	0	-5	-32	-58	-56	-57	-29	-30	-35	-27	-11							
4	0	0	0	0	-1	-10	-24	-28	-30	-19	-19	-20	-20	-18	-15	-8	-3	0	0	0	
3	0	0	0	0	0	-1	-5	-7	-8	-6	-6	-6	-5	-5	-4	-2	-1	0	0	0	0
2	0	0	0	0	0	0	-3	-4	-6	-4	-4	-4	-4	-3	-2	-1	0	0	0	0	0
1	0	0	0	0	0	0	-2	-3	-5	-3	-3	-3	-3	-2	-2	-1	0	0	0	0	0
IX=	1	2	3	4	5	6	7	8	9	10	11	12	13	14	15	16	17	18	19	20	21

Response = Tritium discharge rate at t_f = 10 days.

Value -100 = -8.07×10^{-5}% change in response/% change in λ.

Figure 6.9. Relative Sensitivity Coefficient Field of the Second Response to Radioactive Decay Constant.

upstream region will bring about concentration change in that region which will ultimately contribute to the response change.

We notice that there are some negative sensitivity coefficients for the parameter of transverse dispersivity a_T (also a few for a_L). For example, at element (6,8), 1% increase in a_T results in 0.023% "decrease" in the first response of interest. This seems surprising at first. Let us consider the effect of the transverse dispersivity variation in the region near the source boundary, where the hydraulic velocity is large, to the response of interest. An increase in a_T in a discrete element of that region will increase the outgoing transversal dispersive transport rate in that element, and consequently will result in a concentration decrease in that element. Since the groundwater passing through that element will also flow through the response region ZONE-1, the concentration decrease in that element will ultimately result in the concentration decrease in the downstream region (including the response region) and hence will result in the response decrease. On the other hand, the concentration increase in the region transverse to the groundwater flow direction (e.g., discrete element (7,8)) due to the increase of the incoming dispersive transport flow rate has little contribution to the concentration in the response region because the groundwater is not flowing through that region. Therefore it is not surprising to have some negative sensitivity coefficients of the first response to a_T.

As for the sensitivity coefficients of the second response of interest (tritium discharge rate at t_f = 10 days) to a_L and a_T, we generally have high sensitivity coefficients near the source boundary

and along the groundwater flow path up to the outflow boundary because any change in a_L or a_T in the upstream region of the outflow boundary will affect the concentration on the boundary and hence will contribute to the change in the response.

We next examine the sensitivity coefficients of the first response of interest to the retardation factor R_d and radioactive decay constant λ. We first notice that the sensitivity coefficients for R_d and λ are all negative. That is, any increase in R_d or λ will result in a decrease in the response of interest. This can be seen from the negative sign in the sensitivity equations for R_d and λ (see Equations 6.30, and 6.32). As we can see from Figures 6.4 and 6.5, the sensitivity coefficients for R_d and λ are high near the source boundary, in the upstream region of, and inside the response region ZONE-1. It is conceivable that the change of R_d inside the response region or in its upstream region will have higher impact on the response change than in any other regions. This is because the resultant concentration change in the upstream region, or inside the response region will be transported by the groundwater flow into the response region and contribute to the response change. In contrast, it is more difficult for the concentration change in any other regions to reach the response region because of the low hydraulic velocities.

As for the sensitivity coefficients of the second response of interest to R_d and λ, we can see from Figures 6.8 and 6.9 that the response is in general sensitive to the variations of R_d and λ in the upstream region of the outflow boundary.

In summary, the sensitive region of a specified response of interest to each one of the four input parameters is determined by (1) groundwater flow, and (2) geometric location of the response region in the groundwater flow system. That is, the higher the hydraulic velocity is in a region, the more sensitive the response is to the parameter variation in that region. And the sensitive region is in general situated in the upstream area with respect to the response region. In all cases, we see that R_d is the most sensitive parameter, and λ is the least sensitive parameter. The sensitivity coefficient for λ is about three orders of magnitude smaller than that for R_d.

CHAPTER VII

VALIDATION OF THE SENSITIVITY METHODOLOGY

In this chapter, the sensitivity results obtained from both direct calculation and the general sensitivity analysis based on generalized perturbation theory will be presented and compared against each other. This comparison can serve as a validation process for the general sensitivity theory. The linearity ranges of the parameters within which the perturbation theory will give good prediction of the response of interest were estimated.

A. Comparisons of Sensitivity Coefficients

The quantities to be compared are the total relative sensitivity coefficients of the specified response of interest to the specified input parameters. We assume that the specified input parameter is perturbed uniformly over the system region (i.e., the perturbation of the parameter is space-independent). For example, if the longitudinal dispersivity a_L is perturbed by one percent, the a_L value in each computational discrete-element is perturbed by 1%. Consequently, the total relative sensitivity coefficient of the response to the specified input parameter is calculated by integrating the relative sensitivity coefficient density field over the space of system region. In the discrete-element formulation, the total relative sensitivity coefficient is calculated by summing up the product of the relative sensitivity coefficient density and the area of each discrete-element in the system region.

The procedure for the calculation of the total relative sensitivity coefficient by direct-calculation approach is outlined as follows. We perturbed only one parameter in the vicinity of its reference value at one time while holding all other parameters at their reference values. Let R_r represent the response of interest calculated by running the radionuclide transport code with all the input parameters at their reference values. If we wish to calculate the sensitivity coefficient of response to the i^{th} parameter α_i, we perturb α_i by p percent to become α_i' while all the other parameters remain at their reference values. In other words, the input data set has the form

$$\underline{\alpha}_i' = (\alpha_1, \alpha_2, \cdots, \alpha_i', \cdots \alpha_N) \tag{7.1}$$

where $\alpha_i' = \alpha_i\ (1 + 0.01\ p)$ (7.2)

and p is usually a small number (e.g., 1 or 2) to attain a linear behavior of the response in the vicinity of the reference point. Another response of interest R_α' was calculated by running the same computer code with the perturbed input data $\underline{\alpha}_i'$. Now the total relative sensitivity coefficient of response R_r to parameter α_i by means of direct-calculation approach was calculated as

$$S_\alpha = \frac{(R_\alpha' - R_r)/R_r}{0.01\ p} . \tag{7.3}$$

Then the total relative sensitivity coefficients of response R_r to all the other parameters by the direct-calculation approach were calculated in the same way.

We now compare the total relative sensitivity coefficients obtained by using the generalized perturbation theory and direct-calculation approaches for two cases. The four input parameters considered in the sensitivity coefficients comparison are longitudinal and transverse dispersivities a_L, a_T, retardation factor R_d, and radioactive decay constant λ. The reference input parameter data for the two cases was listed in Table 3.1 (example 1) on page 54. The steady-state hydraulic velocity field was presented in Figure 3.4, page 52.

In the first case of sensitivity coefficient comparison, the responses of interest were specified to be the space-average tritium concentrations in region ZONE-1 as shown in Figure 5.1, page 95, at final times t_f = 2 and 8 days. In the second case, the responses of interest were specified to be the tritium discharge rates on the outflow boundary at final times t_f = 2 and 8 days. The total relative sensitivity coefficients of the responses of interest specified for both cases to the specified four input parameters were computed by means of both the direct calculation and the perturbation method approaches, and the results were given in Tables 7.1, 7.2 and Tables 7.3 and 7.4, respectively.

Among the four parameters of interest, R_d and λ have negative sensitivity coefficients. That is, an increase in the value of R_d or λ causes a decrease in the response. As can be seen in the radionuclide transport equation (Equation 2.8), an increase in R_d will result in a

Table 7.1. Comparison of Relative Sensitivity Coefficients Computed by Both Direct-Calculation and Perturbation-Theory Methods for Sensitivity Comparison Case 1[a] at t_f = 2 Days

Input[b] Parameter	Relative Sensitivity Coefficients		
	Direct Calculation	Perturbation Prediction	Discrepancy[c] (%)
a_L (1%)	1.0358	0.9754	5.83
a_T (1%)	0.6002	0.5991	0.19
R_d (1%)	-2.8274	-2.8777	-1.78
λ (100%)	-2.2423×10^{-4}	-2.2623×10^{-4}	-0.89

[a]The specified response is the space-average tritium concentration in region ZONE-1 (see Figure 5.1, page 95) at the specified final time t_f.

[b]The percentage in the parenthses represents the perturbation of the associated parameter in the direct calculation.

[c]Discrepancy is defined to be $100 \times \left(\frac{\text{Direct-Perturbation}}{\text{Direct}} \right)$ %.

Table 7.2. Comparison of Relative Sensitivity Coefficients Computed by Both Direct-Calculation and Perturbation-Theory Methods for Sensitivity Comparison Case 1 at t_f = 8 Days

Input Parameter	Relative Sensitivity Coefficients		
	Direct Calculation	Perturbation Prediction	Discrepancy (%)
a_L (1%)	0.4654	0.4970	-6.79
a_T (1%)	0.1193	0.1231	-3.19
R_d (1%)	-1.6121	-1.6258	-0.85
λ (100%)	-8.1769×10^{-4}	-7.8232×10^{-4}	4.33

Table 7.3. Comparison of Relative Sensitivity Coefficients Computed by Both Direct-Calculation and Perturbation-Theory Methods for Sensitivity Comparison Case 2[a] at t_f = 2 Days

Input Parameter	Relative Sensitivity Coefficients		
	Direct Calculation	Perturbation Prediction	Discrepancy (%)
a_L (1%)	1.9216	1.8400	4.17
a_T (1%)	0.3581	0.3600	-0.47
R_d (1%)	-4.0822	-4.1950	-2.74
λ (100%)	-2.4835×10^{-4}	-2.4288×10^{-4}	2.20

[a]The specified response is the tritium discharge rate on the outflow boundary at the specified final time t_f.

Table 7.4. Comparison of Relative Sensitivity Coefficients Computed by Both Direct-Calculation and Perturbation-Theory Methods for Sensitivity Comparison Case 2 at t_f = 8 Days

Input Parameter	Relative Sensitivity Coefficients		
	Direct Calculation	Perturbation Prediction	Discrepancy (%)
a_L (1%)	1.5167	1.5455	-1.90
a_T (20%)	7.523×10^{-3}	7.405×10^{-3}	1.57
R_d (1%)	-3.5229	-3.6895	-4.73
λ (100%)	-9.3836×10^{-4}	-9.5347×10^{-4}	-1.61

decrease in the effective radionuclide moving speed in the porous medium ($\bar{v}/R_d$), and hence a decrease in the concentration field. Since the response of interest is specified to be the linear functional of the concentration field, a decrease in concentration will result in a decrease in response of interest.

Examining Tables 7.1 and 7.2, we see that the space-average tritium concentrations in region ZONE-1 predicted at the two indicated final times are most sensitive to the retardation factor R_d and most insensitive to the radioactive decay constant λ. For example, if the retardation factor R_d is increased by 1%, then the response will decrease by 2.88%. Whereas 1% increase in λ only results in 0.0002% decrease in the response. In the second case, we see from Tables 7.3 and 7.4 that the tritium discharge rate predicted at the same two final-times as in

the first case are also most sensitive to R_d and most insensitive to λ. In both cases, the sensitivity priority for the four parameters are R_d, a_L, a_T, and λ in the order of decreasing sensitivity. It means that R_d is the most important parameter and λ is the least important one in the calculation of the response.

As can be seen from Tables 7.1 through 7.4, the agreements between the sensitivity coefficients computed by direct-calculation method and those predicted by the generalized perturbation theory are good for the four addressed parameters in both cases. The discrepancies for the parameters are small (less than 7%). The good agreement in the comparison of sensitivity coefficients by the two methods has shown that the generalized perturbation theory is valid and useful in predicting the sensitivity coefficients for the problem of radionuclide transport by groundwater flow.

One should note that the sensitivity coefficients computed by the direct-calculation method depend on the perturbation value imposed on the specified parameter. One percent of the reference data value was used to perturb the input parameters in the direct calculations except the radioactive decay constant and the transverse dispersivity in one case, whose sensitivity coefficients are very small. Large perturbation values were used for these parameters in order to gain enough numerical accuracy.

One would also like to know how the response behaves near the reference point in contrast to the perturbation prediction. We shall present the response behavior with respect to the parameter

along with the response-parameter line predicted by the generalized perturbation theory in the following section.

B. Ranges of Linearity for the Radionuclide Transport Responses

The perturbation sensitivity analysis technique developed in this dissertation for the radionuclide transport simulation is based on the generalized perturbation theory. Consequently, the response variation computed by the perturbation method is only accurate to the first-order change of the input parameter data, but is insensitive to the first-order variations of the concentration fields resulting from the parameter perturbation. As previously discussed in Chapter IV, sensitivity coefficients obtained by the perturbation method can be used to predict the changes in the specified response R due to changes in the input parameter value α, i.e.,

$$(\Delta R/R)\% = S_{\alpha}(\Delta\alpha/\alpha)\% \tag{7.4}$$

where S_{α} represents the relative sensitivity coefficient of response R to parameter α. One would like to ask the question: "How much can a parameter value be perturbed from its reference value without making the perturbation sensitivity analysis technique break down in predicting the response changes (i.e., without giving rise to large errors in the response prediction)?" This question can be answered by determining the linearity range of the parameter for the response in the neighborhood of the reference data point. In this section we shall make a comparison between the responses obtained by both the direct-calculation and perturbation-theory methods due to the same parameter changes.

Longitudinal and transverse dispersivities a_L, a_T and retardation factor R_d were chosen as the input parameters to illustrate the predictive aspect of the perturbation-theory method. The two specified responses of interest were: (1) space-average tritium concentration in region ZONE-1 shown in Figure 5.1, page 95, at final time t_f = 2 days, and (2) tritium discharge rate at t_f = 2 days. The percent response changes from the reference-state values were plotted against the percent changes of the parameters from their reference values in both positive and negative directions as presented in Figures 7.1 through 7.6 for the two specified responses. The straight lines passing through the reference data point (i.e., coordinate (0,0) in Figures 7.1-7.6) represent the response vs parameter lines predicted by the generalized perturbation theory. The slopes of these straight lines give the relative sensitivity coefficients computed by the generalized perturbation theory. One should note that each pair of the specified response and parameter corresponds to a unique sensitivity coefficient computed by the perturbation method at the reference data point. Thus, the predicted response change corresponding to a given percent change of the parameter can be determined by multiplying the relative sensitivity coefficient with that percent change. As for the direct-calculation method, the response changes were obtained by making percent changes (positive as well as negative) in the specified input parameter, then rerunning the radionuclide transport code RADMIG with all the other input parameters fixed at their reference values. Thus, one can construct a response versus parameter curve by repeating the radionuclide transport calculation with altered input parameter values.

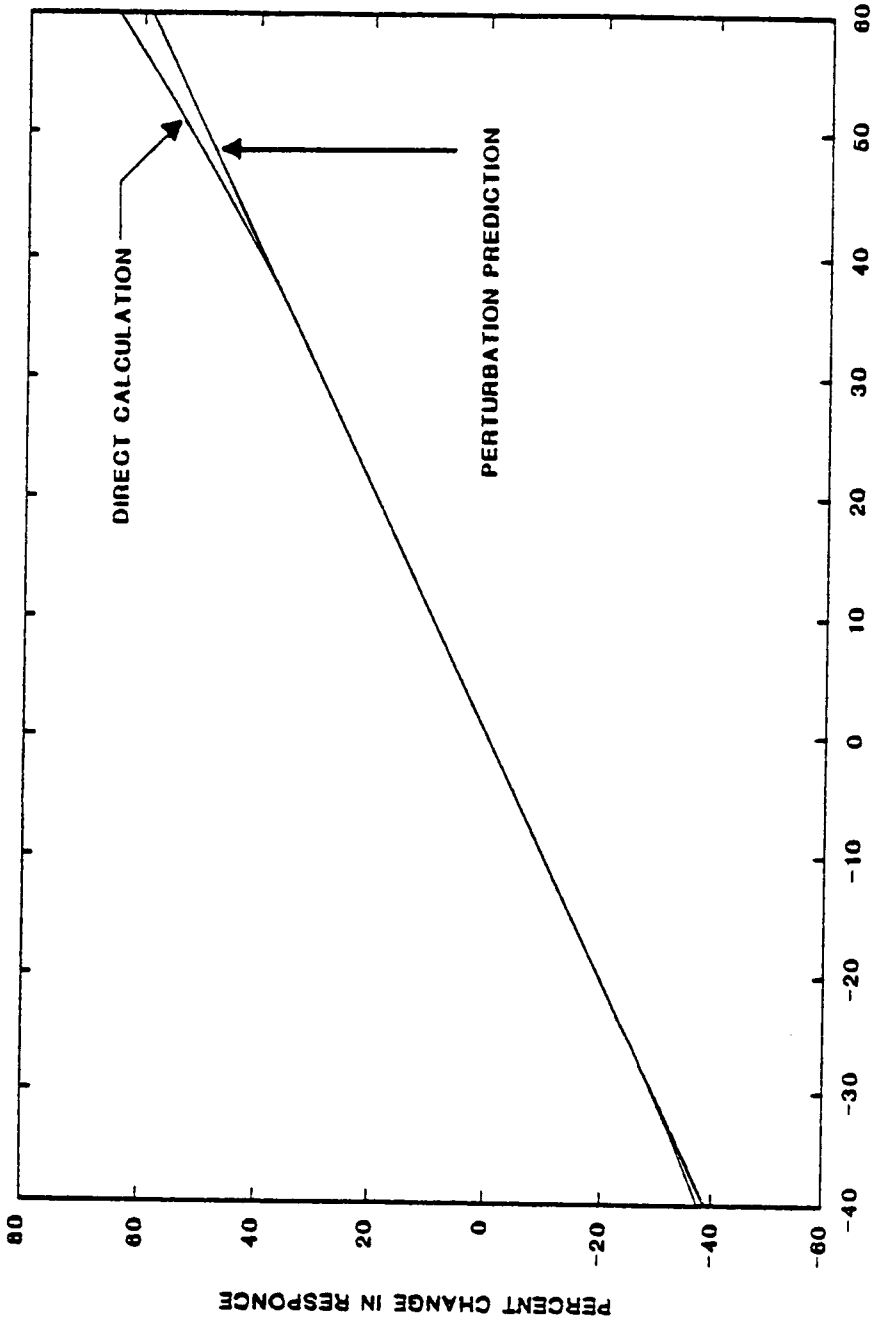

Figure 7.1. Space-Average Tritium Concentration in ZONE-1 at t_f = 2 Days as a Function of Longitudinal Dispersivity.

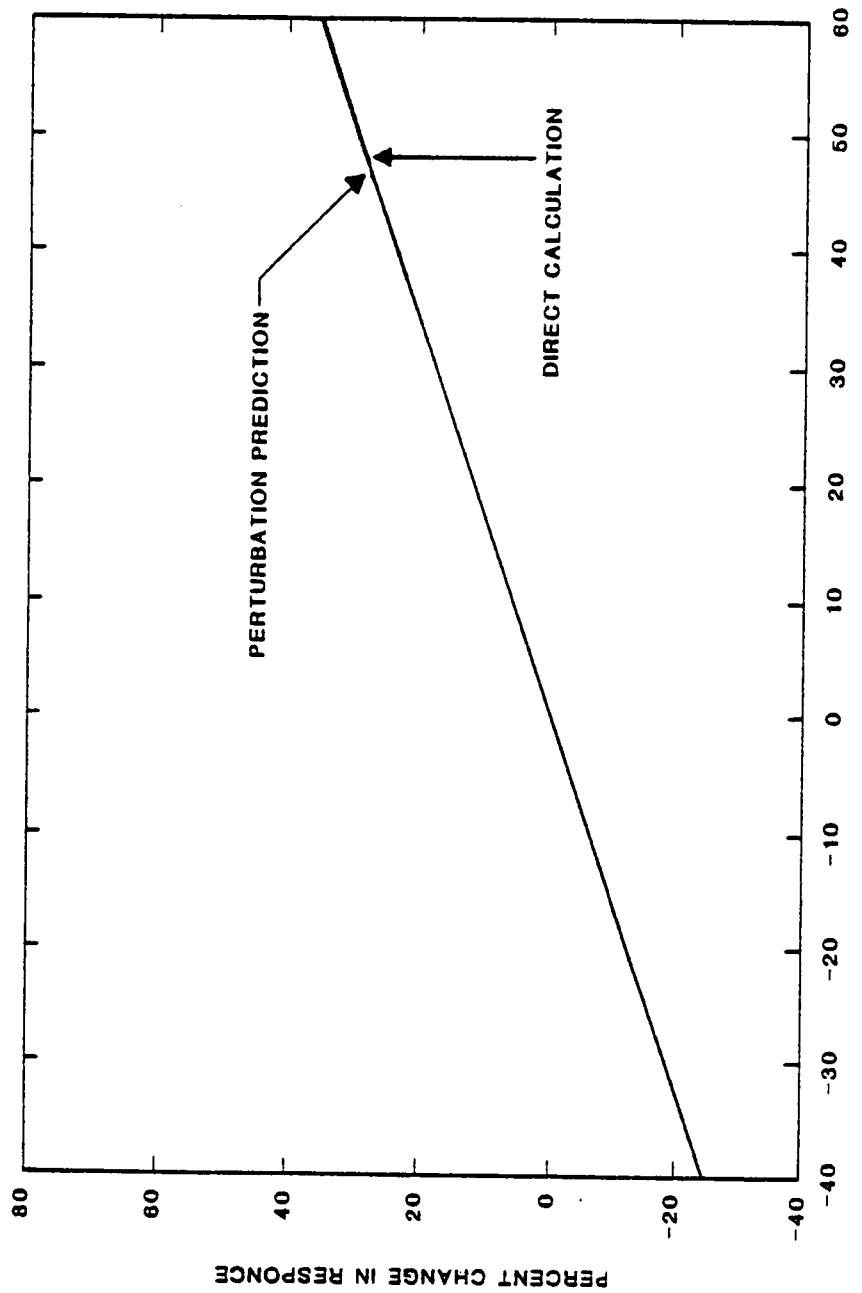

Figure 7.2. Space-Average Tritium Concentration in ZONE-1 at t_f = 2 Days as a Function of Transverse Dispersivity.

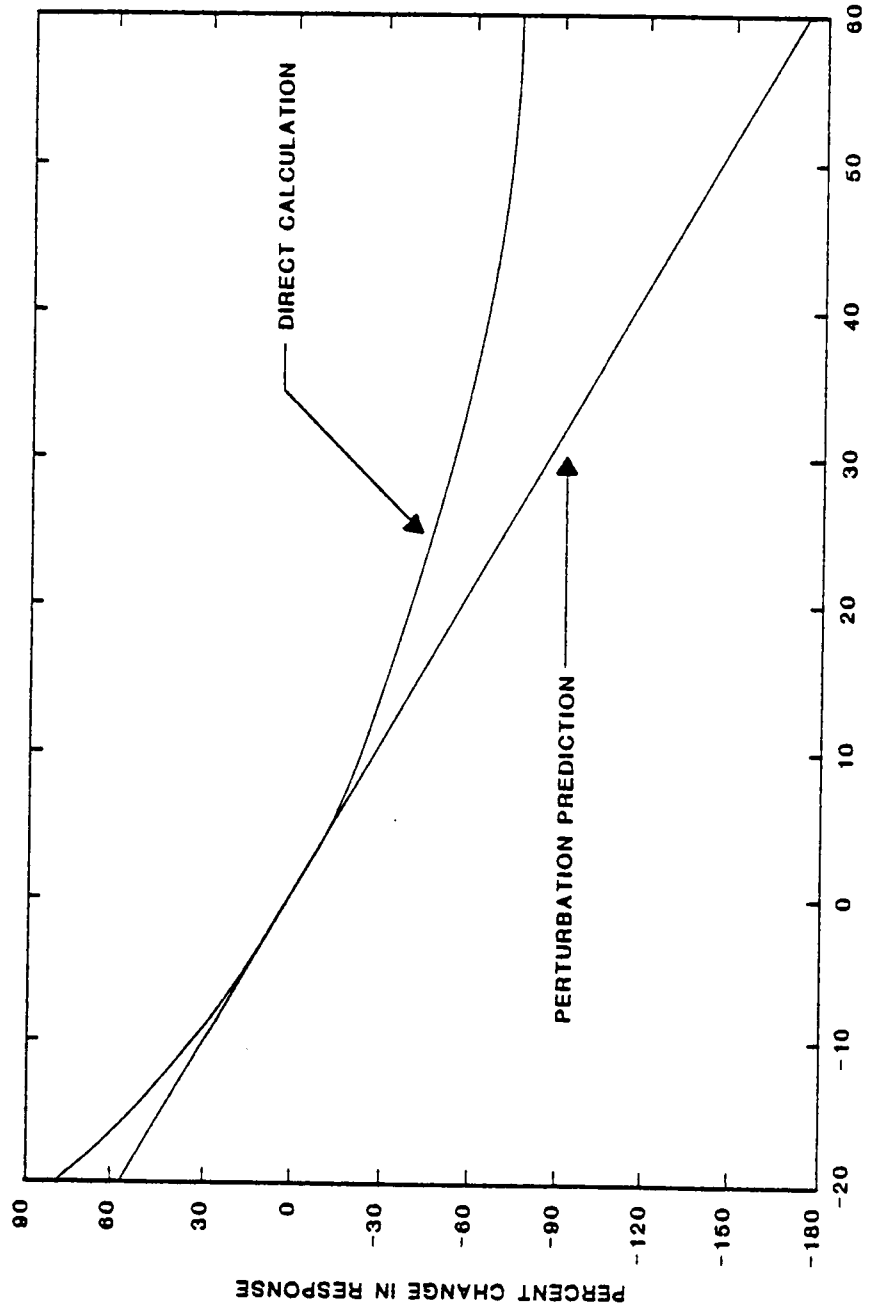

Figure 7.3. Space Average Tritium Concentration in ZONE-1 at t_f = 2 Days as a Function of Retardation Factor.

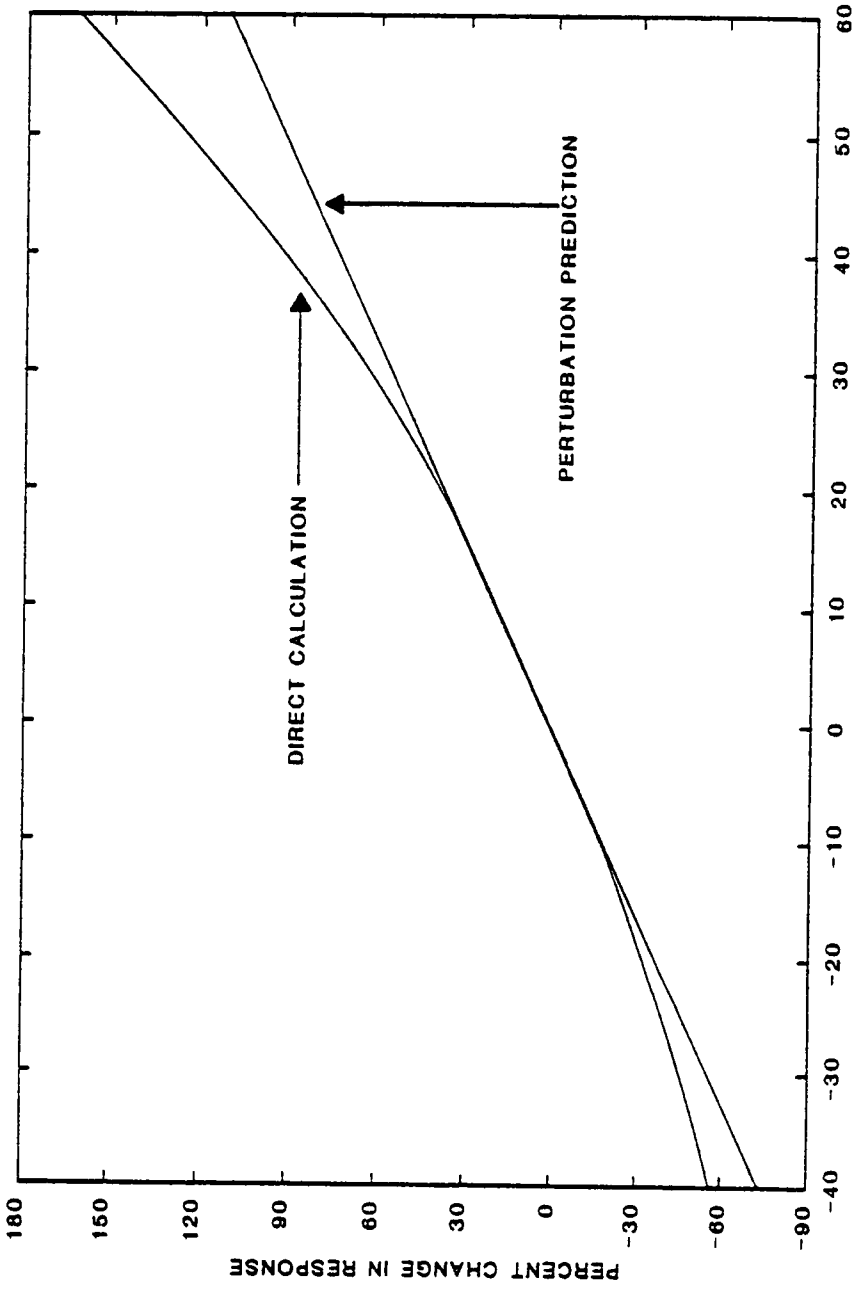

Figure 7.4. Tritium Discharge Rate at t_f = 2 Days as a Function of Longitudinal Dispersivity.

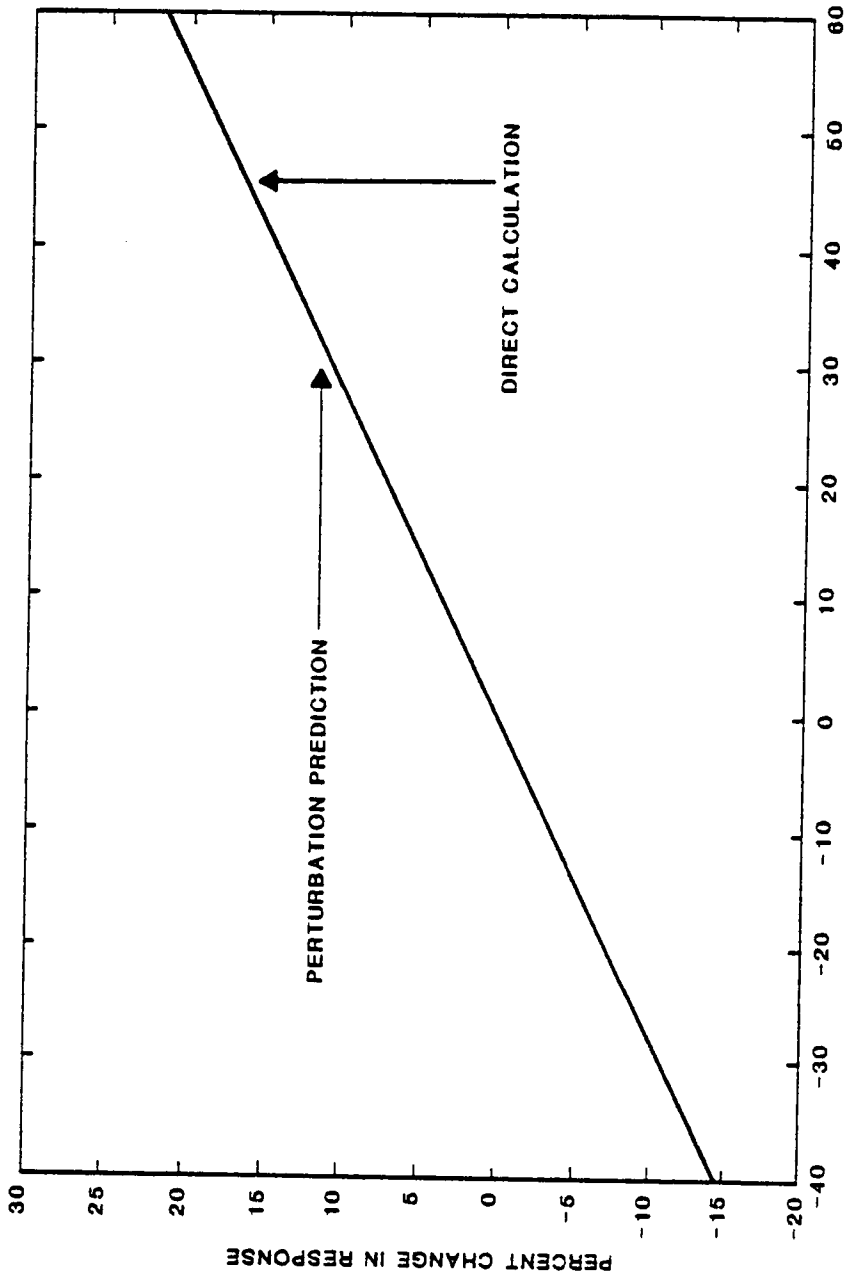

Figure 7.5 Tritium Discharge Rate at t_f = 2 Days as a Function of Transverse Dispersivity.

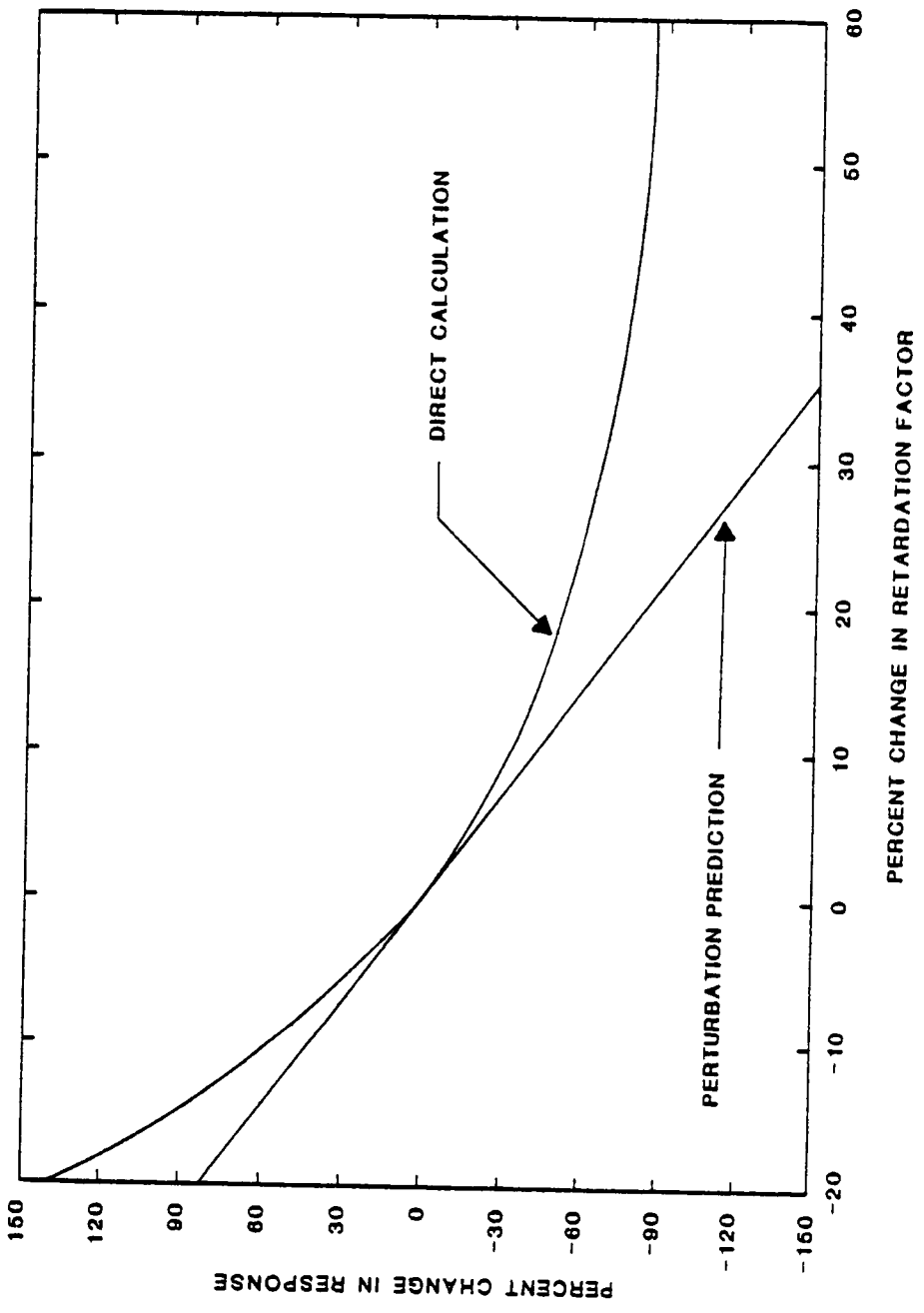

Figure 7.6. Tritium Discharge Rate at t_f = 2 Days as a Function of Retardation Factor.

As can be seen from Figures 7.1 through 7.6, the response behavior near the reference point is linear in both specified response cases. The agreement between the perturbation prediction and direct calculation for the response changes is good in the linearity ranges of the parameters listed in Table 7.5 for the two response cases. Now, the response change with respect to the reference-state response value arising from any parameter change within its linearity range can be obtained by multiplying the relative sensitivity coefficient for the parameter calculated by the perturbation method with the specified parameter percent change. The response so calculated will be as accurate as that obtained by running the radionuclide transport code with the varied

Table 7.5. Linearity Ranges of the Parameters in the Radionuclide Transport Calculations

	Input Parameter Range (%)		
Response Case 1	a_L	a_T	R_d
From	-35	-60	-8
To	40	60	8
	Input Parameter Range (%)		
Response Case 2	a_L	a_T	R_d
From	-12	-80	-4
To	18	80	4

parameter data. The graphical comparison of the response shown in Figures 7.1 through 7.6 further demonstrates the validation and usefulness of the generalized perturbation theory in predicting the response change in the radionuclide transport calculation.

The advantage of using the perturbation method to get the perturbed response for a parameter change within its linearity range is the following. Once the relative sensitivity coefficient of the response to the parameter has been determined at the reference-state, the perturbed response can be calculated by using Equation 7.4 without having to repeat the radionuclide transport calculation. Thus, the computation cost can be saved.

However, as can be seen from Figures 7.1 through 7.6, the response is no longer linear if the perturbation of the parameter is extended beyond its linearity range in both positive and negative directions. Then the perturbation method cannot be employed to accurately predict the response changes due to such large parameter changes.

CHAPTER VIII

SUMMARY, CONCLUSIONS AND RECOMMENDATIONS FOR FURTHER STUDY

Transport of radionuclides by groundwater flow in saturated-unsaturated porous media has been regarded as an important pathway for radioactive wastes to reach the biosphere from the low-level radioactive wastes shallow-land burial trench. The simulation of radionuclide transport and the prediction of radiation dose to man are necessitated in the assessment of the environmental impact of the radioactive wastes disposal to the biosphere, and can be performed by employing numerical models for the simulations of both the groundwater flow and radionuclide transport. Sensitivity analysis for the radionuclide transport by groundwater flow which was developed using generalized perturbation theory allows one to identify the most sensitive input parameters and the sensitive regions; to estimate changes in the computed response of interest (e.g., dose to man) arising from changes in the input parameter data without resorting to recomputation of the response. The following is a summary of the work that has been done and conclusions of the findings in this study.

A transient, two-dimensional computer code RADMIG for the simulation of radionuclide transport by groundwater flow has been developed using Fluid in Discrete Element (FLIDE) numerical formulation. This code was employed to simulate tritium transport in a hypothetical groundwater flow system and compute the specified response of interest for three example problems. The steady-state groundwater flow data in

the system region was obtained by running a groundwater flow transport code based on the Galerkin finite-element model and transferring the flow data into discrete-element form as input data to RADMIG. The time-dependent isoconcentration contour graphs were presented for each case.

The sensitivity analysis methodology for the radionuclide transport problem has been developed, based on generalized perturbation theory, which can be used to assess the uncertainty and sensitivity of the response of interest (e.g., total radionuclide discharge rate or space-average concentration at a final time) due to changes in the input parameter data. The adjoint transport equation was derived from the radionuclide transport equation using the variational principle formulation of generalized perturbation theory. Boundary conditions for the adjoint transport equation were formulated. Since the adjoint transport was characterized as a final-value problem, the final conditions were formulated for each type of response under consideration. The sensitivity coefficients were formulated for each of five input parameters and were computed by "folding" the time-dependent concentration and adjoint fields together.

The adjoint transport equation was solved using the adjoint transport code ADJMIG which was developed by modifying the radionuclide transport code RADMIG. The adjoint transport equation was solved to obtain time-dependent adjoint fields for two responses of interest. It was shown that the adjoint function can be interpreted as "importance" of a radionuclide in a groundwater flow system to a computed response of interest. This response-importance field is closely related to the groundwater flow pattern and the response region. It was

illustrated that the response-importance was transported by the reversed groundwater flow from the response region. It was concluded that the time-dependent adjoint fields can provide some physical insight into the importance of the groundwater flow to the response.

The relative sensitivity coefficient formulations have been implemented into the computer code SENCOF which was used to compute the relative sensitivity coefficient fields of two responses (space-average concentration and total discharge rate) to four input parameters. The procedure for radionuclide transport sensitivity analysis was outlined. The sensitivity coefficient field shows the sensitive regions of the parameter in which the response of interest is most sensitive to the parameter variation. It was concluded that the sensitive region is in general situated in the upstream area with respect to the response region in the groundwater flow system. It was also noted that the sensitive regions for the parameters are largely dependent upon (1) groundwater flow pattern, and (2) geometrical location of the response region.

The radionuclide transport sensitivity theory has been validated by comparing the relative sensitivity coefficients of responses of interest to each one of the input parameters, obtained from the use of the perturbation sensitivity analysis (prediction) and direct-substitution-type analysis (direct-calculation). The responses of interest under consideration included the space-average tritium concentrations and tritium discharge rates at different final times. Uniform percent changes of parameters through the system region were used for both prediction and direct-calculation approaches to obtain the relative sensitivity coefficients which represent percent changes in responses

due to 1% change in the addressed parameters. The agreement between the sensitivity results from both prediction and direct-calculation approaches is good for the specified parameters.

The advantage of using generalized perturbation theory to address the sensitivity analysis for the radionuclide transport problem is that only two computer runs are required for each specified response of interest to obtain the sensitivity coefficients of the response to all of the parameters. The two computer runs are respectively the radionuclide and adjoint transport simulations with the referenced input parameter data, in order to obtain the concentration and adjoint fields. However, as for the direct-calculation approach, the radionuclide transport code RADMIG must be run for every change made in the input data for each of the input parameters in order to compute the response changes. For a CPU-time-consuming code, the reduction in computation cost resulting from using the generalized perturbation approach is substantial.

The generalized perturbation sensitivity analysis has its limitation in predicting the response change due to input parameter changes. In view of the first-order property of the perturbation method, the perturbation of the input parameter should not exceed the range of linearity in the vicinity of its reference point. The responses versus dispersivities and retardation factor near the reference values have been presented using direct-calculation approach, together with the response-parameter lines predicted by use of the generalized perturbation method.

In conclusion, the radionuclide-transport sensitivity analysis based on generalized perturbation theory can provide a very effective and useful means in assessing the sensitivity problem for the radionuclide transport by groundwater flow. However, because this dissertation is the first attempt in applying the perturbation theory to the radionuclide transport problem, there remain some areas which deserve further study. The following is a list of recommendations for further investigations.

(a) Apply the perturbation sensitivity analysis methodology to groundwater flow transport problems to address the sensitivity of groundwater flow to the soil properties (e.g., hydraulic conductivity, specific storage).

(b) Perform the radionuclide-transport sensitivity analysis using other numerical models for radionuclide transport by groundwater flow (e.g., finite-element, method of characteristics).

(c) Apply perturbation sensitivity theory to realistic contaminant (radioactive or non-radioactive) transport problems. Use time-dependent groundwater flow data as input to mass transport model, which will be obtained from the simulation of a transient groundwater flow transport model.

LIST OF REFERENCES

LIST OF REFERENCES

1. Debuchananne, G. D., and W. W. Wood, "Hydrologic Consideration Related to Management of Radioactive Waste," chapter 3, Radioactive Waste in Geologic Storage, American Chemical Society, 1979.

2. Frind, E. O., and M. J. Verge, "Three-Dimensional Modeling of Groundwater Flow Systems," Water Resour. Res., Vol. 14, No. 5, 844-856, 1978.

3. Narasimhan, T. N., and P. A. Witherspoon, "Numerical Model for Saturated-Unsaturated in Deformable Porous Media," Water Resour. Res., Vol. 13, No. 3, 657-663, 1977.

4. Narasimhan, T. N., P. A. Witherspoon and A. L. Edwards, "Numerical Model for Saturated-Unsaturated Flow in Deformable Porous Media," Water Resour. Res., Vol. 14, No. 2, 255-261, 1978.

5. McEllwee, C. D., and M. A. Yukler, "Sensitivity of Groundwater Models with Respect to Variations in Transmissivity and Storage," Water Resour. Res., Vol. 14, No. 3, 451-459, 1978.

6. Narasimhan, T. N., and P. A. Witherspoon, "An Integrated Finite Difference Method for Analyzing Fluid Flow in Porous Media," Water Resour. Res., Vol. 12, No. 1, 57-63, 1976.

7. Narasimhan, T. N., S. P. Neuman and P. A. Witherspoon, "Finite Element Method for Subsurface Hydrology Using a Mixed Explicit-Implicit Scheme," Water Resour. Res., Vol. 14, No. 5, 863-877, 1978.

8. Wiggert, D. C., and E. B. Wylie, "Numerical Predictions of Two-Dimensional Transient Groundwater Flow by the Method of Characteristics," Water Resour. Res., Vol. 12, No. 5, 971-977, 1976.

9. Reeves, M., and J. Duguid, "Water Movement through Saturated-Unsaturated Porous Media: A Finite Element Galerkin Model," ORNL-4927, 1975.

10. DeWiest, "Flow Through Porous Media," Academic Press, N.Y. 1969.

11. Aikens, Jr., A. E., et al., "Generic Methodology for Assessment of Radiation Doses from Groundwater Migration of Radionuclides in LWR Waste at Shallow Land Burial Trenches," prepared by Dames and Moore for the Atomic Industrial Forum, AIF/NESP-015, 1979.

12. Bredehoeft, J., and G. Pinder, "Mass Transport in Flowing Groundwater," Water Resour. Res., Vol. 9, 194-210, 1973.

13. Pinder, G., "A Galerkin Finite-Element Simulation of Groundwater Contamination of Long Island, New York," Water Resour. Res., Vol. 9, 1657-1670, 1973.

14. Rubin, J., and R. V. James, "Dispersion-Affected Transport of Reacting Solutes in Saturated Porous Media: Galerkin Methods Applied to Equilibrium-Controlled Exchange in Unidirectional Steady Water Flow," Water Resour. Res., Vol. 9, 1332-1356, 1973.

15. Duguid, J., and M. Reeves, "Material Transport Through Saturated-Unsaturated Porous Media: A Finite Element Galerkin Model," ORNL-4928, 1976.

16. Pickens, J. F., and W. C. Lennox, "Numerical Simulation of Water Movement in Steady Groundwater Flow Systems," Water Resour. Res., Vol. 12, No. 2, 171-179, 1976

17. Konikow, L. F. and Bredehoeft, J. D., "Computer Model of Two-Dimensional Solute Transport and Dispersion in Ground Water," chapter C2, Techniques of Water-Resources Investigations of the U. S. Geological Survey.

18. Lapidus, L., and N. Amundson, "Mathematics of Adsorption in Beds, VI. The Effect of Longitudinal Diffusion in Ion Exchange and Chromatographic Columns," J. Phys. Chem., Vol. 56, 984-998, 1952.

19. Oster, C., J. Sonnichsen and R. Jaske, "Numerical Solution to the Convective Diffusion Equation," Water Resour. Res., Vol. 6, 1746-1752, 1970.

20. Bredehoeft, J., "Comment on Numerical Solution to the Convective Diffusion Equation by C. A. Oster, J. C. Sonnichsen and R. T. Jaske," Water Resour. Res., Vol. 9, 194-210, 1973.

21. Hadermann, J., "Radionuclide Transport Through heterogeneous Media," Nuclear Technology, Vol. 47, 312-323, 1980.

22. Gray, W. G., "Numerical Solution Techniques for the Convective Dispersive Equation," ANS Transaction, Vol. 33, 120-121, 1979.

23. Guymon, G. L., "A General Numerical Solution of the Two-Dimensional Diffusion-Convection Equation by the Finite Element Method," Water Resour. Res., Vol. 6, 1611-1617, 1970.

24. Eraslan, A. H., "A Transient, Two-Dimensional Discrete-Element, Far-Field Model for Thermal Impact Analysis of Power Plant Discharges in Coastal and Offshore Region. Part I: General Description of the Mathematical Model and the Results of an Application," ORNL-4940, 1975.

25. Eraslan, A. H. "A Transient, Two-Dimensional, Discrete-Element Model for Far-Field Analysis of Thermal Discharges in Coastal Regions," Progress in Astronautics and Aeronautics, Vol. 36, AIAA publication, 1975.

26. Eraslan, A. H., "A Tidal-Transient, Far-Field Model for Offshore Thermal Discharges," ANS Transactions, Vol. 18, 1974.

27. Eraslan, A. H., et al., "Development of a Unified Transport Approach for the Assessment of Power Plant Impact," ORNL/NUREG/TM-89, 1977.

28. Eraslan, A. H., K. H. Kim and J. L. Harris, "A Systematic Application of Transient, Multi-Dimensional Models for Complete Analysis of Thermal Impact in Regions with Severe Reversing Flow Conditions," Waste Heat Management and Utilization Conference, Miami Beach, Florida, 1977.

29. Eraslan, A. H., "A Tidal-Transient, Two-Dimensional Multi-Layer Discrete-Element Model for Simulating Natural and Power Plant Induced Hydrodynamic Conditions in Large Receiving Water Bodies," ESM/ENV-77-04, USDI project report, 1977.

30. Roache, P. J., Computational Fluid Dynamics, Hermosa Publishers, Albuquerque, N. M., 1976.

31. Bell, M. J., "The Nuclear Regulatory Commission's Low-Level Waste Management Program," ANS Transactions, 1977.

32. Heath, C. A., "The Department of Energy Program for Long-Term Isolation of Radioactive Waste," chapter 3, Radioactive Waste in Geologic Storage, American Chemistry Society, 1979.

33. Williams, M. L., and C. R. Weisbin, "Sensitivity and Uncertainty Analysis for Functionals of the Time-Dependent Nuclide Density Field," ORNL-5393, 1978.

34. Oblow, E. M., "Sensitivity Theory for Reactor Thermal-Hydraulic Problems," Nucl. Sci. Eng., 68, 322-337, 1978.

35. Oblow, E. M., et al., "General Sensitivity Theory for Radiation Transport," ORNL/TM-4110, 1974.

36. Oblow, E. M., "Reactor Cross-Section Sensitivity Studies Using Transport Theory," ORNL/TM-4437, 1974.

37. Weisbin, C. R., et al., "Application of FORSS Sensitivity and Uncertainty Methodology to Fast Reactor Benchmark Analysis," ORNL/TM-5563, 1976.

38. Oblow, E. M., "Sensitivity Theory from a Differential Viewpoint," Nucl. Sci. Eng., 59, 187-189, 1976.

39. Pomraning, G. C., "Variation Principle for Eigenvalue Equation," J. Math. Phys. 8, 149, 1967.

40. Stacey, Jr., W. M., Variational Methods in Nuclear Reactor Physics, Academic Press, N. Y., 1974.

41. Williams, M. L., "Perturbation and Sensitivity Theory for Reactor Burnup Analysis," Ph.D. Dissertation, the University of Tennessee, 1979.

42. Courant, R., Friedrichs, K. and Lewy, H., "On the Partial Difference Equations of Mathematical Physics," IBM Journal, 215-234, March, 1967.

43. Lilly, D. K., "On the Computational Stability of Numerical Solutions of Time-Dependent Non-Linear Geophysical Fluid Dynamics Problems," U. S. Weather Bureau Monthly Weather Review, Vol. 93, No. 1, 11-26, 1965.

44. DuFort, E. C., and S. P. Frankel, "Stability Conditions in the Numerical Treatment of Parabolic Differential Equations," Math Tables and Other Aids to Computation, Vol. 7, 135-152, 1953.

45. Von Neumann, J., and R. D. Richtmyer, "A Method for the Numerical Calculation of Hydrodynamic Shocks," J. Appl. Phys., Vo. 21, 232-257, 1950.

46. Hirt, C. W., "Heuristic Stability Theory for Finite-Difference Equations," Journal of Computational Physics, Vol. 2, 339-355, 1968.

47. Eraslan, A. H., Personal communication.

APPENDIX

APPENDIX

DERIVATION OF THE VARIATION OF K WITH RESPECT TO C

This appendix is devoted to deriving from Equation 4.27 the variation of K with respect to C as expressed in Equation 4.28. Here we suppress all the independent variables for the sake of notation simplicity.

Let the linear radionuclide transport operator L operate on the variation of C,

$$L\,\delta C = -R_d\theta\frac{\partial \delta C}{\partial t} + \nabla\cdot\bar{\bar{D}}\nabla\delta C - \nabla\cdot\bar{v}\delta C - R_d\theta\lambda\delta C \ . \tag{A.1}$$

Define the adjoint transport operator L* from L as

$$L^* = R_d\theta\frac{\partial}{\partial t} + \nabla\cdot\bar{\bar{D}}^{+}\nabla + \bar{v}\cdot\nabla - R_d\theta\lambda \tag{A.2}$$

where $\bar{\bar{D}}^{+}$ is the transpose of the hydrodynamic dispersion coefficient tensor $\bar{\bar{D}}$. Operating L* on the Lagrangian multiplier ψ^* which will be called adjoint function hereafter,

$$L^*\psi^* = R_d\theta\frac{\partial \psi^*}{\partial t} + \nabla\cdot\bar{\bar{D}}^{+}\nabla\psi^* + \bar{v}\cdot\nabla\psi^* - R_d\theta\lambda\psi^* \ . \tag{A.3}$$

Multiply Equation A.1 by ψ^* and integrate the resultant equation over x, z in the system region, and t from initial time 0 to final time t_f. Then multiply Equation A.3 by δC and integrate over x, z, t in the same way. Subtract these two equations to obtain

$$[\psi^* L\,\delta C]_{x,z,t} - [\delta C L^* \psi^*]_{x,z,t} = -\left[R_d\theta\psi^* \frac{\partial \delta C}{\partial t} + R_d\theta\delta C \frac{\partial \psi^*}{\partial t}\right]_{x,z,t}$$

$$+ [\psi^* \nabla\cdot\bar{\bar{D}}\nabla\delta C - \delta C \nabla\cdot\bar{\bar{D}}^+\nabla\psi^*]_{x,z,t} - [\psi^*\nabla\cdot\bar{v}\,\delta C + \delta C\bar{v}\cdot\nabla\psi^*]_{x,z,t} . \quad (A.4)$$

The first term on the right-hand side (RHS) of Equation A.4 can be reduced to

$$\left[R_d\theta\psi^* \frac{\partial \delta C}{\partial t} + R_d\theta\delta C \frac{\partial \psi^*}{\partial t} \right]_{x,z,t} = \left[\frac{\partial R_d\theta\psi^*\delta C}{\partial t} \right]_{x,z,t}$$

$$= [R_d\theta\psi^*\delta C]_{x,z,t=t_f} - [R_d\theta\psi^*\delta C]_{x,z,t=0} \quad (A.5)$$

We now simplify the second term on RHS of Equation A.4. We notice that both ψ^* and δC are scalar fields, both $\bar{\bar{D}}\nabla\delta C$ and $\bar{\bar{D}}^+\nabla\psi^*$ are vectors because the gradient of a scalar is a vector and a vector operated on by a tensor yields another vector. From vector calculus, we have the equation for the divergence of a vector field multiplied by a scalar field,

$$\nabla\cdot(f\bar{v}) = f\nabla\cdot\bar{v} + \bar{v}\cdot\nabla f. \quad (A.6)$$

Then we have

$$\nabla\cdot\psi^*\bar{\bar{D}}\nabla\delta C = \psi^*\nabla\cdot\bar{\bar{D}}\nabla\delta C + \bar{\bar{D}}\nabla\delta C\cdot\nabla\psi^*, \quad (A.7)$$

and

$$\nabla\cdot\delta C\bar{\bar{D}}^+\nabla\psi^* = \delta C\nabla\cdot\bar{\bar{D}}^+\nabla\psi^* + \bar{\bar{D}}^+\nabla\psi^*\cdot\nabla\delta C. \quad (A.8)$$

It can be shown that the last terms on RHS of Equations A.7, A.8 are equal, i.e.,

$$\bar{\bar{D}}\nabla\delta C\cdot\nabla\psi^* = \bar{\bar{D}}^+\nabla\psi^*\cdot\nabla\delta C. \tag{A.9}$$

From Equations A.7 through A.9, we obtain

$$\psi^*\nabla\cdot\bar{\bar{D}}\nabla\delta C - \delta C\nabla\cdot\bar{\bar{D}}^+\nabla\psi^* = \nabla\cdot\psi^*\bar{\bar{D}}\nabla\delta C - \nabla\cdot\delta C\bar{\bar{D}}^+\nabla\psi^* \ . \tag{A.10}$$

By using the divergence theorem, the second term on RHS of Equation A.4 becomes

$$\left[\psi^*\nabla\cdot\bar{\bar{D}}\nabla\delta C - \delta C\nabla\cdot\bar{\bar{D}}^+\nabla\psi^*\right]_{x,z,t}$$

$$= \int_0^{t_f}\int_V \nabla\cdot(\psi^*\bar{\bar{D}}\nabla\delta C - \delta C\bar{\bar{D}}^+\nabla\psi^*)d\bar{r}dt$$

$$= \int_0^{t_f}\int_S \hat{n}\cdot(\psi^*\bar{\bar{D}}\nabla\delta C - \delta C\bar{\bar{D}}^+\nabla\psi^*)d\bar{r}dt \ , \tag{A.11}$$

where V and S represent the volume and the boundary surface of the system region, respectively.

Using Equation A.6 again, we have

$$\nabla\cdot\psi^*\bar{v}\delta C = \psi^*\nabla\cdot\bar{v}\delta C + \bar{v}\delta C\cdot\nabla\psi^*. \tag{A.12}$$

Substituting Equation A.12 into the last term of Equation A.4 and employing the divergence theorem, we get

$$[\psi^* \nabla \cdot \bar{v} \delta C + \delta C \bar{v} \cdot \nabla \psi^*]_{x,z,t}$$

$$= \int_0^{t_f} \int_V \nabla \cdot \psi^* \bar{v} \delta C d\bar{r} dt. \qquad \text{(A.13)}$$

Combining Equations A.4, A.5, A.11, and A.13, substituting into Equation 4.26, the variation of K with respect to C becomes

$$\delta K_C = \left(\frac{\partial R}{\partial C} \right)_{ref} \delta C + [\delta C L^* \psi^*]_{x,z,t} + [R_d \theta \psi^* \delta C]_{x,z,t=0}$$

$$- [R_d \theta \psi^* \delta C]_{x,z,t=t_f} + \int_0^{t_f} \int_S \hat{n} \cdot (\psi^* \bar{\bar{D}} \nabla \delta C$$

$$- \delta C \bar{\bar{D}}^+ \nabla \psi^* - \psi^* \bar{v} \delta C) d\bar{r} dt. \qquad \text{(A.14)}$$

Now Equation A.14 can be written as Equation 4.27.

VITA

Hanchang Henry Chen was born in Canton, China on May 2, 1948. He attended elementary school in I-Lan, Taiwan. After graduation from I-Lan High School he entered Tsing-Hua University, Hsinchu, Taiwan in 1965. In June 1970, he obtained a Bachelor of Science degree in Nuclear Engineering. After serving in the military service for a year, he continued his graduate study in the Nuclear Engineering Department at Tsing-Hua University. Upon receipt of his Master of Science degree in Nuclear Engineering, he accepted an instructor position in the Nuclear Engineering Department of Tsing-Hua University, where he had served for three years. In the fall of 1976, he accepted a research assistantship to begin work towards the Doctor of Philosophy degree at the University of Tennessee.

The author is a member of Phi Kappa Phi and the American Nuclear Society. After graduation, he will continue working in engineering with Technology for Energy Corporation, where he is currently employed. He was married to the former Margaret Suchao Huang of Tainan, Taiwan in 1973. They now have two sons.